AD 285 569

ASD-TDR-62-432

INVESTIGATION OF DIFFUSION BARRIERS FOR REFRACTORY METALS

TECHNICAL DOCUMENTARY REPORT NR ASD-TDR-62-432

July 1962

Directorate of Materials and Processes
Aeronautical Systems Division
Air Force Systems Command
Wright-Patterson Air Force Base, Ohio

Project Nr 7312, Task Nr 731201

(Prepared under Contract Nr AF33(616)-6354 by MANLABS, INC., Cambridge, Massachusetts; E. M. Passmore, J. E. Boyd, B. S. Lement, authors.)

Aeronautical Systems Division, Dir/Materials & Processes, Metals & Ceramics Lab, Wright-Patterson AFB, Ohio.
Rpt Nr ASD-TDR-62-432, INVESTIGATION OF DIFFUSION BARRIERS FOR REFRACTORY METALS. Final report, July 1962, 95 p., incl. illus., tables & 30 refs.

Unclassified Report

Thirty-three base barrier combinations involving the four refractory metals W, Mo, Ta, and Cb and 12 potential barrier metals having melting points over 1700°C were evaluated for relative interdiffusion behavior at 1700°C and 1800°C. The relative extent of interdiffusion decreases with increasing base-barrier solidus temperature, although wide variations occur for melting points up to

(over)

2100°C. Interdiffusion in the Mo-Cr combination was found to be substantially reduced by the presence of a Re barrier.

Re, Ru, and Ir barriers appear optimum for W base metal; W, Re, Ru, and Ir appear optimum for Ta; and W, Re, Os, and Zr appear optimum for Cb.

The thickness (X) of the total interdiffusion zone as well as of the intermediate phase layers in the W-Re, Mo-Re, Ta-Re, and Cb-Re combinations was found to increase with time (t) in accordance with the relationship $X^n = kt$, with values of n in the range 1.4 to 4.9.

1. Barrier Coatings
2. Interdiffusion
3. Refractory Metals

I. AFSC Project 7312 Task 731201
II. Contract AF 33(616)-6354
III. ManLabs, Inc., Cambridge, Mass.
IV. E. M. Passmore, J. E. Boyd, B. S. Lement
V. Aval fr OTS
VI. In ASTIA collection

Aeronautical Systems Division, Dir/Materials & Processes, Metals & Ceramics Lab, Wright-Patterson AFB, Ohio.
Rpt Nr ASD-TDR-62-432, INVESTIGATION OF DIFFUSION BARRIERS FOR REFRACTORY METALS. Final report, July 1962, 95 p., incl. illus., tables & 30 refs.

Unclassified Report

Thirty-three base barrier combinations involving the four refractory metals W, Mo, Ta, and Cb and 12 potential barrier metals having melting points over 1700°C were evaluated for relative interdiffusion behavior at 1700°C and 1800°C. The relative extent of interdiffusion decreases with increasing base-barrier solidus temperature, although wide variations occur for melting points up to

(over)

2100°C. Interdiffusion in the Mo-Cr combination was found to be substantially reduced by the presence of a Re barrier.

Re, Ru, and Ir barriers appear optimum for W base metal; W, Re, Ru, and Ir appear optimum for Ta; and W, Re, Os, and Zr appear optimum for Cb.

The thickness (X) of the total interdiffusion zone as well as of the intermediate phase layers in the W-Re, Mo-Re, Ta-Re, and Cb-Re combinations was found to increase with time (t) in accordance with the relationship $X^n = kt$, with values of n in the range 1.4 to 4.9.

1. Barrier Coatings
2. Interdiffusion
3. Refractory Metals

I. AFSC Project 7312 Task 731201
II. Contract AF 33(616)-6354
III. ManLabs, Inc., Cambridge, Mass.
IV. E. M. Passmore, J. E. Boyd, B. S. Lement
V. Aval fr OTS
VI. In ASTIA collection

Aeronautical Systems Division, Dir/Materials & Processes, Metals & Ceramics Lab, Wright-Patterson AFB, Ohio.
Rpt Nr ASD-TDR-62-432, INVESTIGATION OF DIFFUSION BARRIERS FOR REFRACTORY METALS. Final report, July 1962, 95 p., incl. illus., tables & 30 refs.

Unclassified Report

Thirty-three base barrier combinations involving the four refractory metals W, Mo, Ta, and Cb and 12 potential barrier metals having melting points over 1700°C were evaluated for relative interdiffusion behavior at 1700°C and 1800°C. The relative extent of interdiffusion decreases with increasing base-barrier solidus temperature, although wide variations occur for melting points up to

(over)

1. Barrier Coatings
2. Interdiffusion
3. Refractory Metals

I. AFSC Project 7312 Task 731201
II. Contract AF 33(616) -6354
III. ManLabs, Inc., Cambridge, Mass.
IV. E. M. Passmore, J. E. Boyd, B. S. Lement
V. Aval fr OTS
VI. In ASTIA collection

2100°C. Interdiffusion in the Mo-Cr combination was found to be substantially reduced by the presence of a Re barrier.

Re, Ru, and Ir barriers appear optimum for W base metal; W, Re, Ru, and Ir appear optimum for Ta; and W, Re, Os, and Zr appear optimum for Cb.

The thickness (X) of the total interdiffusion zone as well as of the intermediate phase layers in the W-Re, Mo-Re, Ta-Re, and Cb-Re combinations was found to increase with time (t) in accordance with the relationship $X^n = kt$, with values of n in the range 1.4 to 4.9.

Aeronautical Systems Division, Dir/Materials & Processes, Metals & Ceramics Lab, Wright-Patterson AFB, Ohio.
Rpt Nr ASD-TDR-62-432, INVESTIGATION OF DIFFUSION BARRIERS FOR REFRACTORY METALS. Final report, July 1962, 95 p., incl. illus., tables & 30 refs.

Unclassified Report

Thirty-three base barrier combinations involving the four refractory metals W, Mo, Ta, and Cb and 12 potential barrier metals having melting points over 1700°C were evaluated for relative interdiffusion behavior at 1700°C and 1800°C. The relative extent of interdiffusion decreases with increasing base-barrier solidus temperature, although wide variations occur for melting points up to

(over)

1. Barrier Coatings
2. Interdiffusion
3. Refractory Metals

I. AFSC Project 7312 Task 731201
II. Contract AF 33(616) -6354
III. ManLabs, Inc., Cambridge, Mass.
IV. E. M. Passmore, J. E. Boyd, B. S. Lement
V. Aval fr OTS
VI. In ASTIA collection

2100°C. Interdiffusion in the Mo-Cr combination was found to be substantially reduced by the presence of a Re barrier.

Re, Ru, and Ir barriers appear optimum for W base metal; W, Re, Ru, and Ir appear optimum for Ta; and W, Re, Os, and Zr appear optimum for Cb.

The thickness (X) of the total interdiffusion zone as well as of the intermediate phase layers in the W-Re, Mo-Re, Ta-Re, and Cb-Re combinations was found to increase with time (t) in accordance with the relationship $X^n = kt$, with values of n in the range 1.4 to 4.9.

FOREWORD

This report was prepared by ManLabs, Inc. under USAF Contract No. AF33(616)-6354. This contract was initiated under Project No. 7312, "Finishes and Materials Preservation", Task No. 731201, "Surface Treatments and Coatings". The work was administered under the direction of the Directorate of Materials and Processes, Deputy Commander/Technology, Aeronautical Systems Division, with Mr. N.M. Geyer acting as project engineer.

This report covers work conducted from May 1960 to March 1962.

The authors wish to acknowledge the assistance of Sim Adler, Joseph Davis, and (Miss) Irita Vilks during the course of the program.

2-31C, 500, 8-31-62

ABSTRACT

Thirty-three base barrier combinations involving the four refractory metals: W, Mo, Ta, Cb; and 12 potential barrier metals having melting points over 1700°C were evaluated for relative interdiffusion behavior at 1700°C. Further evaluation of promising W and Ta-base combinations was carried out at 1800°C. In general, the relative extent of interdiffusion decreases with increasing base-barrier solidus temperature, although wide variations occur for melting points up to 2100°C. Alloying of Mo and Cb base metals was found to have no significant effect on interdiffusion with Re. Interdiffusion in the Mo-Cr combination was found to be substantially reduced by the presence of a Re barrier.

The base-barrier interdiffusion studies were supplemented by consideration of such factors as alloy melting point and barrier-coating interdiffusion in selecting optimum barrier metals for each base metal. As a result, Re, Ru, and Ir barriers appear optimum for W base metal; W, Re, Ru, and Ir appear optimum for Ta; and W, Re, Os, and Zr appear optimum for Cb.

The thickness (X) of the total interdiffusion zone as well as of the intermediate phase layers in the W-Re, Mo-Re, Ta-Re, and Cb-Re combinations was found to increase with time (t) in accordance with $X^n = kt$, with values of n in the range 1.4 to 4.9. Approximate over-all interdiffusion coefficients, D_s, of 3.4×10^{-6}, 9.0×10^{-5}, 1.9×10^{-8}, and 5.1×10^{-8} cm^2/sec were found for the W-Re, Mo-Re, Ta-Re, and Cb-Re combinations, respectively.

This report has been reviewed and is approved.

I. Perlmutter
Chief, Physical Metallurgy Branch
Metals and Ceramics Laboratory
Directorate of Materials and
Processes

TABLE OF CONTENTS

Section		Page
I.	INTRODUCTION	1
	A. The Diffusion Barrier Concept	1
	B. Previous Work	1
	C. Selection of Potential Barrier Metals	1
	D. Scope of the Investigation	4
II.	EXPERIMENTAL PROCEDURE	5
	A. Materials	5
	B. Preparation of Couples	5
	C. Evaluation of Couples	8
III.	RESULTS AND DISCUSSION	12
	A. Evaluation of Base-Barrier Combinations	12
	B. Interdiffusion Kinetics in Some Optimum Combinations	72
IV.	SUMMARY OF RESULTS	84
	REFERENCES	86

LIST OF FIGURES

Figure		Page
1	Schematic diagram of molybdenum clamp and assembled apparatus	7
2	Arrangement of Knoop microhardness indentations in the diffusion zone of a Cb-Re couple, annealed 8.3 hours at 1900°C	11
3	W-Re, pressure weld no. 4a-4; microstructure and microindentation measurements of interdiffusion after annealing 4 hours at 1700°C	22
4	W-Os, pressure weld no. 4a-4; microstructure and microindentation measurements of interdiffusion after annealing 4 hours at 1700°C	23
5	W-Ru, pressure weld no. 6a, annealed 4 hours at 1700°C	24
6	W-Ir, pressure weld no. 3-4; microstructure and microindentation measurements of interdiffusion after annealing 4 hours at 1700°C	25
7	W-Hf, pressure weld no. 6a, annealed 4 hours at 1700°C	26
8	W-Rh, pressure weld no. 6a, annealed 4 hours at 1700°C	27
9	W-Cr, pressure weld no. 6a, annealed 4 hours at 1700°C	28
10	W-V, pressure weld no. 6a, annealed 4 hours at 1700°C	29
11	Mo-W, pressure weld no. 6a, annealed 4 hours at 1700°C	30
12	Mo-Re, pressure weld no. 5, annealed 1 hour at 1700°C	31
13	Mo-Re, pressure weld no. 4b-4; microstructure and microindentation measurements of interdiffusion after annealing 4 hours at 1700°C	32
14	Mo-Ta, pressure weld no. 4b-4; microstructure and microindentation measurements of interdiffusion after annealing 4 hours at 1700°C	33
15	Mo-Ir, pressure weld no. 5, annealed 1 hour at 1700°C	34
16	Mo-Ir, pressure weld no. 3-4; microstructure and microindentation measurements of interdiffusion after annealing 4 hours at 1700°C	35
17	Mo-Cb, pressure weld no. 4b-4; microstructure and microindentation measurements of interdiffusion after annealing 4 hours at 1700°C	36

LIST OF FIGURES (Cont.)

Figure		Page
18	Mo-Hf, pressure weld no. 6a, annealed 4 hours at 1700°C .	37
19	Mo-Rh, pressure weld no. 6a, annealed 4 hours at 1700°C .	38
20	Mo-Cr, pressure weld no. 5, annealed 1 hour at 1700°C .	39
21	Mo-V, pressure weld no. 6a, annealed 4 hours at 1700°C .	40
22	Ta-Re, pressure weld no. 4a-4; microstructure and microindentation measurements of interdiffusion after annealing 4 hours at 1700°C	41
23	Ta-Os, pressure weld no. 4a-4; microstructure and micro-indentation measurements of interdiffusion after annealing 4 hours at 1700°C	42
24	Ta-Ru, pressure weld no. 6b, annealed 4 hours at 1700°C .	43
25	Ta-Ir, pressure weld no. 3-4; microstructure and micro-indentation measurements of interdiffusion after annealing 4 hours at 1700°C	44
26	Ta-Hf, pressure weld no. 6b, annealed 4 hours at 1700°C .	45
27	Cb-Re, pressure weld no. 4b-4; microstructure and microindentation measurements of interdiffusion after annealing 4 hours at 1700°C	46
28	Cb-Re, pressure weld no. 6c, annealed 4 hours at 1700°C .	47
29	Cb-Ta, pressure weld no. 4b-4; microstructure and microindentation measurements of interdiffusion after annealing 4 hours at 1700°C	48
30	Cb-Os, pressure weld no. 6b, annealed 4 hours at 1700°C .	49
31	Cb-Ir, pressure weld no. 4b-4; microstructure and micro-indentation measurements of interdiffusion after annealing 4 hours at 1700°C	50
32	Cb-Hf, pressure weld no. 6b, annealed 4 hours at 1700°C .	51
33	Cb-Zr, pressure weld no. 6b, annealed 4 hours at 1700°C .	52
34	Mo (.5Ti) - Re, pressure weld no. 6c, annealed 4 hours at 1700°C	53
35	Cb(F48) - Re, pressure weld no. 6c, annealed 4 hours at 1700°C	54

LIST OF FIGURES (Cont.)

Figure		Page
36	Cb(FS82)-Re, pressure weld no. 6c, annealed 4 hours at 1700°C	55
37	Cb(D31) - Re, pressure weld no. 6c, annealed 4 hours at 1700°C	56
38	W-Re, pressure weld no. 7a, annealed 3 hours at 1800°C	57
39	W-Os, pressure weld no. 7b, annealed 3 hours at 1800°C	58
40	W-Ru, pressure weld no. 7a, annealed 3 hours at 1800°C	59
41	W-Ir, pressure weld no. 7a, annealed 3 hours at 1800°C	60
42	W-Rh, pressure weld no. 7a, annealed 3 hours at 1800°C	61
43	Ta-W, pressure weld no. 7b, annealed 3 hours at 1800°C	62
44	Ta-Re, pressure weld no. 7b, annealed 3 hours at 1800°C	63
45	Ta-Ir, pressure weld no. 7b, annealed 3 hours at 1800°C	64
46	Re-Cr, pressure weld no. 5; annealed 1 hour at 1700°C	65
47	Ir-Cr, pressure weld no. 5, annealed 1 hour at 1700°C	66
48	Re-Rh, pressure weld no. 7a, annealed 3 hours at 1800°C	67
49	Ir-Rh, pressure weld no. 7a, annealed 3 hours at 1800°C	68
50	Mo-Re-Cr, pressure weld no. 5, annealed 1 hour at 1700°C.	69
51	Mo-Ir-Cr, pressure weld no. 5, annealed 1 hour at 1700°C.	70
52	Relationship between extent of interdiffusion and the minimum solidus temperature in several base-barrier alloy systems. Diffusion couples were given the indicated annealing treatments.	71
53	Variation of Knoop indentation length with distance, normal to the interface, in tungsten-rhenium diffusion couples after annealing at 1900°C	77
54	Variation of Knoop indentation length with distance, normal to the interface in molybdenum - rhenium diffusion couples after annealing at 1900°C	78

LIST OF FIGURES (Cont.)

Figure		Page
55	Variation of Knoop indentation length with distance normal to the interface, in tantalum-rhenium diffusion couples after annealing at 1900°C	79
56	Variation of Knoop indentation length with distance, normal to the interface, in columbium-rhenium diffusion couples after annealing at 1900°C	80
57	Growth of interdiffusion zone and intermediate phases in tungsten-rhenium diffusion couples annealed at 1900°C	81
58	Growth of interdiffusion zone and intermediate phases in molybdenum-rhenium diffusion couples annealed at 1900°C	82
59	Growth of interdiffusion zone and intermediate phases in tantalum-rhenium and columbium-rhenium diffusion couples annealed at 1900°C	83

LIST OF TABLES

Table		Page
1	Selection of Potential Base-Barrier Combinations	2
2	Materials	6
3	Etching Procedures for Diffusion Couples	9
4	Summary of Evaluation Experiments on Base-Barrier Combinations, Diffusion-Annealed 4 Hours at 1700°C .	13
5	Summary of Evaluation Experiments on W and Ta-Base Combinations, Diffusion-Annealed Three Hours at 1800°C .	18
6	Summary of Interdiffusion Measurements in Combinations of Promising Barriers and Oxidation Resistant Metals .	21
7	Solid Solubilities and Intermediate Phases at 1900°C in Some Optimum Combinations	73
8	Constants in the Equation, $X^n = kt$, Relating Intermediate Phase and Total Interdiffusion Zone Thicknesses to Diffusion-Annealing Time at 1900°C	75

I. INTRODUCTION

A. The Diffusion Barrier Concept

In order to use the major refractory metals (W, Mo, Ta, and Cb) at high temperatures, it is necessary to protect them with an oxidation resistant coating. However, interdiffusion between the coating and the refractory base metal may bring about the deterioration of the properties of both (due to the resultant alloying).

The performance of surface coatings may be enhanced if an intermediate metallic layer is placed between the coating and the base. The principal requirement of this layer is for it to act as a barrier to diffusion. Thus, the rate of interdiffusion between this barrier and the base metal should be much less than that between the oxidation resistant coating and base metal. Furthermore, only a limited amount of interdiffusion should take place between the coating and the barrier, although the barrier itself need not be highly oxidation resistant.

This report primarily deals with a study of interactions between potential barrier metals and W, Mo, Ta and Cb base metals. Interactions between barrier metals and oxidation resistant metals were also studied in order to evaluate more fully the relative efficacy of the various barrier metals. The report covers the continuation of work performed from May 1959 to May 1960 on the same contract[1] and was carried out from May 1960 to March 1962.

B. Previous Work

During the first year, 24 base-barrier metal combinations were evaluated by studying the extent of interdiffusion after holding one hour at 1700°C. Measurements of interdiffusion were made by microscopy, microhardness measurements, and electron micro-beam analysis. Based on these measurements, it was tentatively concluded that Hf was the most promising barrier for W, with Ir and V as alternate choices. Ir appeared to be the best choice for Ta and Mo. No recommendations were made for Cb because of melting of Cb-base combinations at 1700°C.

No correlation was found between interdiffusion behavior and the extent of solid solubility or the presence of intermediate phases in base-barrier systems. The extent of interdiffusion appeared to decrease as the melting points of barrier and base increased; however, there were several exceptions.

C. Selection of Potential Barrier Metals

Originally, 11 barrier metals with melting points above 1700°C were selected as potential barriers for each of the four base metals. The resulting 44 combinations are included in the first column of Table 1. Of these, the following were initially excluded because of extensive solid solubility: W-Cr[2], Ta-Re[3], Ta-V[4], Mo-Re[5], Mo-V[6], Mo-Pt[7], Cb-Re[8,9,10], Cb-Ru[11], Cb-Hf[12], Cb-V[13] and Cb-Zr[14]. However, the results of the first year's program indicated that the melting point of the barrier may be a more important factor than base-barrier solid solubility in affecting the extent

---

Manuscript released by authors May 1962 for publication as an ASD Technical Documentary Report.

Table I

Selection of Potential Base-Barrier Combinations

All Combinations Considered	Minimum Solidus Temperature °C	Previously Evaluated (Partially or Completely)	Selected for Further Evaluation
W-Re	2825[15]	W-Re	W-Re
W-Os	2725[16]		W-Os
W-Ta	see Ta-W		
W-Ru	2205[16]	W-Ru	W-Ru
W-Ir	2420[17]	W-Ir	W-Ir
W-Hf	1930[16]	W-Hf	W-Hf
W-Rh	1830[17]	W-Ru	W-Rh
W-V	1630[6]	W-V	W-V
W-Cr	1890[2]		W-Cr
W-Zr	1650[7]	W-Zr	
W-Pt	1769[13]	W-Pt	
W-Th	1475[13]	W-Th	
Mo-W	2625[13]		Mo-W
Mo-Re	2300[5]		Mo-Re
Mo-Os	2360[17]		Mo-Os
Mo-Ta	2625[13]		Mo-Ta
Mo-Ru	1945[18]	Mo-Ru	
Mo-Ir	N.A.	Mo-Ir	Mo-Ir
Mo-Hf	1915[7]	Mo-Hf	Mo-Hf
Mo-Rh	1930[19]	Mo-Rh	Mo-Rh
Mo-V	N.A.		Mo-V
Mo-Cr	1860[7]	Mo-Cr	Mo-Cr
Mo-Zr	1520[7]	Mo-Zr	
Mo-Pt	1769[7]		
Mo-Th	N.A.	Mo-Th	

Table 1 (Continued)

Selection of Potential Base-Barrier Combinations

All Combinations Considered	Minimum Solidus Temperature °C	Previously Evaluated (Partially or Completely)	Selected for Further Evaluation
Ta-W	(14)		Ta-W
Ta-Re	2690[3]		Ta-Re
Ta-Os	2360[16]		Ta-Os
Ta-Ru	1970[20]		Ta-Ru
Ta-Ir	2250[17]	Ta-Ir	Ta-Ir
Ta-Hf	2100[7]		Ta-Hf
Ta-Rh	1680[17]	Ta-Rh	
Ta-V	1830[4]		Ta-V
Ta-Cr	1700[7]	Ta-Cr	
Ta-Zr	1585[7]	Ta-Zr	Ta-Zr
Ta-Pt	N.A.	Ta-Pt	
Ta-Th	N.A.		
Cb-W	2460[14]		Cb-W
Cb-Re	2400[8,9,10]		Cb-Re
Cb-Os	N.A.		Cb-Os
Cb-Ta	2460[14]		Cb-Ta
Cb-Mo	2350[7]		Cb-Mo
Cb-Ru	N.A.		Cb-Ru
Cb-Ir	N.A.		Cb-Ir
Cb-Hf	N.A.		Cb-Hf
Cb-Rh	N.A.	Cb-Rh	
Cb-V	1810[13]		Cb-V
Cb-Cr	1660[21]		
Cb-Zr	1750[14]		Cb-Zr
Cb-Pt	N.A.	Cb-Pt	
Cb-Th	1435[13]	Cb-Th	

of interdiffusion. Consequently, the originally excluded combinations having high melting point barriers were included in the current program.

One group of potential barrier metals not originally considered are the major refractory base metals themselves, e.g., a W barrier on Ta, Mo, or Cb base metal. In spite of extensive solid solubility, these metals are considered as potential barriers because of their high melting points, and are also included in the first column of Table 1.

Some of the combinations originally considered have been excluded from the current program because of low melting points. Ta-Th, Mo-Pt, and Cb-Cr fall into this category.

The last column in Table 1 consists of the 35 combinations selected for evaluation on the current program. Twelve of these are combinations which were partially evaluated during the previous year, and for which the results were not conclusive. The remaining 23 combinations are new ones, not previously evaluated. They include the 11 combinations previously rejected because of extensive solid solubility, the 6 combinations involving W, Mo, and Ta as barriers, and 6 other combinations which were not previously evaluated because of experimental difficulties.

D. Scope of the Investigation

It was planned to evaluate the 35 potential combinations selected for study by determining the relative extents of interdiffusion after standard diffusion-annealing treatments. From the combinations evaluated, one, or possibly a few, optimum barrier metals were to be chosen for further study. This would involve such areas as: the effect of alloying of the base metal on base-barrier interdiffusion, interdiffusion in barrier-coating combinations, and quantitative interdiffusion studies. The diffusion barrier concept itself was to be evaluated by the investigation of interdiffusion in three-layer, base-barrier-coating systems.

II. EXPERIMENTAL PROCEDURE

A. Materials

The suppliers, forms and estimated purities of the metals used in the current program are listed in Table 2.

B. Preparation of Couples

Pressure welding was used to prepare most of the couples studied in the evaluation tests. Essentially, the technique was similar to that developed during the preceding program. The specimens were polished on both faces, cleaned, and placed inside a cylindrical Mo-0.5 Ti alloy clamp (Fig. 1). The chamber of the clamp was lined with Ta foil before the specimens were inserted. After the specimens were in place, the excess foil was folded over them. The threaded plugs were then tightened securely, thus exerting a compressive force on the diffusion couples.

The entire clamp was wrapped in Ta foil and the whole assembly was vacuum-annealed for one hour at a temperature in the range 750° to 1100°C. On cooling to room temperature, the plugs were re-tightened and the clamp wrapped in fresh Ta foil. The clamp-specimen assembly was then placed inside a mullite tube (Fig. 1), and the tube was flushed with argon for several hours. The clamp was then induction-heated to the diffusion-annealing temperature and held at plus or minus 10°C by means of an automatic on-off-type timer switch. The temperature was measured by means of a Pyrometer Instrument Co. Micro-Optical Pyrometer, sighted on the bottom of a deep hole. The ratio of length to diameter of the hole was high enough (more than 5 to 1) to ensure black-body conditions. The optical pyrometer was calibrated against a tungsten ribbon filament lamp with a quartz sighting window. The lamp was purchased from General Electric and calibrated by the National Bureau of Standards.

For the quantitative interdiffusion studies, the experimental procedures were essentially those previously described for the evaluation experiments. However, some changes were made in order to make the results more quantitatively reliable. All the materials used were first recrystallization-annealed for one hour at 1900°C in order to stabilize the grain structure. After assembly of the metal wafers into the Mo clamp, they were vacuum -annealed for one hour at 1100°C in order to align the wafers in the clamp and to achieve some preliminary degree of pressure welding. However, an experiment in which one series of diffusion couples was retightened after the 1100° treatment (the usual procedure) and an identical series was heated directly to the diffusion-annealing temperature of 1900° without retightening showed that the degree of welding during the prior 1100° treatment was not sufficient to hold the couples together during subsequent diffusion-annealing. Consequently, all other diffusion couples were pressure welded and diffusion-annealed simultaneously at 1900°C. The effect of the pressure applied by the difference in thermal expansion between the Mo clamp and the metals composing the diffusion couples on the measured rates is believed to be insignificant.

Table 2

Materials

Metal	As-Received Form	Supplier	Estimated Purity, %
W	0.030 in. strip	Fansteel Metallurgical	99.9
Re	0.020 in. strip	Chase Brass and Copper	99.98
Os	arc melted buttons	Engelhard Industries	99.8
Ta	0.030 in. strip	Fansteel Metallurgical	99.9
Mo	0.030 in. strip	Fansteel Metallurgical	99.9
Ru	arc melted button	Engelhard Industries	99.8
Ir	0.020 in. strip	Engelhard Industries	99.8
Cb	0.030 in. strip	Fansteel Metallurgical	99.8
Hf	crystal bar	Foote Mineral	97.7*
Rh	0.020 in. strip	Engelhard Industries	99.8
V	0.030 in. strip	A. D. Mackay	99.7
Cr	1/8 in. flake	Union Carbide	99.0**
Zr	0.035 in. strip	A. D. Mackay	99.8

*Remainder mostly Zr.

**Remainder mostly Fe, Zn, and Ni.

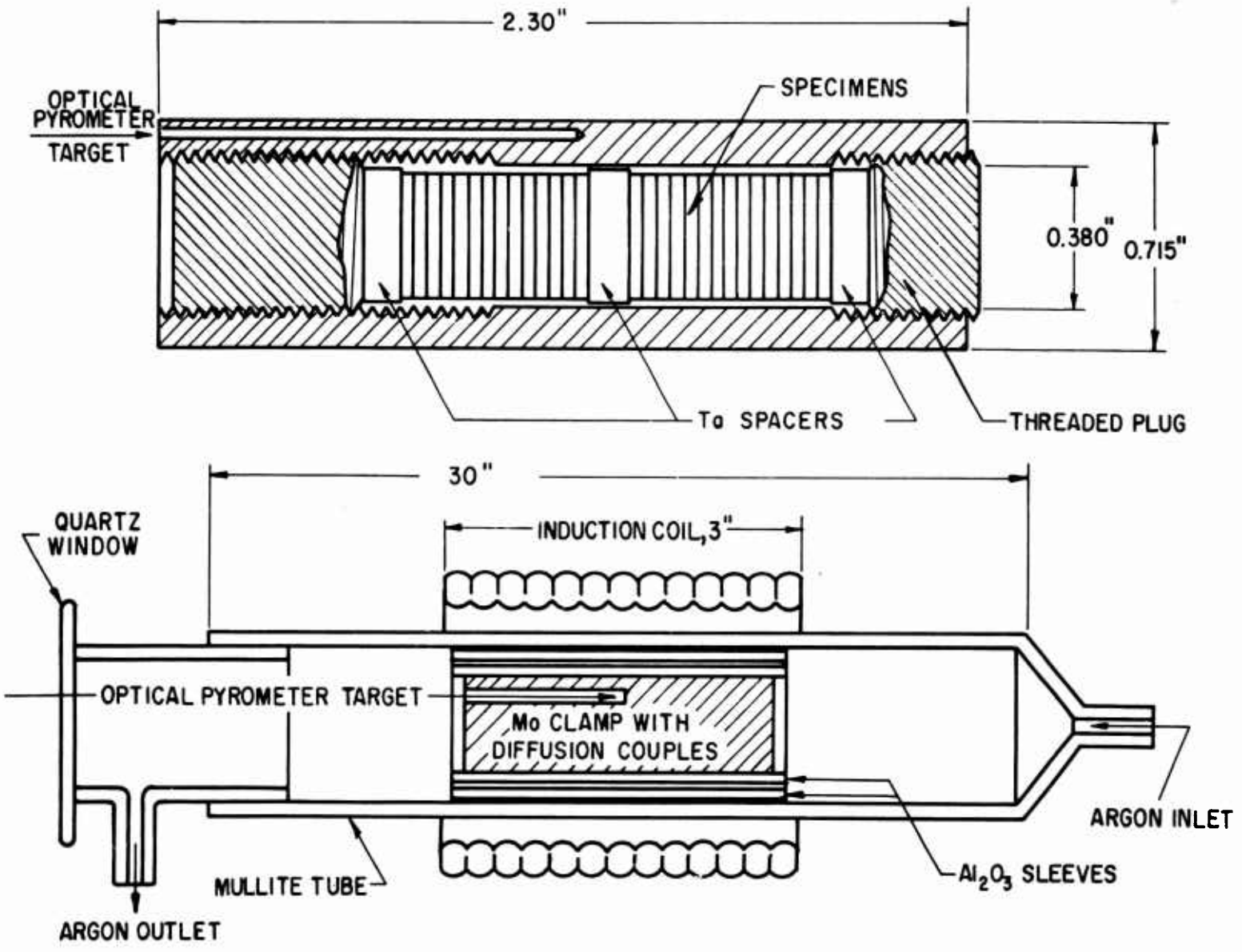

Fig. 1- Schematic diagram of molybdenum clamp (above) and assembled apparatus (below)

Because of the long annealing times, additional care was taken to minimize contamination. The argon used as a protective atmosphere was first passed through Drierite (anhydrous calcium sulfate) to remove water vapor and then over hot Ta foil to remove interstitial impurities from the gas before it reached the Mo clamp. The argon was allowed to flow through the mullite tube for several hours (usually overnight) before the annealing treatment in order to flush out all traces of air. A Ta foil wrapping around the diffusion couples inside the clamp was used (as in the evaluation tests) to remove any impurities that might remain.

C. Evaluation of Couples

As in the previous program, diffusion couples were evaluated by metallography and by microindentation (microhardness) measurements.

1. Metallography — Pressure welds were removed from the Mo clamp and then mounted in plastic. Epoxy resin was used initially, but a lucite mount with a harder layer of bakelite at the surface to be polished was found to be better. Specimens were then ground to a depth approximately 1/3 to 1/2 the specimen diameter on the surface normal to the diffusion interfaces and rough polished with 6-micron diamond dust on a silk lap. They were then polished with Linde B in 5% chromic acid on a soft wool (Forstmann Style No. 18019/1) lap at 400 rpm and finish polished with Linde B on Buehler Microcloth at 200 rpm. Etching solutions and procedures are presented in Table 3. Bright field illumination was generally used for microscopic examination. For couples involving Re polarized light also proved useful to a limited extent.

Intermediate phase layer widths were measured at a single point at the interface in most of the evaluation tests at 1700°C. In each couple a point was chosen where the layer showed the maximum uniform thickness. Layer widths measured in this way were reported to the nearest micron (e.g., 5, 6, or 7).

Average intermediate phase layer widths were reported to the nearest tenth-micron (e.g., 6.0, 6.1 or 6.2) for some of the tests at 1700° and all of those at 1800° and 1900°C. In these measurements, the section of the interface which showed the maximum uniform penetration in a particular couple was selected and an approximate estimate of its length ($B_{max.}$) was made. $B_{max.}$ was usually in the range of several hundred to several thousand microns. Then, an estimate of the uniformity and total width (w) of the phase layer was made in order to decide on the number of measurements (N) and their spacing (b). N and b were kept below the limit at which $B = (N - 1)b = B_{max.}$ Usually 20 measurements were made at a spacing (b) somewhat greater than the layer width ($b > w$). However, as many as 30 measurements were made if the layer was nonuniform and less than 10 microns wide, or as few as 10 measurements were made if the layer was quite uniform and more than 20 microns wide.

2. Microhardness Measurements — Previous measurements had been made by using a 25 gram load and a Vickers (diamond pyramid) indenter. The indentation diagonals were converted to hardness values, which were then plotted as a function of distance from the base-barrier interface.

Table 3

Etching Procedures for Diffusion Couples

Combinations	Etching Solution	Method of Application
Ta-W Mo-W Cb-W W-V Mo-V Mo-Ta Cb-Mo	10 g. $K_3Fe(CN)_6$, 10 g. KOH, 100 cc H_2O (Murakami's reagent)	immersion
Ta-V Cb-V Ta-Re Cb-Re Cb-Ta	30 cc lactic acid, 10 cc HNO_3, 1-10 cc HF	swabbing
W-Rh Mo-Rh	concentrated HCl, followed by immersion in Murakami's reagent	electrolytic, 6v, d-c carbon cathode
W-Re Mo-Re W-Cr Mo-Cr	10% oxalic acid	electrolytic, 6v, d-c carbon cathode
W-Os Mo-Os	10% HCl in ethyl alcohol, followed by immersion in Murakami's reagent	electrolytic, 10v, d-c carbon cathode
Ta-Os Cb-Os	10% HCl in ethyl alcohol, followed by swabbing with 30 cc lactic acid, 10 cc HNO_3, 5-10 cc HF	electrolytic,10v, d-c carbon cathode
W-Ru W-Ir	20% HCl in H_2O, saturated with NaCl, followed by immersion in Murakami's reagent	electrolytic, 10v, a-c carbon cathode
Ta-Ru Cb-Ru Ta-Ir Cb-Ir	20% HCl in H_2O, saturated with NaCl, followed by swabbing with 30 cc lactic acid, 10 cc HNO_3, 5-10 cc HF	electrolytic, 10v, a-c carbon cathode
W-Hf Ta-Hf Mo-Hf Cb-Hf Cb-Zr	30 cc lactic acid, 10 cc HNO_3, 0.1-0.5 cc HF	swabbing

In the current program, measurements were made by using a 100 gram load and a Knoop indenter. The indentations were carefully placed in parallel rows, with additional indentations made near the interface (Fig. 2) in order to resolve the rapid change in hardness with distance in this region. The length of the indentation was plotted as a function of distance from the interface in order to assess the extent of interdiffusion. In preparing specimens for testing, care was taken to ensure that disturbed (work-hardened) metal was removed from the surface and that no appreciable difference in level existed between the two metals across the interface. Such differences were encountered if the metals composing the diffusion couple differed substantially in hardness and resulted in fallacious hardness minima (indentation length maxima) at the interfaces.

Measurements were initially made using both the Vickers and Knoop diamonds on the same couples, so that results could be compared with those obtained on the previous program. Approximately equal values of extents of interdiffusion were found to result from the use of both techniques. However, it is believed that the long (narrow) Knoop indentation and heavier load employed gave better resolution of the diffusion zone than was obtained with the pyramidal-shaped Vickers indentation.

Hardness increments at the interfaces of the diffusion couples were calculated by determining the difference between the maximum hardness at the interface (or the hardness in the barrier metal, which ever was greater) and the minimum hardness in the base metal (outside the diffusion zone).

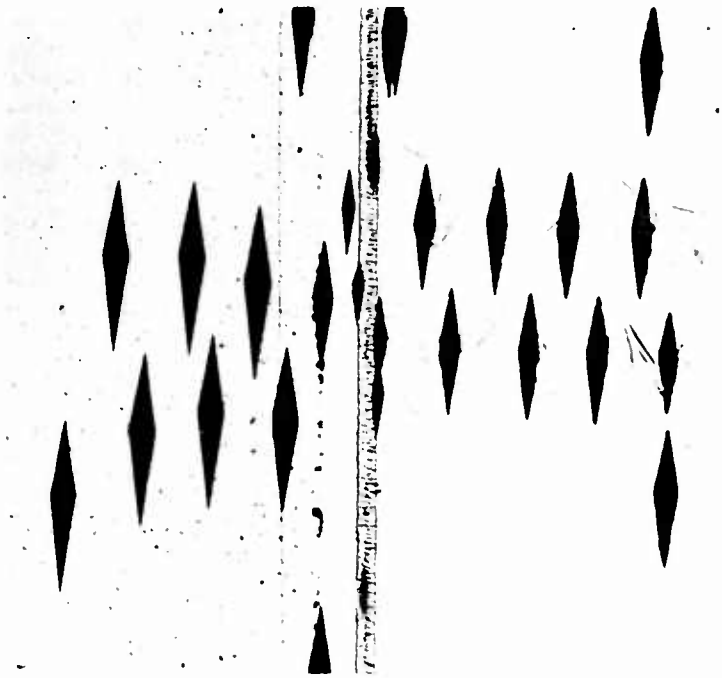

Fig. 2 - Arrangement of Knoop microhardness indentations in the diffusion zone of a Cb-Re couple, annealed 8.3 hours at 1900°C.

III. RESULTS AND DISCUSSION

A. Evaluation of Base-Barrier Combinations

1. Microstructures

Microstructures of the interdiffusion zones in typical diffusion couples are shown in Figs. 3 to 51. Intermediate phase layers at the interfaces were found in 19 of the 30 base-barrier combinations evaluated for interdiffusion during the current program. In most cases, only one intermediate phase was found at the interface; but in the W-Re, Ta-Os, Ta-Ir, Mo-Re, Mo-Ir, Cb-Os, and Cb-Ir combinations, more than one was found. The largest number, 3, were present in the Ta-Ir and Cb-Ir combinations. In most combinations, the number of phases found at the interface agrees with the published equilibrium phase diagram. However, in some cases, after the shorter annealing time of one hour (at 1700°C), fewer phases were found than predicted. This observation can be attributed either to slow nucleation or to a very low growth rate[22]. In no cases were more phases found than reported in the equilibrium diagram.

In a few combinations the solid solution regions in the interdiffusion zone could be clearly distinguished microscopically. In the W-Hf (Fig. 7), Mo-Hf (Fig. 18), Ta-Hf (Fig. 26), and Cb-Hf (Fig. 32) combinations, the extensive solid solution regions formed during diffusion-annealing were made evident by the two-phase structures resulting from eutectoid reactions during cooling.

As will be discussed further on, the relative extents of interdiffusion indicated by the widths of the solid solution regions were useful in evaluating some of those combinations where such regions were evident.

Porosity was formed in the interdiffusion zones of many of the combinations evaluated, especially in those exhibiting the most interaction. Such porosity is usually attributed to the precipitation of vacancies resulting from the unequal diffusion rates of the metals composing each diffusion couple. It occurs in that region of the couple which is losing atoms[23], i.e., the side of the interface occupied by the element which diffuses faster. Thus, in principle, the over-all direction of mass flow can be inferred from the presence and location of the porosity. The validity of this interpretation was confirmed by examination of several couples at low magnification. At the edges of the couples, it was observed that the intermediate phases formed on the side of the original interface opposite the band of porosity. From such observations, the predominant direction of flow was estimated in each combination and is listed in Table 4. This table also shows that in combinations where both elements interdiffuse at approximately equal rates, no porosity was formed, even though the over-all rate of interdiffusion was very fast, e.g., W-Cr (Fig. 9).

2. Relative Extents of Interdiffusion at 1700°C

Knoop indentation lengths are plotted against distance in a direction normal to the interface for diffusion couples annealed at 1700°C in Fig. 3 to 51.

Table 4

Summary of Evaluation Experiments on

Base-Barrier Combinations, Diffusion-Annealed 4 Hours

at 1700°C

Combination		Intermediate Phase Layer Thickness, Microns				Total Interdiffusion		Predominant Diffusion	Hardness Increment	Maximum Hardness
Base	Barrier	Base Side	Center	Barriers	Total	Zone, Microns	Porosity	Direction	KHN	KHN
W	Re	4	-	2	6	~ 50	none	equal	230	750
W	Os	-	-	-	6	≤ 50	some	into W	215	700
W	Ru	-	-	-	2	≤ 50	some	into W	100	570
W	Ir	-	-	-	3	~ 50	some	into W	380	890
W	Hf	-	-	-	5	365	none	into W	410	810
W	Rh	-	-	-	18.2	~ 50	some	into W	230	670
W	V	-	-	-	0	≤ 50	some	into W	175	645
W	Cr	-	-	-	0	170	none	equal	465	935
W	Pt*	-	-	-	8*	110-200*	none*	equal*	500*	950**
(from ref. (1))										
Ta	Re	-	-	-	3	≤ 50	none	into Re	195	470
Ta	Os	7	-	3	10	30	none	equal	600	890
Ta	Ru	-	-	-	20	45	none	into Ta	920	1050
Ta	Ir	4	10	12	26	40	none	into Ta	990	1350
Ta	Hf	-	-	-	0	630	none	into Ta	410	470
Ta	V*	-	-	-	0	125*	equal*	into Ta	415*	595*
Mo	W	-	-	-	0	≤ 50	some	equal	265	470
Mo	Re	6	-	3	9	60	none	into Re	960	1162
Mo(0.5Ti)	Re	4	-	3	7	≤ 50	none	into Re	280	490
Mo	Os*	-	-	-	10*	≤100*	none*	into Mo*	620*	850*
Mo	Ta	-	-	-	0	≤ 50	none	uncertain	120	340

* One-hour annealing treatment

** VHN, approximately equal to KHN.

Table 4 (Continued)

Summary of Evaluation Experiments on

Base-Barrier Combinations, Diffusion-Annealed 4 Hours

at 1700°C

Combination		Intermediate Phase Layer Thickness, Microns				Total Interdiffusion		Predominant Diffusion	Hardness Increment	Maximum Hardness
Base	Barrier	Base Side	Center	Barriers	Total	Zone, Microns	Porosity	Direction	KHN	KHN
Mo	Ir	4.5	-	15	19.5	90	some	into Ir	770	985
Mo	Hf	-	-	-	10	630	some	into Mo	470	680
Mo	Rh	-	-	-	17	115	some	into Mo	880	1100
Mo	V	-	-	-	0	≤ 50	some	into Mo	115	340
Mo	Cr*	-	-	-	0	190, 270*	some*	into Mo*	290, 425*	515, 645
Cb	W	-	-	-	-	≤ 50	none	uncertain	130	380
Cb	Re	-	-	-	5, 6	≤ 50	none	into Re	715, 745	890, 985
Cb/27 Ta /IZr (FS82)	Re	-	-	-	6	≤ 50	none	into Re	880	1040
Cb/14W/ 5Mo/IZr (F48)	Re	-	-	-	4	≤ 50	none	into Re	725	1015
Cb/10Ti/ 10 Mo (D31)	Re	-	-	-	6	≤ 50	little	into Re	725	1015
Cb	Os	2	-	8	10	≤ 50	some	into Cb	505*	705*
Cb	Mo	-	-	-	-	≤ 50	none	equal	70	275
Cb	Ta	-	-	-	-	≤ 50	little	into Ta	105	370
Cb	Ir	13	10	12	35	≤ 50	none	into Cb	720	985
Cb	Hf	-	-	-	-	630	none	into Cb	450	510
Cb	Zr	-	-	-	-	≤ 50	none	into Cb	205	285

* One-hour annealing treatment

Plots are shown for an annealing time of four hours in most cases, although data are also presented for Mo-Re and Mo-Ir couples after one-hour anneals. The Mo-Cr couple was annealed for one hour only.

The characteristic shape of the curves consisted of relatively constant indentation lengths in both the base and the barrier metals outside the interdiffusion zone, in which there was usually a sharp minimum in the length. In combinations with this type of length vs distance curve, it was possible to estimate the approximate extent of interdiffusion by determining the distance between the points at which the indentation length reached constant values in the base and in the barrier respectively.

In some combinations, e.g., Mo-W (Fig. 11), Mo-V (Fig. 21), Ta-Os (Fig. 23) and Cb-Zr (Fig. 33), no minimum in indentation length occurred; but it was still possible to estimate the extent of interdiffusion because of a large difference in hardness between the base and the barrier. In all these combinations, the extents of interdiffusion so determined are listed in Table 4.

In most cases, the extent of interdiffusion estimated from the microindentation tests was larger than that evident from the microstructural effects observed. However, as discussed before, extensive solid solution regions were observed in the W-Hf, Mo-Hf, Ta-Hf, and Cb-Hf combinations. In these combinations, the extent of interdiffusion listed in Table 4 was based on microindentation tests of the base metal side and on the microstructure of the Hf side of each couple. This procedure gave a higher value than using microhardness or microstructural determinations alone. Results shown in Table 4 for the Ta-Ru (Fig. 24) and Mo-Os (not illustrated) combinations may be open to question because of cracks which apparently occurred at the interfaces after the diffusion-annealing treatments.

As shown in Table 4, a wide range in the extent of interdiffusion due to annealing at 1700°C occurred between the base-barrier combinations involving Cr and Hf barrier metals and those involving W, Re, V, and some of the higher melting point noble metals (Os, Ru, Ir, and Rh). In a later section, the interpretation of these interdiffusion measurements is covered from the standpoint of selecting promising combinations for further study.

Values of hardness increments at the interface and of maximum hardness (found at the interface) are also given in Table 4. These parameters offer some indication of the presence of hard (and presumably brittle) regions at the interface. Brittle phases would be expected to inhibit good bonding of the barrier to the base and lead to early failure of the coating system. Since many of base-barrier combinations showing the least interdiffusion contain intermediate phases along with both high interfacial hardness and hardness increment, it appears likely that the occurrence of brittle constituents is to a large degree unavoidable in protective coating systems.

3. Selection of Promising Combinations for Further Study

Using such arbitrary criteria as 60 microns maximum extent of interdiffusion for an anneal of four hours at 1700°C, 30 microns for an anneal of

one hour at 1700°C, and minimum base-barrier alloy melting points of 1900° for W-base and 1850° for Ta-base combinations, 20 of the 33 combinations evaluated were chosen as promising. The melting point criteria for W-base and Ta-base combinations were chosen in view of the anticipated application temperatures. An implied melting point criterion of 1700°C for Mo-base and Cb-base combinations is evident.

In order of decreasing barrier melting points, the 20 combinations are:

-	Mo-W	Ta-W	Cb-W
W-Re	Mo-Re	Ta-Re	Cb-Re
W-Os	-	Ta-Os	Cb-Os
-	Mo-Ta	-	Cb-Ta
-	-	-	Cb-Mo
W-Ru	-	Ta-Ru	-
W-Ir	-	Ta-Ir	Cb-Ir
-	Mo-V	-	-
-	-	-	Cb-Zr

4. Effect of Alloying of the Base Metal on Mo-Re and Cb-Re Base-Barrier Interdiffusion

As a typical promising barrier metal, Re was chosen for interdiffusion studies using the following alloy base metals:

Alloy Designation	Composition
Mo + 0.5 Ti	Mo + 0.5 Ti
F48	Cb + 14W + 5 Mo + 1Zr
FS82	Cb + 27Ta + 0.8Zr
D31	Cb + 10Ti + 10Mo

Results of evaluation experiments after subjecting these alloy base metals to a diffusion-annealing treatment of four hours at 1700°C are summarized in Table 4 and illustrated in Figs. 35 to 37. Comparison of the extent of interdiffusion in the Mo + 0.5 Ti alloy - Re couple with that in the Mo-Re one after the same diffusion-annealing treatment indicates that the alloying may have decreased the interdiffusion somewhat. However, the limited amount of interdiffusion in both couples and the fact that they were prepared in different pressure welds do not permit an accurate comparison. The interdiffusion behaviors of the three Cb alloy - Re combinations are not significantly different from that of Cb-Re, as shown in Table 4. The extents of interdiffusion in all four combinations are 50 microns or less.

5. Relative Extents of Interdiffusion in Promising W- and Ta-Base Combinations at Higher Diffusion-Annealing Temperatures

Interdiffusion in some of the promising W-base and Ta-base combinations subjected to a diffusion-anneal of three hours at 1800°C is illustrated in

Figs. 38 to 45 and summarized in Table 5. As observed for the same combinations after annealing at 1700°C, intermediate phases were found at all the interfaces except that of the Ta-W combination. W-Re (Fig. 38) and W-Ir (Fig. 41) have two phases each, whereas Ta-Ir (Fig. 45) has three. The others (W-Os, W-Ru, W-Rh, and Ta-Re) each have one intermediate phase, in agreement with the published phase diagrams. The widths of the intermediate phase layers are approximately the same after an annealing treatment of three hours at 1800°C as were found after four hours at 1700°. This indicates that the two time-temperature combinations are sufficiently equivalent to apply the same criterion regarding the maximum tolerable extent of interdiffusion (60 microns) to both the 1700° and 1800°C tests.

Porosity was found on the barrier sides of the interdiffusion zones in the W-Os, W-Ru, W-Ir, W-Rh, and Ta-Ir couples, indicating that diffusion occurs at an appreciably faster rate from the barrier into the base than in the opposite direction. In the Ta-W and Ta-Re combinations, porosity was found on the base side of the interdiffusion zone, indicating more rapid diffusion of the base into the barrier. W-Re is the only combination annealed at 1800°C in which no porosity formed, thus indicating approximately equal diffusion rates for the base and the barrier. As shown by comparison of Table 5 with Table 4, the observations of porosity described above for the 1800° anneal are in agreement with those made on combinations annealed at 1700°C.

Because of increased facility in using the microindentation technique by the time the diffusion-couples annealed at 1800° were evaluated, the actual measured extents of interdiffusion are listed in Table 5, even though all of them with the exception of W-Rh, are below 50 microns, which was considered the lower limit of reliability for most of the previous tests (at 1700°C). All the combinations evaluated at 1800°C satisfy the criterion of 60 microns maximum extent of interdiffusion, which they also did at 1700°C. The extents of interdiffusion increase in the order W-Os, W-Re, W-Ir, W-Ru, and W-Rh for W-base combinations, and in the order Ta-W, Ta-Re, and Ta-Ru for the Ta-base combinations. For both Ta and W base metals, the extent of interdiffusion appears to increase roughly in the order of decreasing barrier melting point.

6. Correlation between Interdiffusion and Base-Barrier Phase Relations

For most of the combinations evaluated at a diffusion-annealing temperature of 1700°C, as summarized in Table 4, qualitative relationships exist between the interdiffusion behavior and the binary phase relations. There is a tendency for the extent of interdiffusion to decrease with increasing melting point of either the barrier metal or the solidus temperature of the alloy composition having the lowest melting point (e.g., a eutectic temperature). The correlation appears to be better with the alloy solidus temperature than with the barrier melting point. All the combinations with solidus temperatures above 2100°C exhibit relatively little interdiffusion, 60 microns or less. For combinations with solidus temperatures up to 2100°C, however, the interdiffusion varies from 50 microns or less for the W-V, Mo-V, and Ta-Ru combinations to 630

Table 5

Summary of Evaluation Experiments on W and Ta-Base Combinations, Diffusion-Annealed Three Hours at 1800°C

Combination		Annealing Temperature, °C	Intermediate Phase Layer Thickness, microns				Total Interdiffusion Zone, microns	Porosity	Predominant Diffusion Direction	Hardness Increment, KHN	Maximum Hardness, KHN
Base	Barrier		Base Side	Center	Barrier	Total					
W	Re	1800	4.1	-	2.1	6.2	≤ 20	none	equal	0	
W	Os	1800	-	-	-	6.1	10	some	into W	790	1230
W	Ru	1800	-	-	-	2.5	40	some	into W	350	810
W	Ir	1800	-	-	-	3.2	30	some	into W	190	645
W	Rh	1800	-	-	-	23.5	60	some	into W	265	735
Ta	W	1800	-	-	-	-	20	some	into W	450	770
Ta	Re	1800	-	-	-	4.0	15	little	into Re	265	305
Ta	Ir	1800	11.9	5.5	10.8	28.2	40	some	into Ta	1175	1480

microns for both the Mo-Hf and Ta-Hf combinations, annealed for four hours. The wide variation does not appear to be related to any obvious characteristic of the alloy systems, such as melting point, solid solubilities, or intermediate phases. Even within the restricted groups of combinations containing Hf, Cr, or V, no systematic relationships were found.

For combinations exhibiting restricted interdiffusion, the limited resolution of the microindentation technique initially made it difficult to compare the relative extents of interdiffusion in couples if they were 50 microns or less. As work progressed, however, more competence with the microindentation technique was gained. Partly as a result, a quantitative relationship between interdiffusion and melting point became evident for a restricted group of promising combinations, as described below.

The extent of interdiffusion is plotted against the minimum alloy solidus temperature in Fig. 52 for several combinations for which the microindentation data is considered reliable. The extent of interdiffusion after annealing for three hours at 1800°C appears to decrease progressively with increasing temperature for combinations between W and such Pt-group metals as, Rh, Ru, Ir, and Os. As shown in Fig. 52, several other combinations appear to follow similar relationships although the data are not as complete. Data were plotted for Ta-Ru and Ta-Os after diffusion-annealing for four hours at 1700°C, since they were not available for three hours at 1800°. Within a reasonable experimental scatter, the Ta-Ru, Ta-Ir, and Ta-Os combinations appear to follow the same curve as the W-base combinations.

7. Interdiffusion in Barrier-Coating Combinations

In addition to the selection of Re for study of interdiffusion with alloy base metals, both Re and Ir barrier metals were chosen for interdiffusion studies with the oxidation resistant metal, Cr. Interdiffusion measurements of combinations of Cr with other promising barrier metals, such as W, Ta, and Mo, were already available from previous base-barrier studies. The results of interdiffusion measurements on Re-Cr and Ir-Cr couples annealed for one hour at 1700°C are illustrated in Figs. 46 and 47 and summarized in Table 6. The total interdiffusion zones varied from a minimum of 105 microns (Re-Cr) to over 360 microns (Ta-Cr). Thus, the extents of interdiffusion between the base metals Ta, Mo, W, and the Cr coating metal are higher than those between the best barrier, Re, and the Cr coating.

Consideration should be given to the effect of the barrier metal on the oxidation properties of the coating, as well as on the total extent of interdiffusion. Of the 5 barrier metals for which interdiffusion data with Cr are available, only Ir exhibits resistance to oxidation[24]. Consequently, much more interdiffusion between Ir and Cr could be tolerated than between Cr and any of the other 4 barrier metals. On the other hand, although Re possesses poor oxidation resistance at high temperatures[24], it nevertheless exhibits the least extent of interdiffusion with Cr. Thus, Ir and Re can be tentatively selected as the most promising of the 5 barrier metals screened for interactions with Cr.

Interdiffusion was also studied in combinations of the oxidation-resistant metal Rh with Re and Ir barrier metals. Since W was also selected as a promising barrier metal for the base metals Mo, Ta, and Cb, W-Rh was considered as a barrier-coating combination.

Table 6 shows that interdiffusion in the barrier-coating combinations increases in the order Ir-Rh, W-Rh, Re-Rh. Fig. 48 shows that a substantial amount of porosity formed in the Re-Rh combination. The relatively poor characteristics of the Re-Rh barrier-coating combination tends to offset the good performance of the W-Re base-barrier combination in comparing the potential effectiveness of Re with Ir as a barrier metal for W. However, the use of a duplex barrier layer of Re and Ir may offer a chance of combining the advantages of both barrier metals for a specific application.

8. Interdiffusion in Three-Layer, Mo-Barrier-Cr Combinations

Results of interdiffusion measurements carried out on three-layer couples after annealing for one hour at 1700°C are illustrated in Figs. 50 and 51 and summarized in Table 6. Diffusion barriers consisting of 38 micron thick wafers of either Ir or Re were used in each case, sandwiched between thick wafers of Mo and Cr. In the same clamp, a 2-layer Mo-Cr couple (Fig. 20) was also annealed for purposes of comparison. In each case, the over-all extent of interdiffusion was measured from the Mo to the Cr, through the barrier layer.

Despite the additional distance introduced by the presence of the unconsumed barrier layer (about 25 microns), the over-all interdiffusion was reduced from 190 to 145 microns by the presence of the Re barrier, a reduction of about 25%. If the Re is considered as an integral part of the base, the extent of base-coating interdiffusion (between the Re and the Cr) is 105 microns, which constitutes a reduction of 45% from that in the Mo-Cr couple.

In the case of the Mo-Ir-Cr combination, the total extent of interdiffusion from the Mo to the Cr (through the Ir barrier) is about the same as that in the Mo-Cr combination, principally because of extensive interdiffusion between the Ir and the Cr. If the viewpoint is adopted that the Ir is an integral part of the coating, the three-layer couple can be considered equivalent to a two-layer couple consisting of a Mo base and a duplex coating (Ir + Cr). On this basis, the extent of interdiffusion may be considered as that between the Mo and the Ir. Since this interdiffusion zone was measured as 50 microns after 1 hour at 1700°C, the presence of the Ir interdiffusion barrier resulted in a reduction of about 75% compared to the Mo-Cr combination.

Thus, depending on the viewpoint adopted in estimating the extent of interdiffusion, the presence of a Re barrier layer results in a reduction of 25 to 45% in the extent of interdiffusion between Mo and Cr, whereas an Ir barrier layer results in a reduction of 0 to 75%.

9. Selection of Optimum Barrier Metals

In order to distinguish the relative merits of the 20 promising combinations more closely, the following factors were considered:

Table 6

Summary of Interdiffusion Measurements in Combinations of Promising Barriers and Oxidation Resistant Metals

Combination	Annealing Temperature, °C	Time, Hrs.	Intermediate Phase Layer Thickness microns			Total Interdiffusion Zone, microns	Porosity	Predominant Diffusion Direction	Hardness Increment, KHN	Maximum Hardness, KHN
			Barrier (or Base) Side	Coating Side	Total					
W-Cr	1700	1	-	-	0	170	none	equal	465	935
Re-Cr	1700	1	-	-	8	105	none	equal	730	1040
Mo-Cr	1700	1	-	-	0	190, 270	none	into Mo	290, 430	290, 515
Ir-Cr	1700	1	12	8	20	185	none	into Cr	645	1040
Mo-Re-Cr	1700	1	-	-	-	145	none	into Mo	510	705
Mo-Ir-Cr	1700	1	-	-	-	215	some	into Mo	655	890
W-Rh	1800	3	-	-	18.2	$\leq$ 50	some	into W	230	670
Re-Rh	1800	3	-	-	20	115	much	into Re	350	550
Mo-Rh	1700	4	-	-	17	115	some	into Mo	880	1100
Ir-Rh	1800	3	-	-	0	30	some	into Ir	105	340

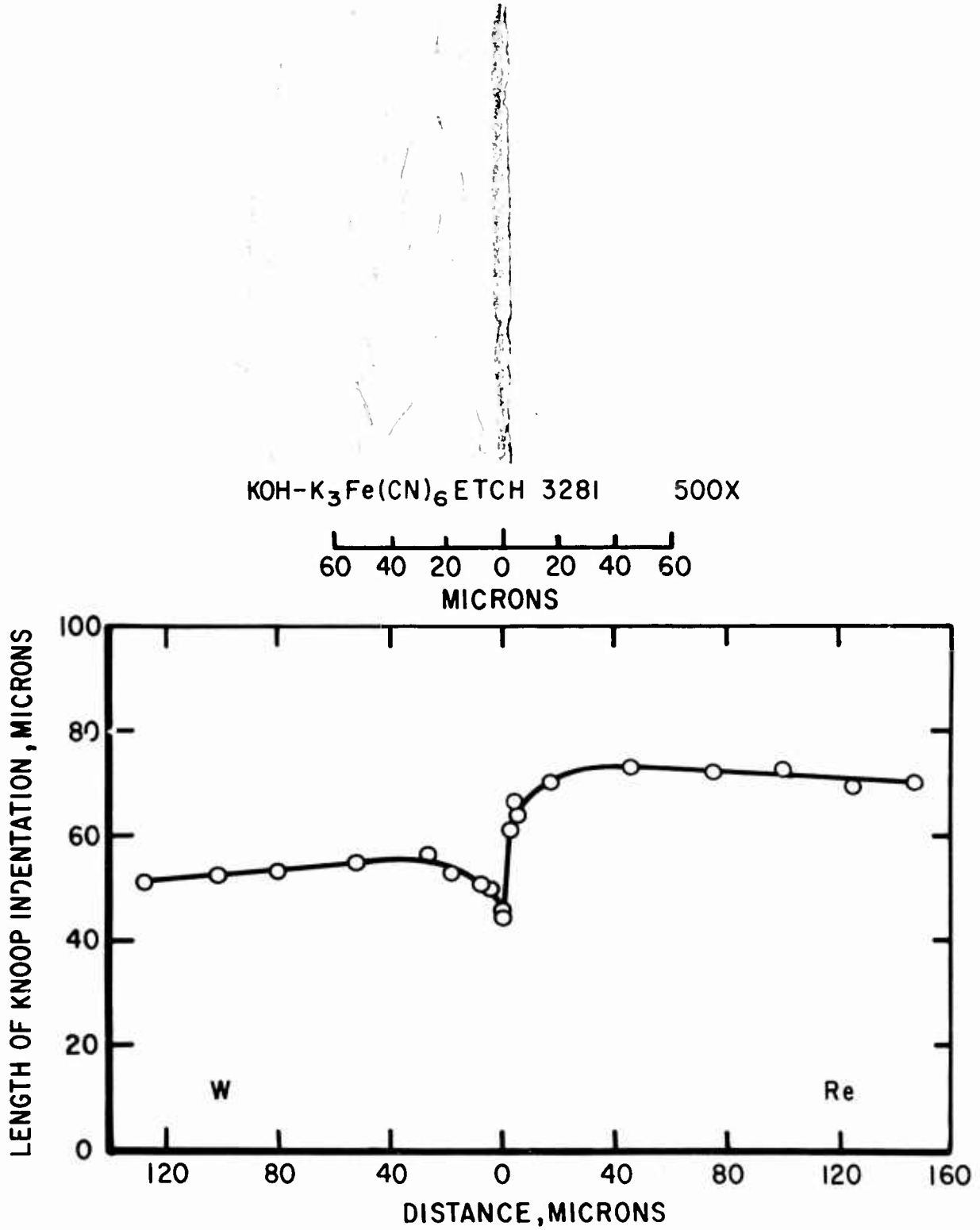

Fig.3 - W - Re, pressure weld no. 4a-4; microstructure and microindentation measurements of interdiffusion after annealing 4 hours at 1700°C.

KOH-$K_3Fe(CN)_6$ ETCH 3282 500X

60 40 20 0 20 40 60
MICRONS

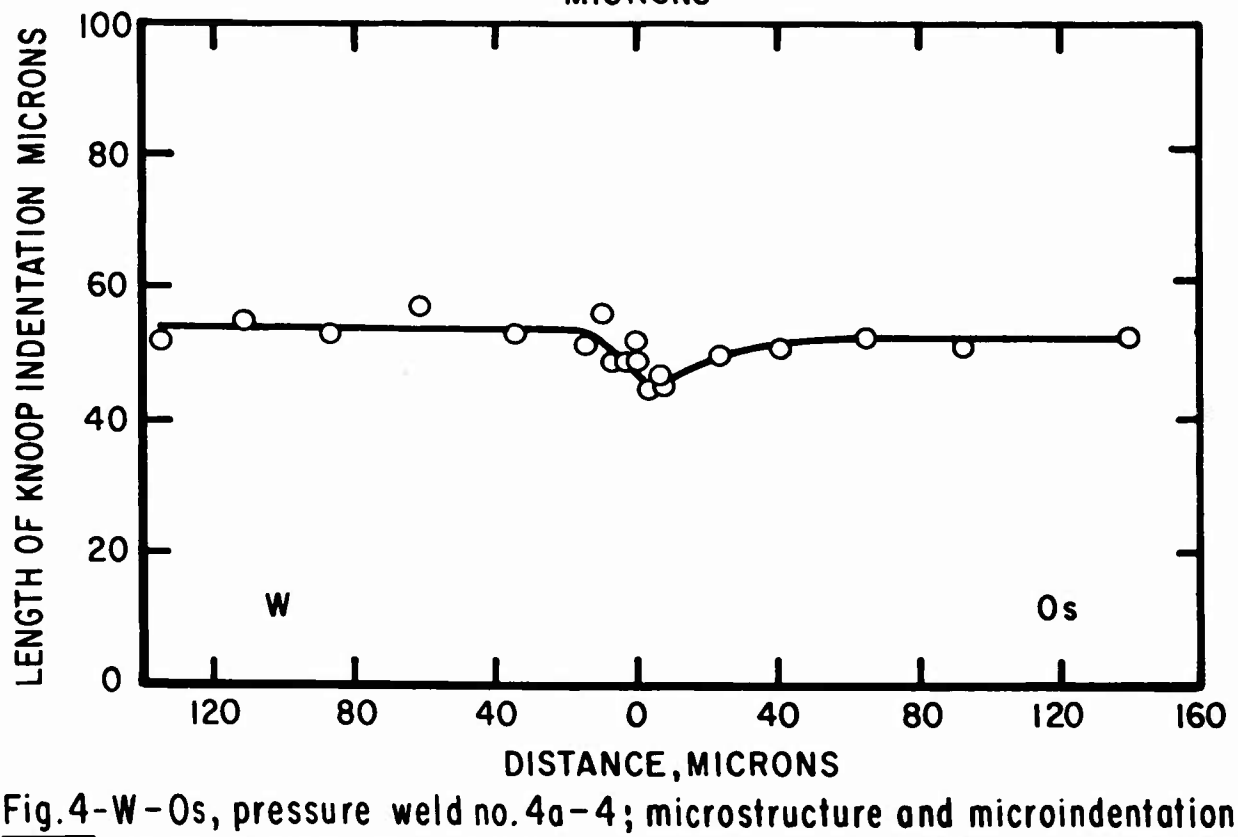

Fig. 4-W-Os, pressure weld no. 4a-4; microstructure and microindentation measurements of interdiffusion after annealing 4 hours at 1700°C.

KOH, $K_3FE(CN)_6$ ETCH 3592 500X

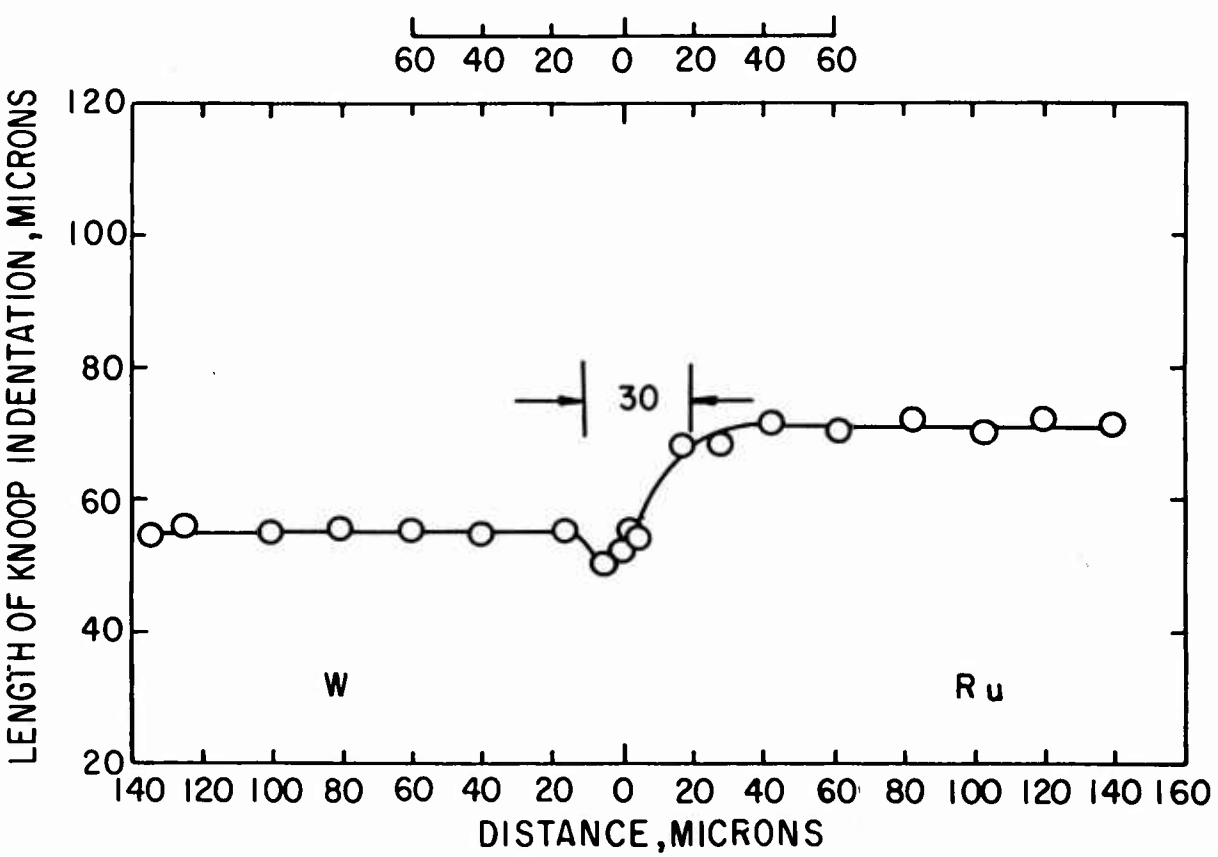

Fig.5-W-Ru, pressure weld no.6a, annealed 4 hours at 1700 °C

$KOH-K_3Fe(CN)_6$ ETCH 3290 500X

60 40 20 0 20 40 60
MICRONS

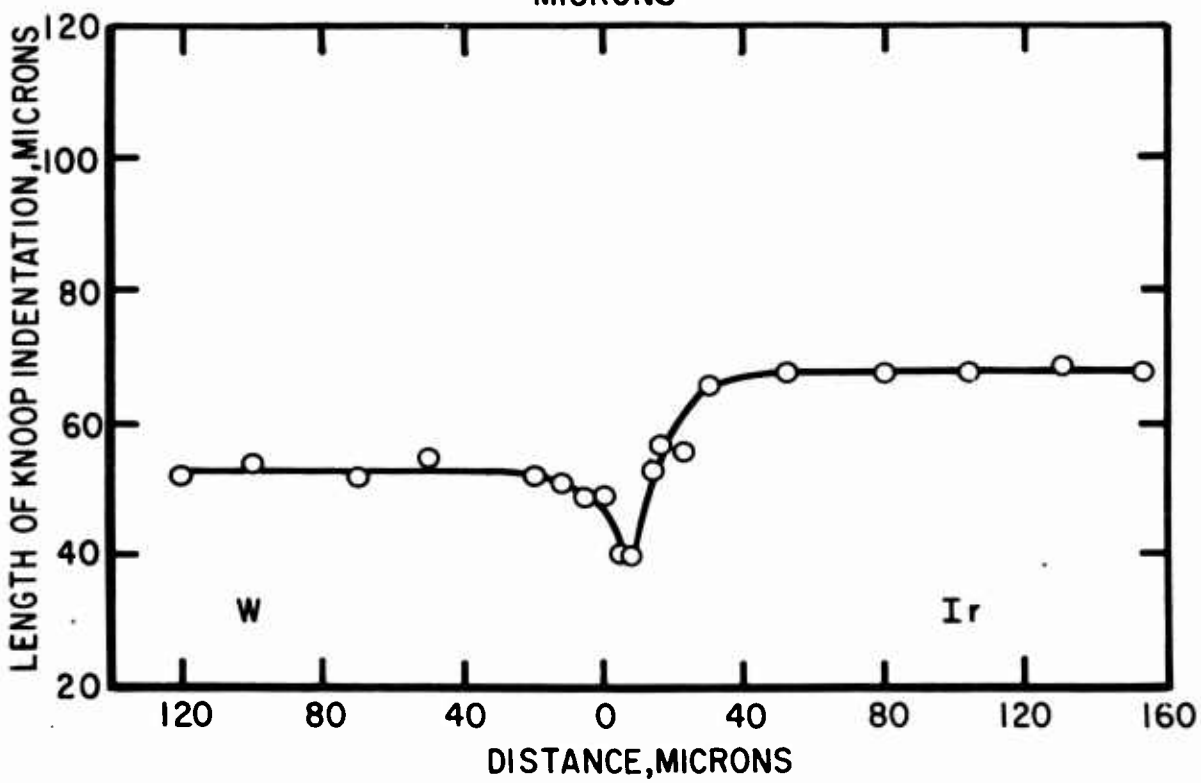

Fig.6 - W - Ir, pressure weld no. 3-4 ; microstructure and microindentation measurements of interdiffusion after annealing 4 hours at 1700° C.

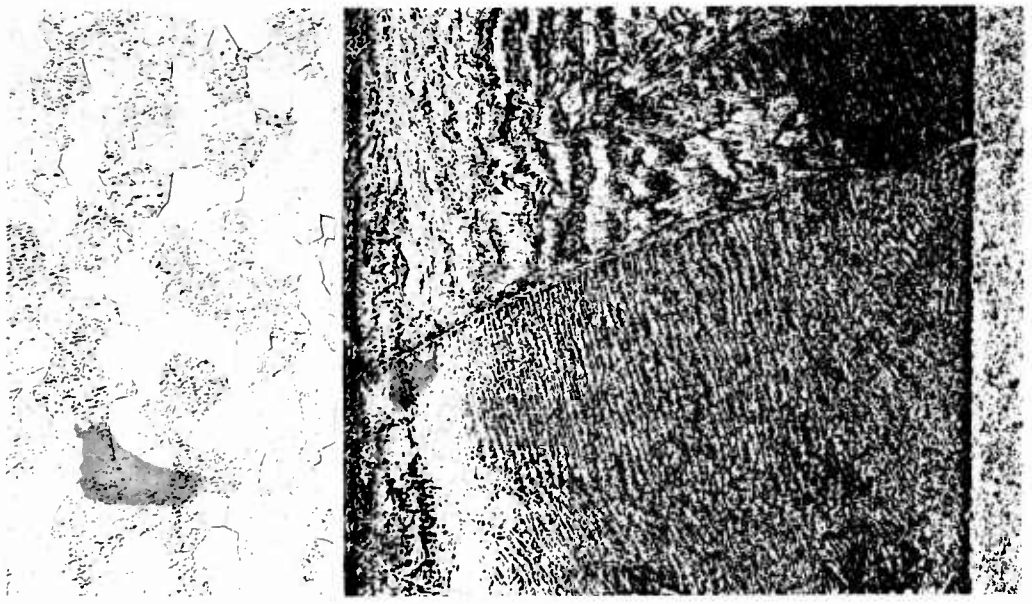

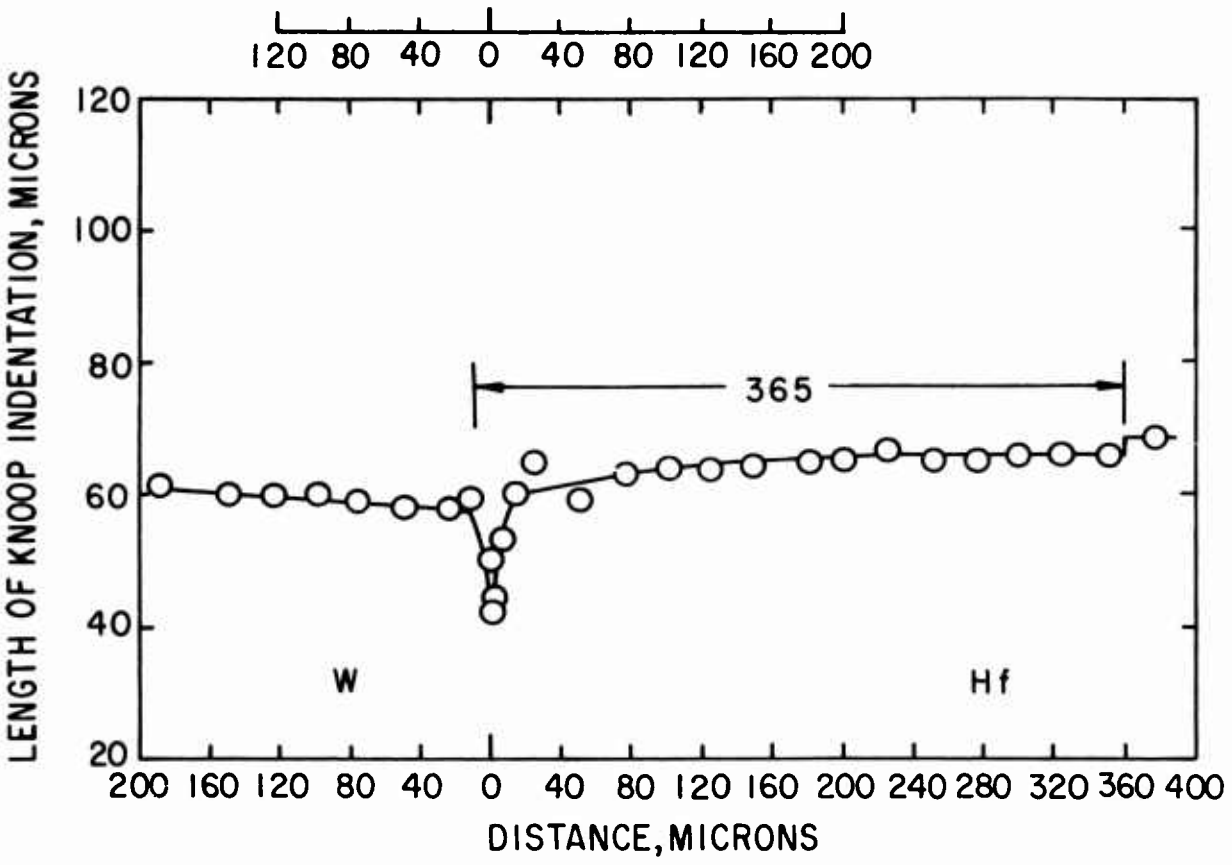

Fig.7- W-Hf, pressure weld no. 6a, annealed 4 hours at 1700 °C

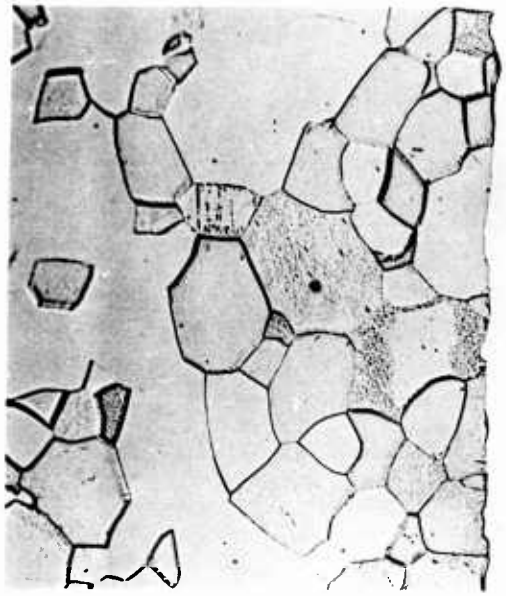

KOH, $K_3Fe(CN)_6$ ETCH 3819 500 X

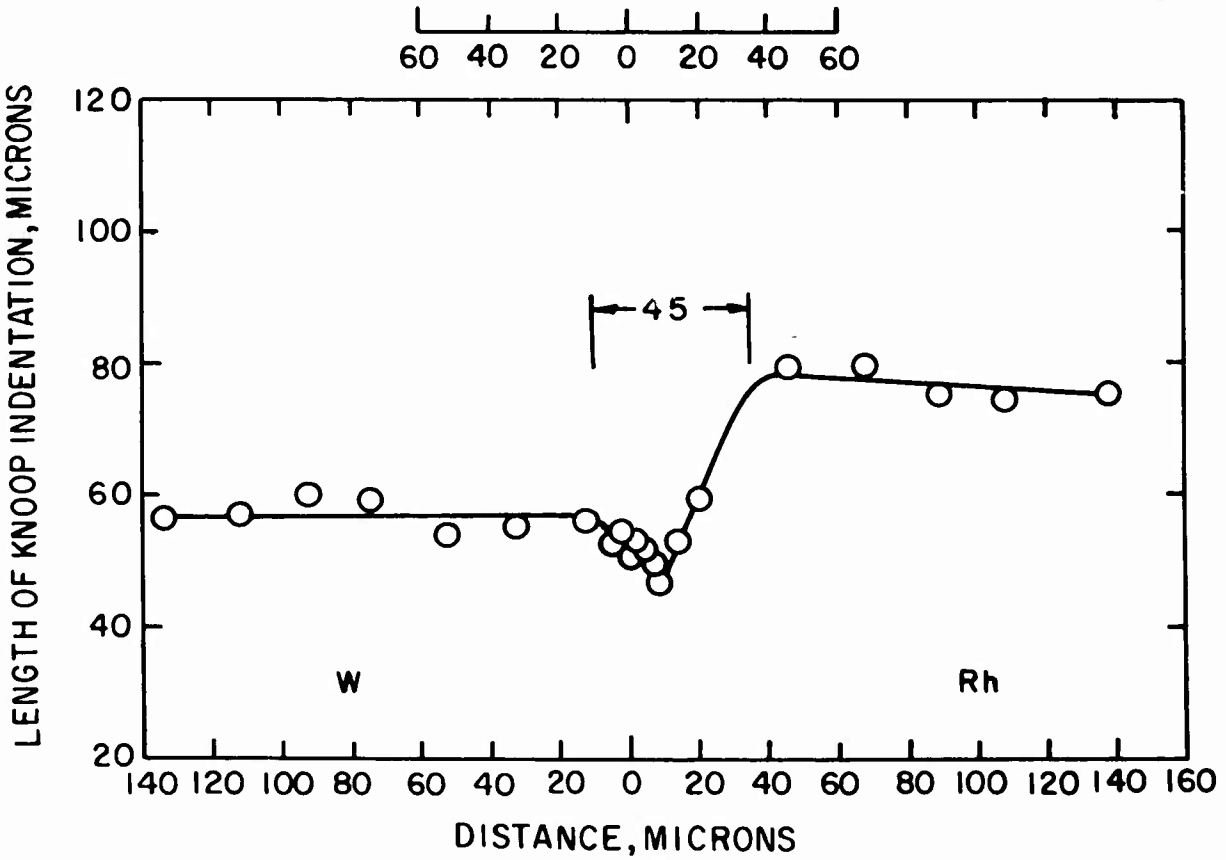

Fig. 8- W-Rh, pressure weld no. 6a, annealed 4 hours at 1700 °C

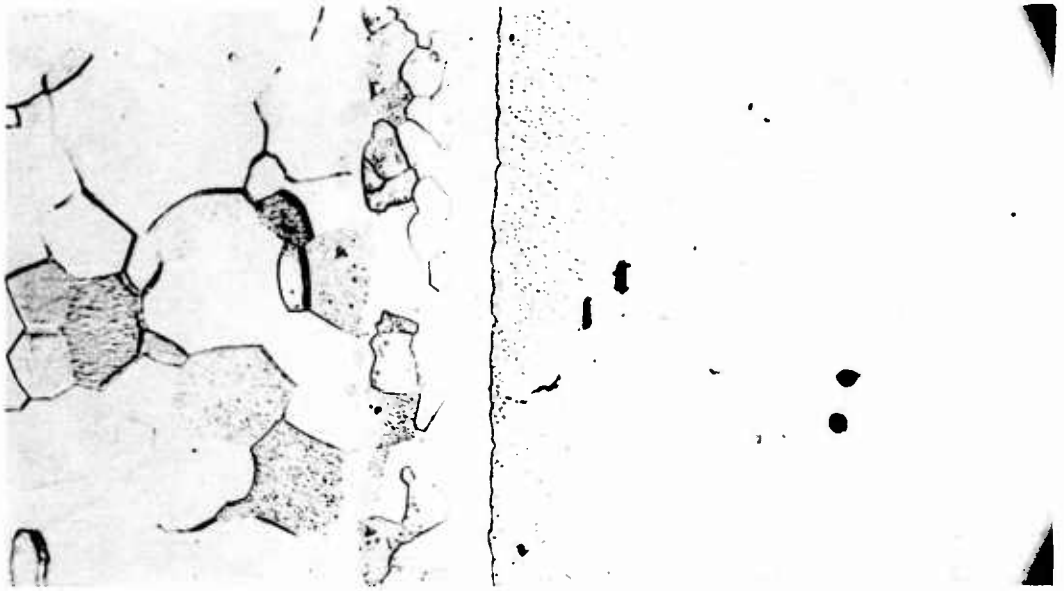

OXALIC ACID ETCH 3605 500X

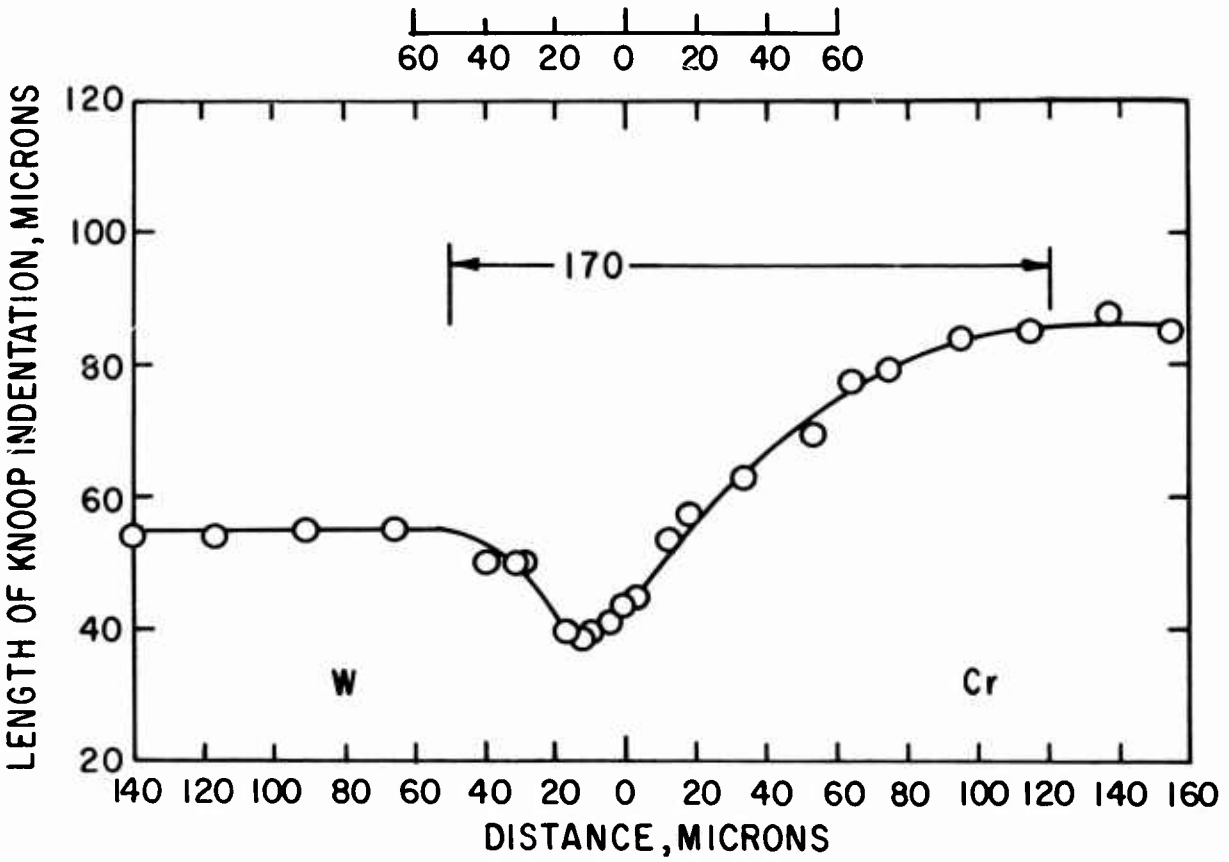

Fig.9- W - Cr, pressure weld no.6a, annealed 4 hours at 1700°C.

KOH, $K_3FE(CN)_6$ ETCH 3591 500 X

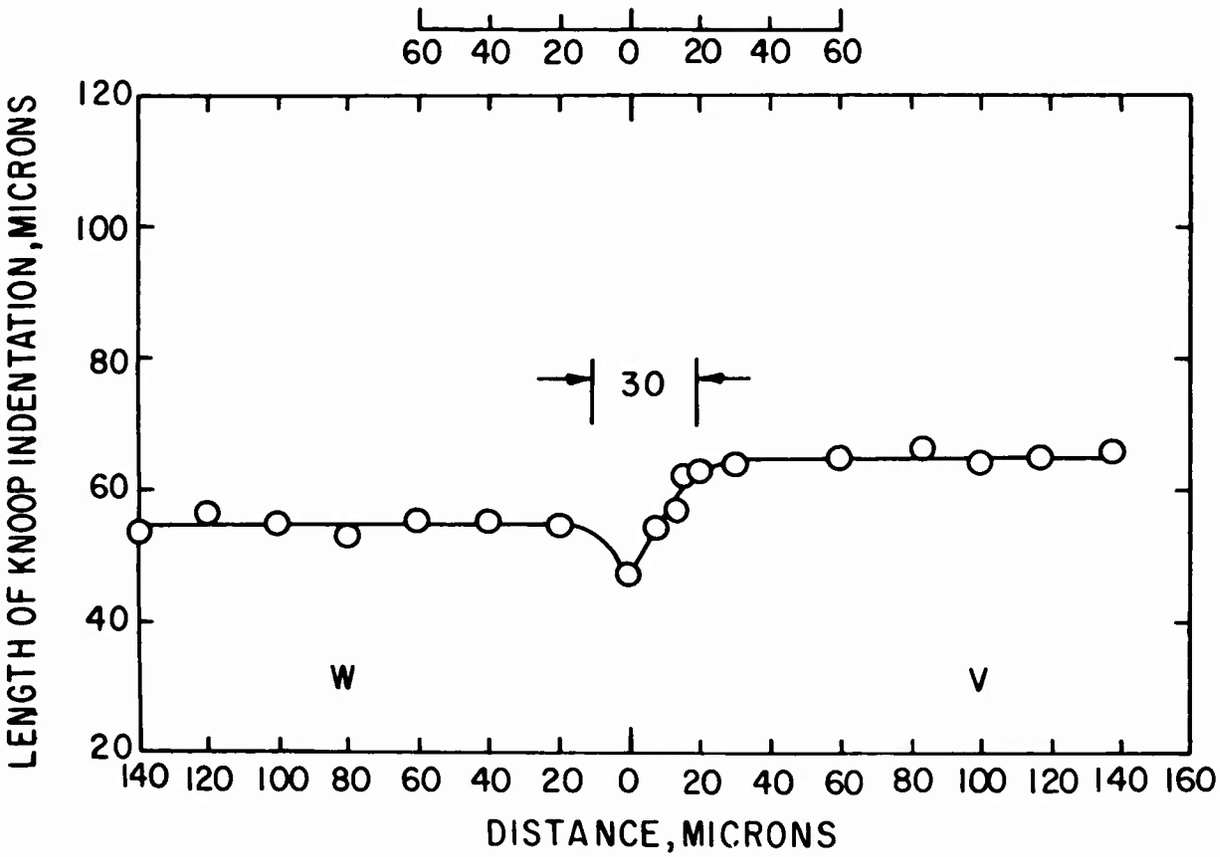

Fig.10- W – V, pressure weld no. 6a, annealed 4 hours at 1700 °C

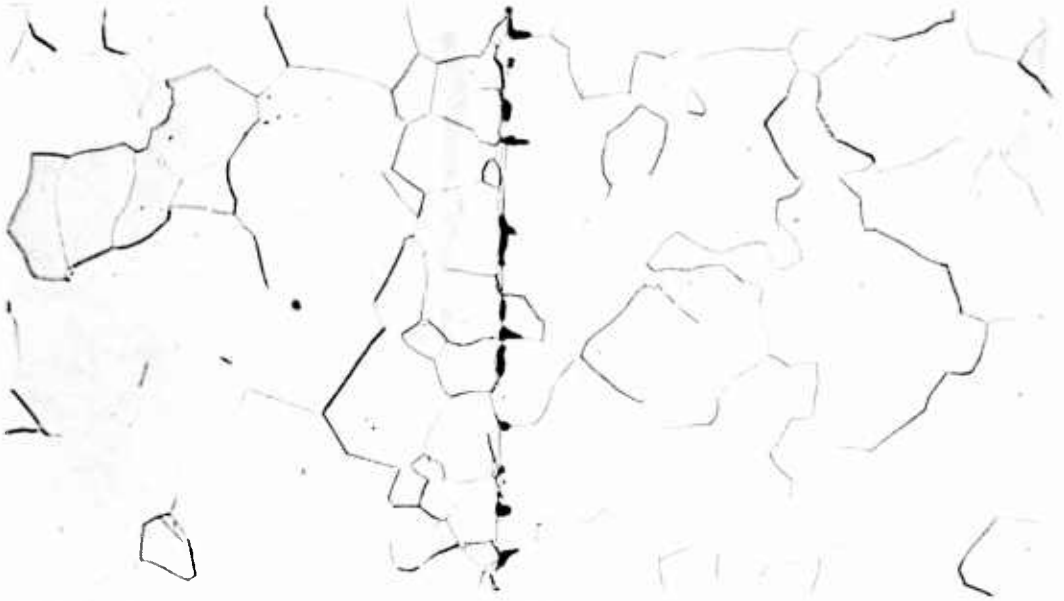

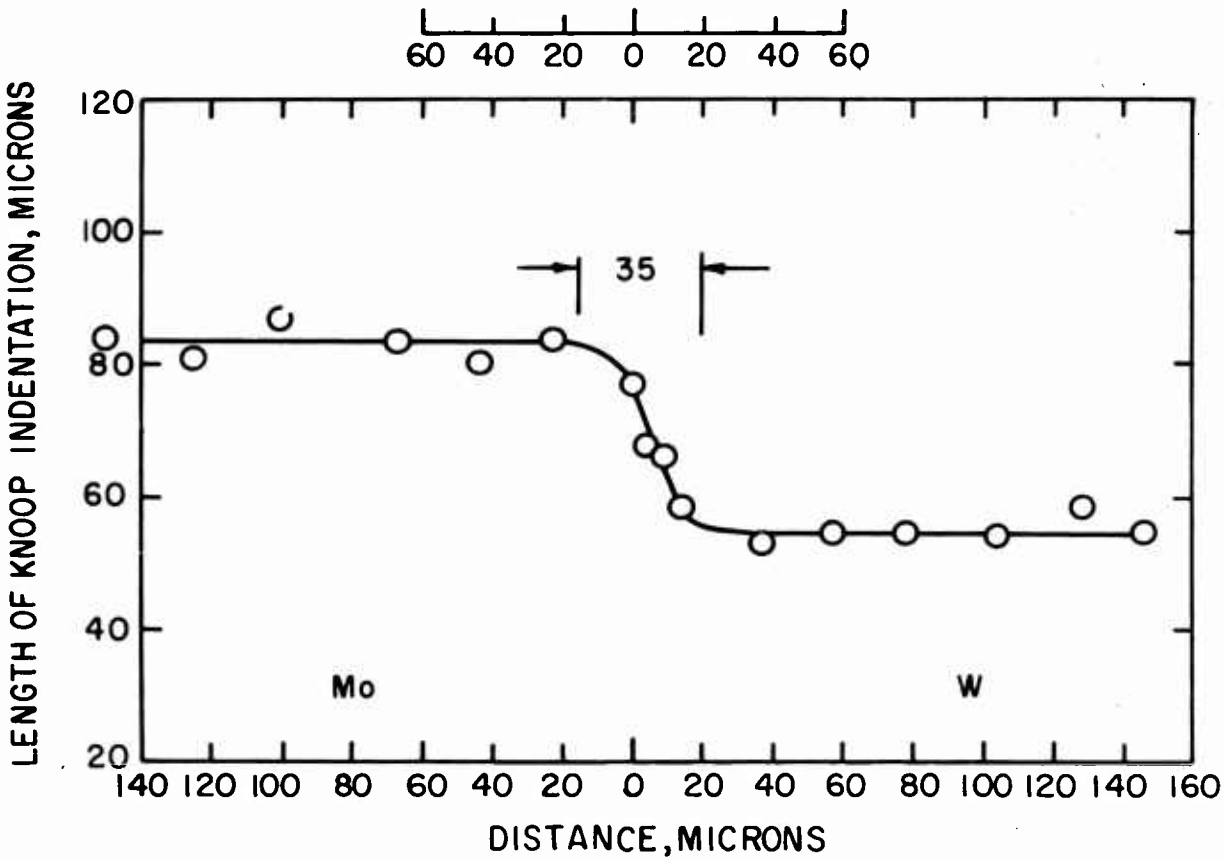

Fig.11- Mo–W, pressure weld no.6a, annealed 4 hours at 1700 °C

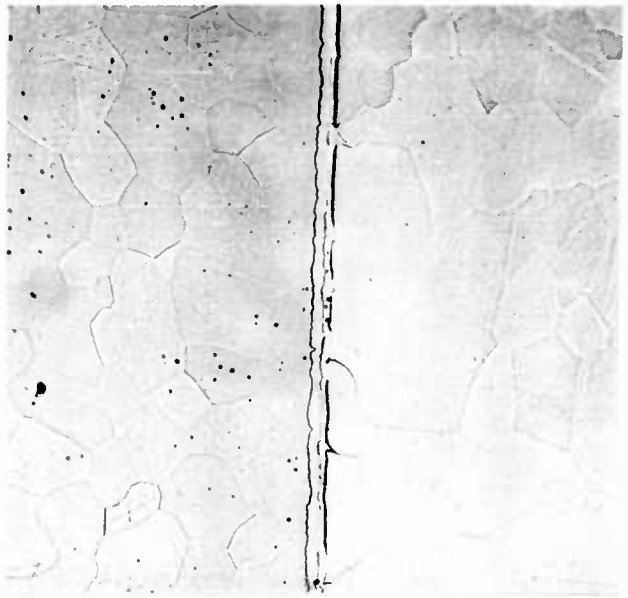

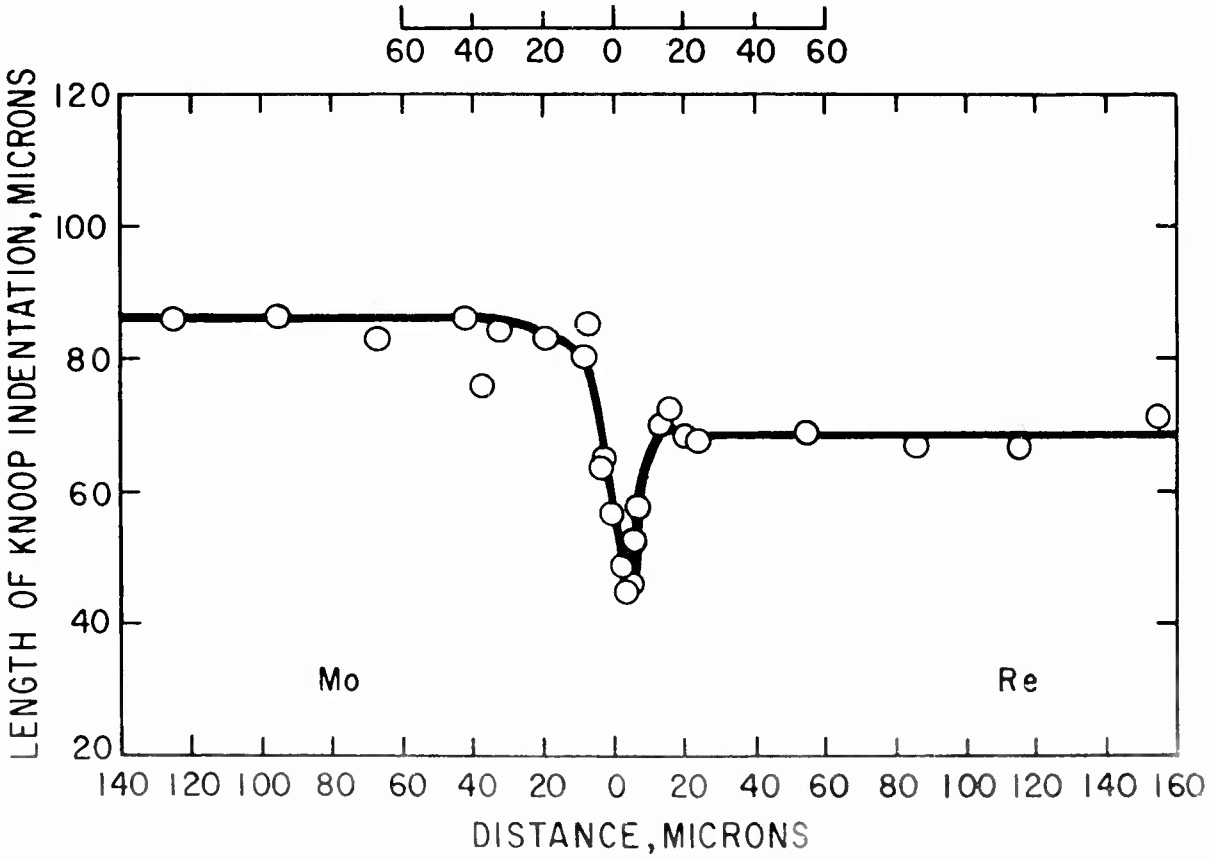

Fig.12- Mo – Re, pressure weld no. 5, annealed 1 hour at 1700°C

KOH-$K_3Fe(CN)_6$ETCH 3302 500X

60 40 20 0 20 40 60

MICRONS

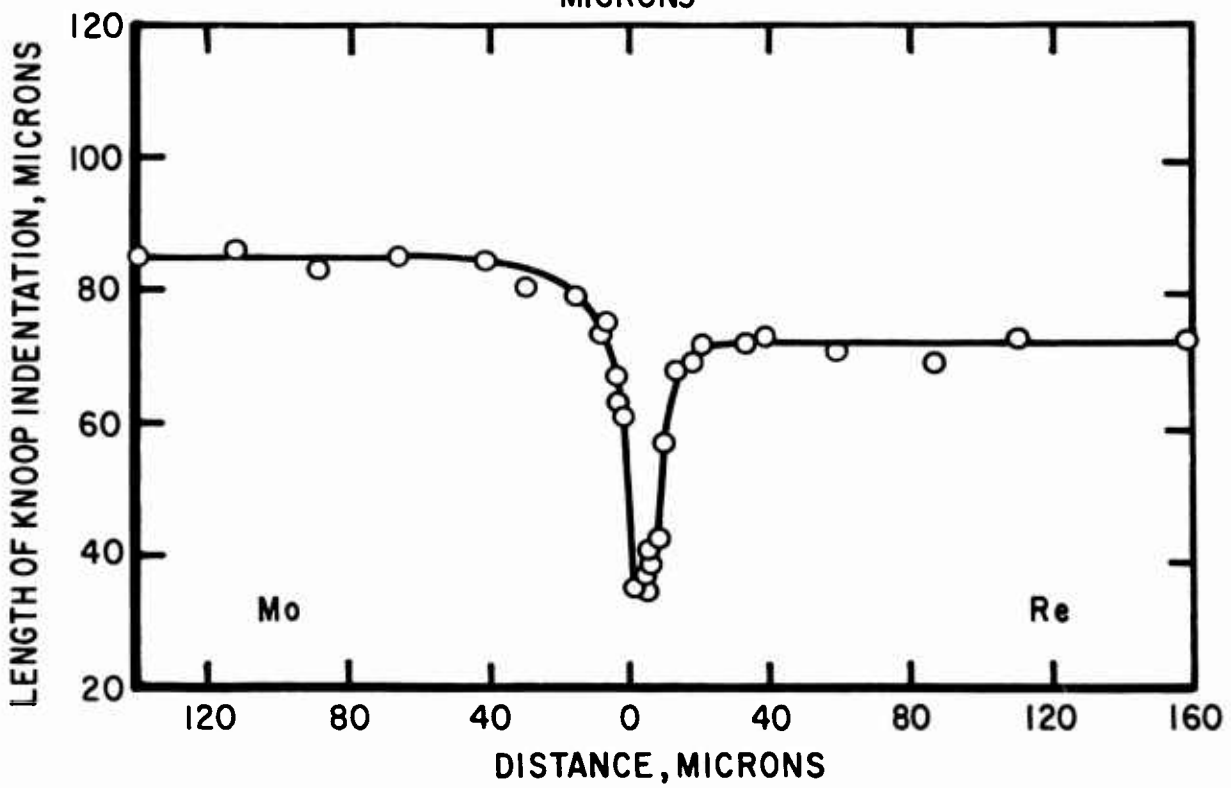

Fig.13- Mo–Re, pressure weld no. 4b–4; microstructure and microindentation measurements of interdiffusion after annealing 4 hours at 1700° C.

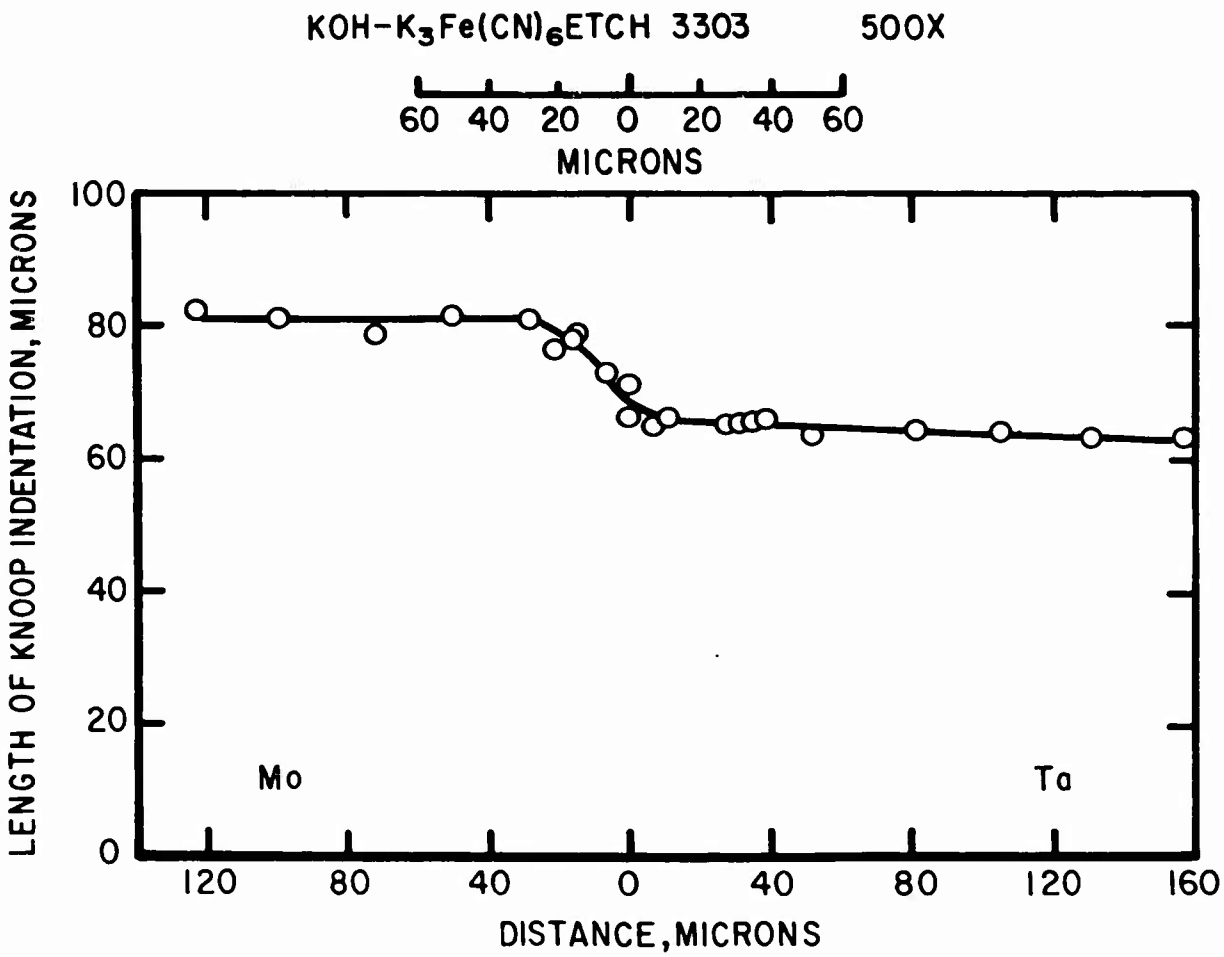

Fig.14- Mo-Ta, pressure weld no. 4b-4; microstructure and microindentation measurements of interdiffusion after annealing 4 hours at 1700°C

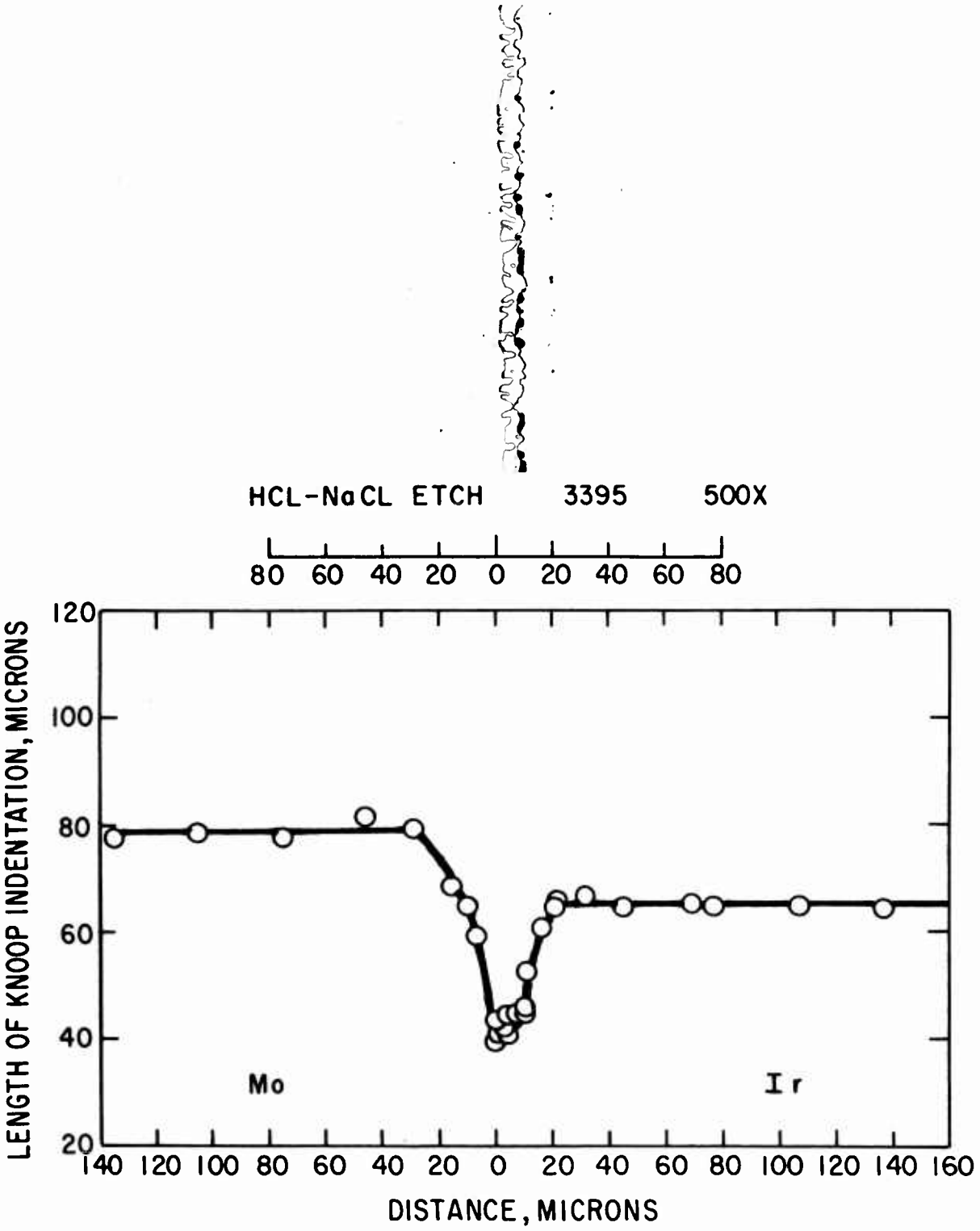

Fig. 15- Mo - Ir, pressure weld no.5, annealed 1 hour at 1700°C

Fig.16-Mo-Ir, pressure weld no.3-4; microstructure and microindentation measurements of interdiffusion after annealing 4 hours at 1700°C.

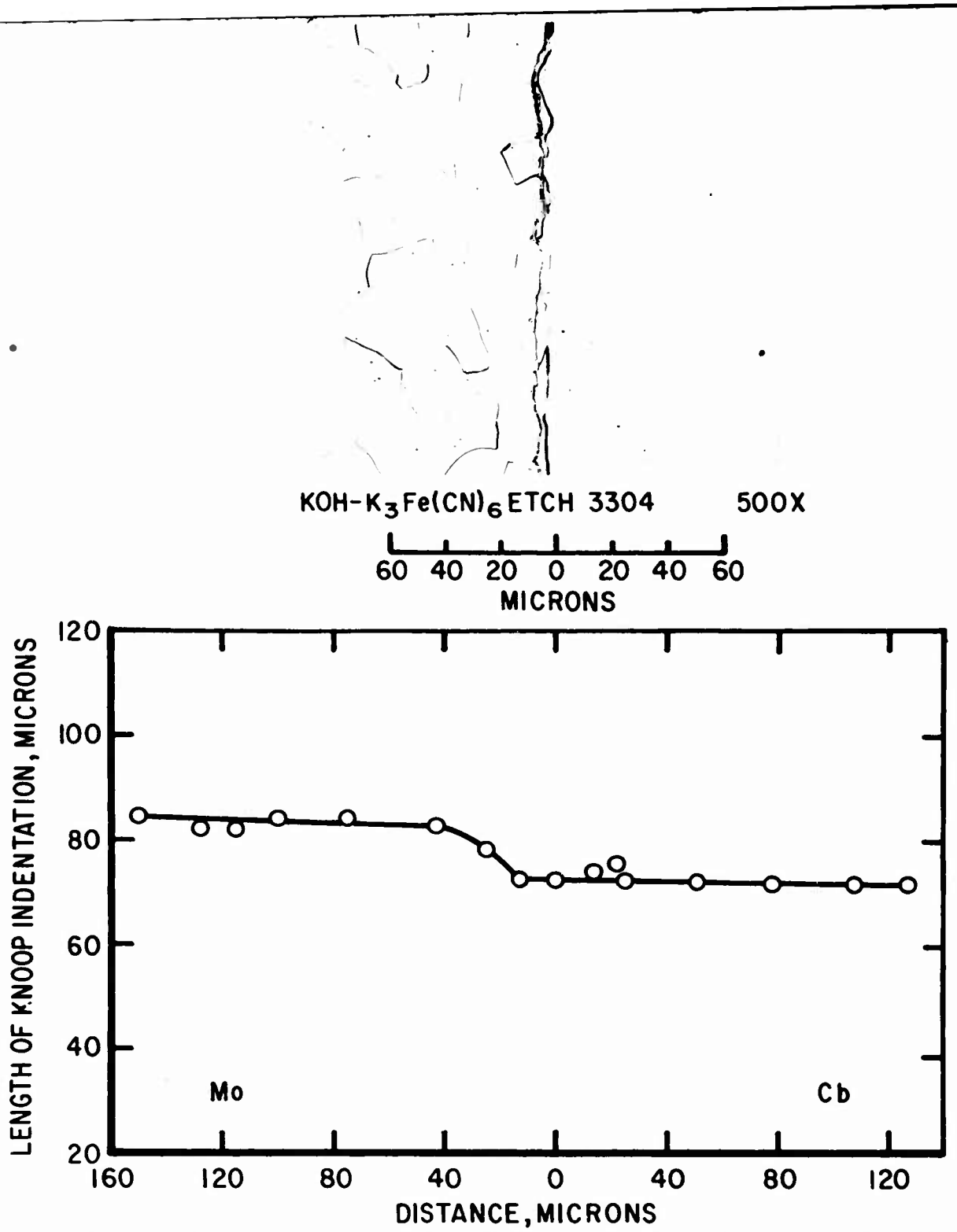

Fig.17- Mo-Cb, pressure weld no. 4b-4; microstructure and microindentation measurements of interdiffusion after annealing 4 hours at 1700°C.

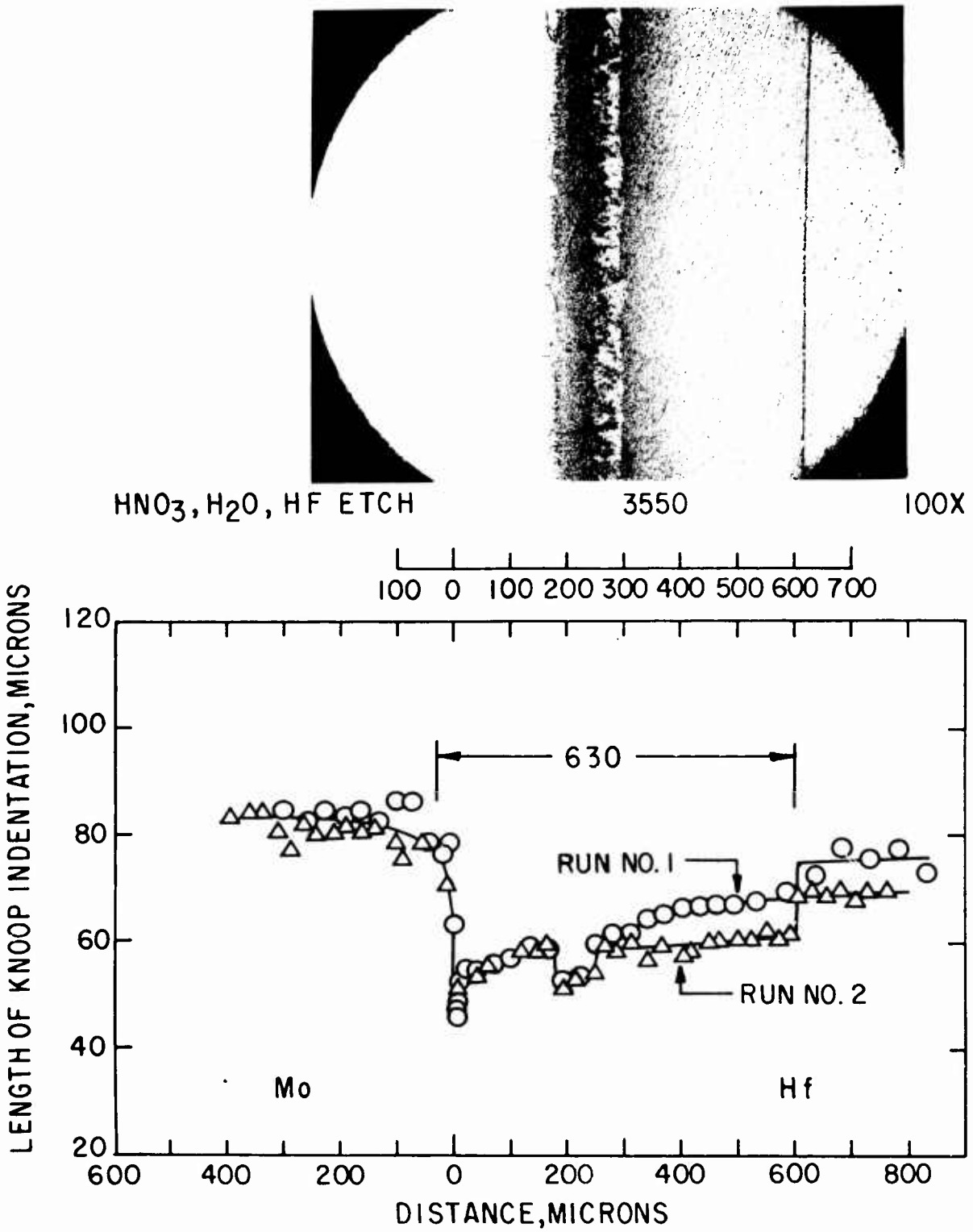

Fig. 18 - Mo - Hf, pressure weld no. 6a, annealed 4 hours at 1700°C

KOH, $K_3Fe(CN)_6$ ETCH 3820 500 X

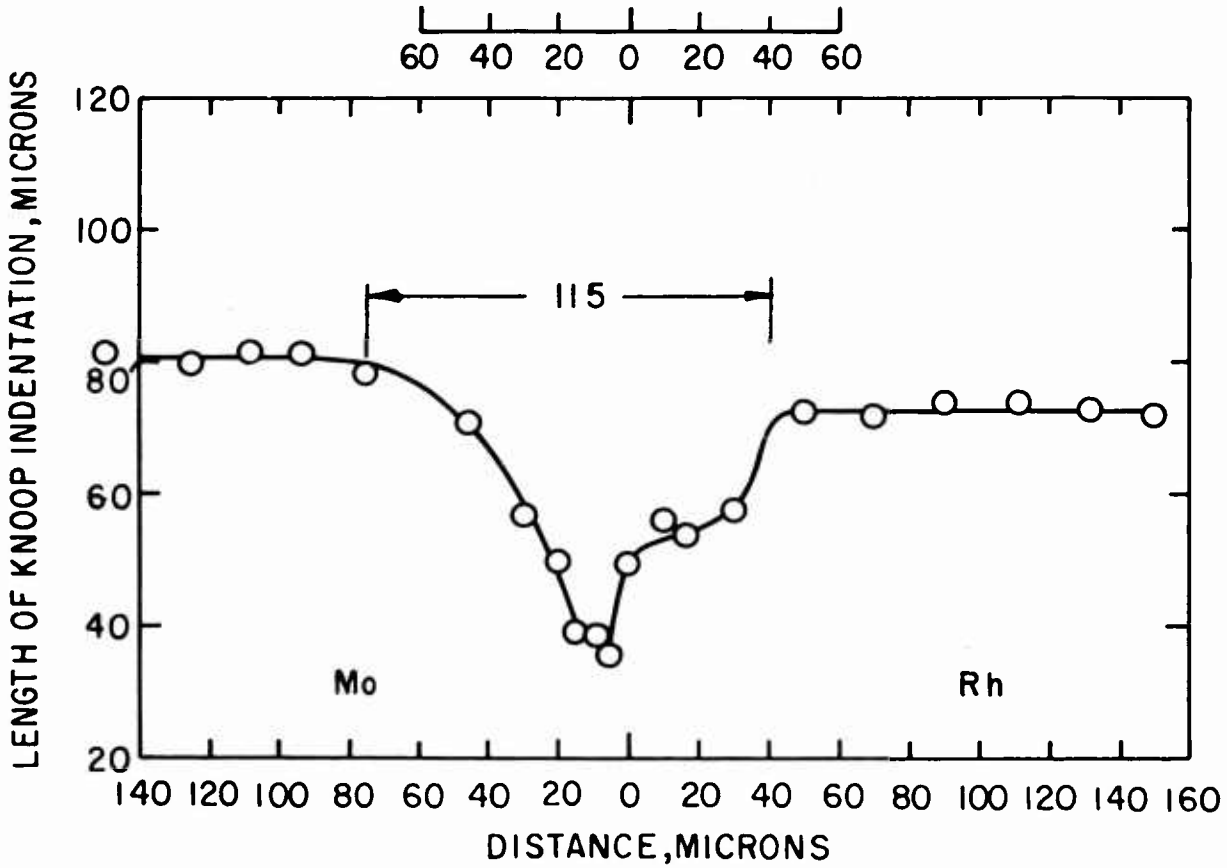

Fig.19- Mo-Rh, pressure weld no.6a, annealed 4 hours at 1700°C

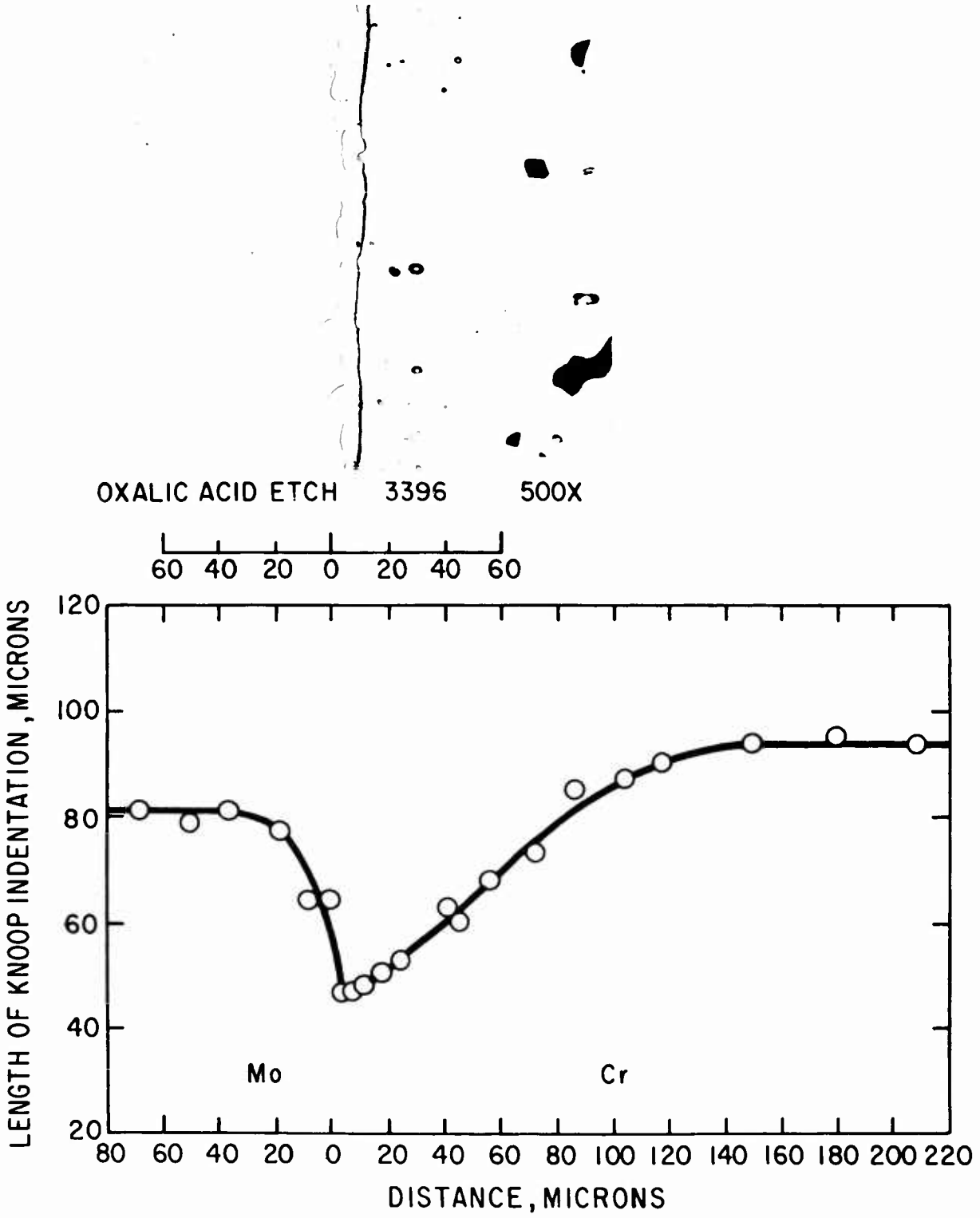

Fig.20 - Mo-Cr, pressure weld no. 5, annealed 1 hour at 1700°C

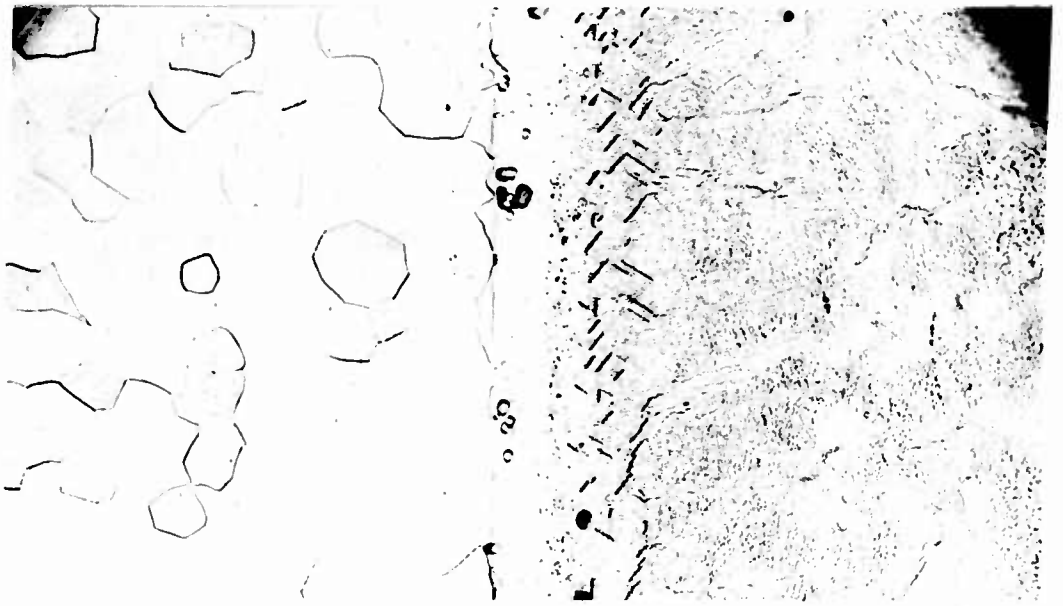

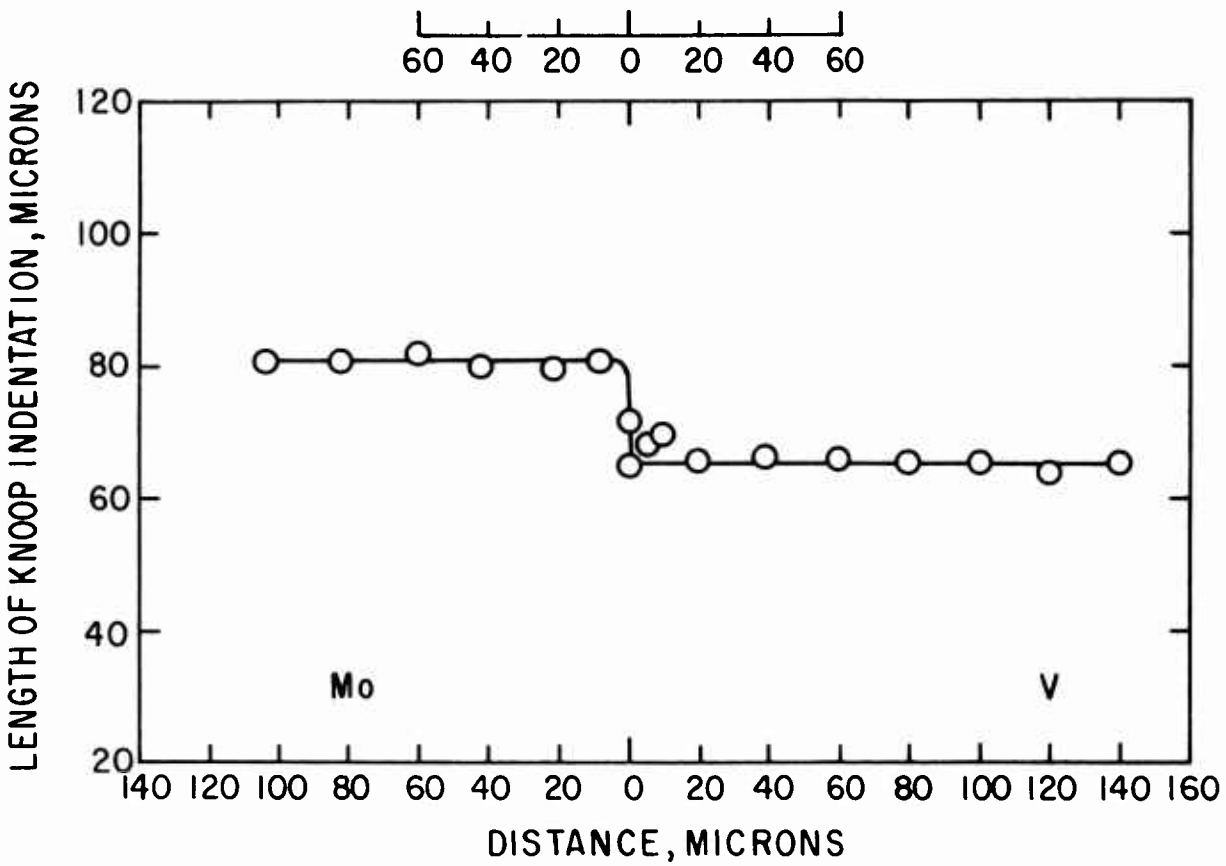

Fig.21-Mo-V, pressure weld no.6a, annealed 4 hours at 1700°C

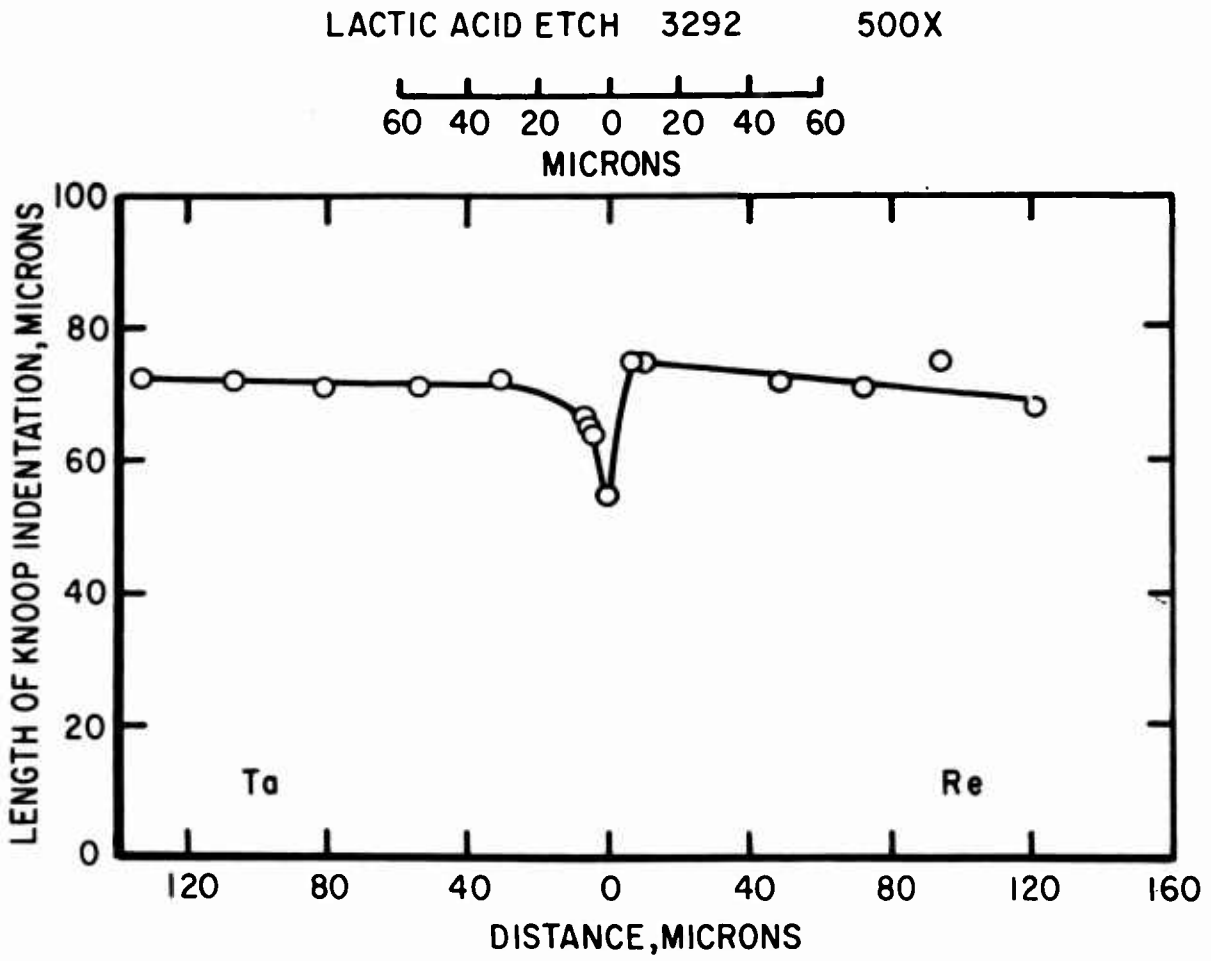

Fig.22- Ta – Re, pressure weld no. 4a-4 ; microstructure and microindentation measurements of interdiffusion after annealing 4 hours at 1700°C.

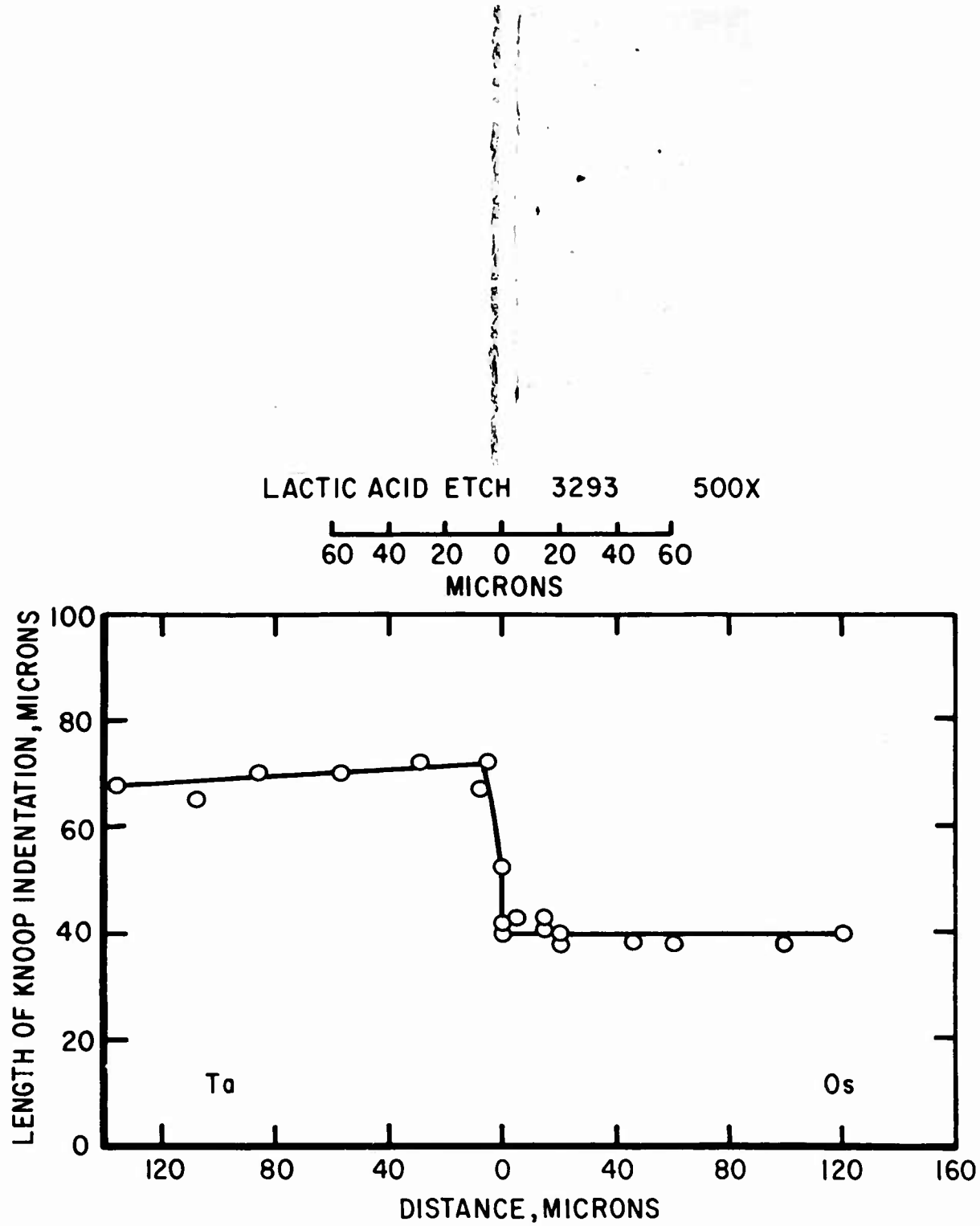

Fig.23- Ta - Os, pressure weld no. 4a-4; microstructure and microindentation measurements of interdiffusion after annealing 4 hours at 1700°C.

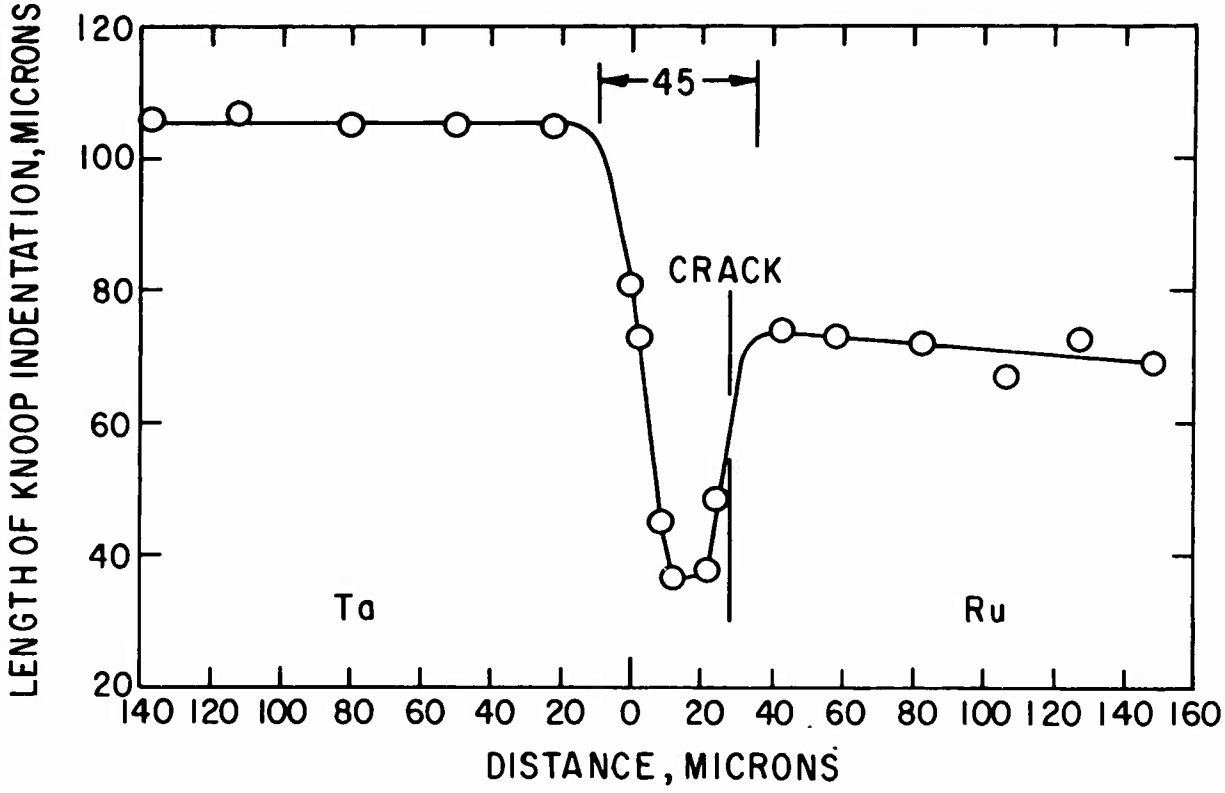

Fig.24- Ta - Ru, pressureweld no. 6b, annealed 4 hours at 1700 °C

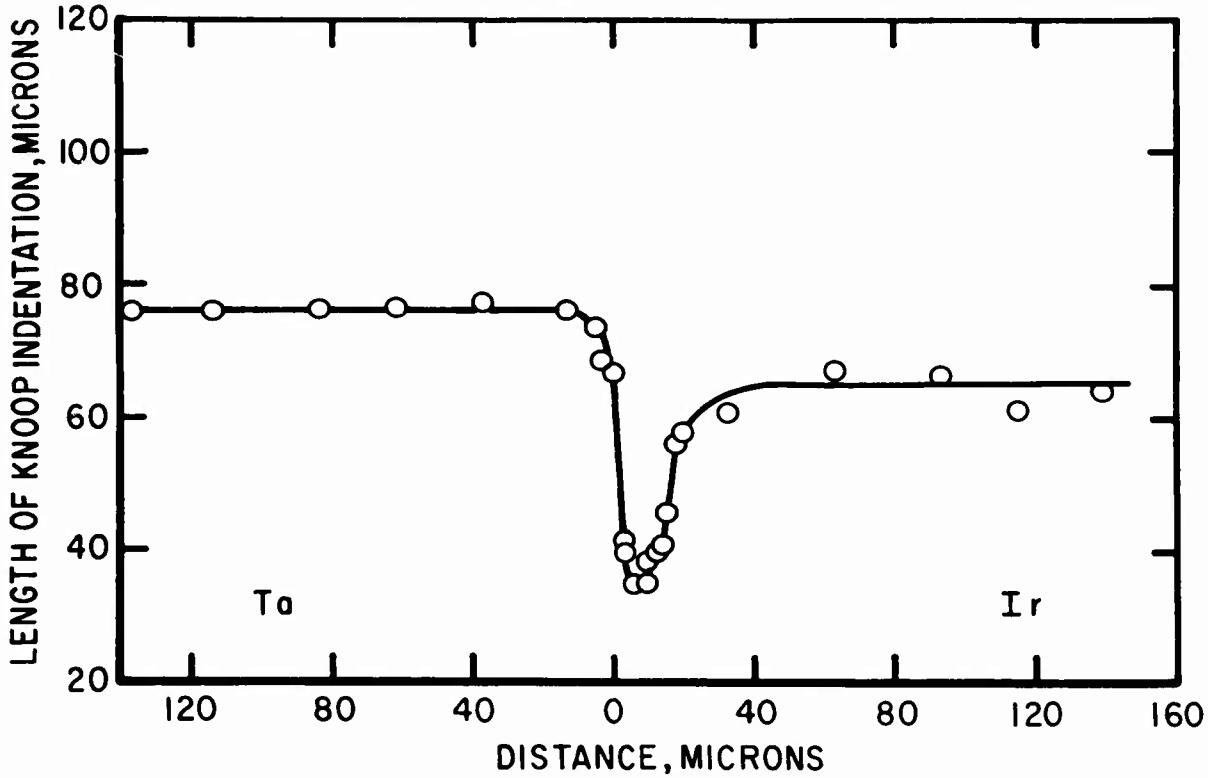

Fig.25-Ta-Ir, pressure weld no. 3-4 ; microstructure and microindentation measurements of interdiffusion after annealing 4 hours at 1700°C

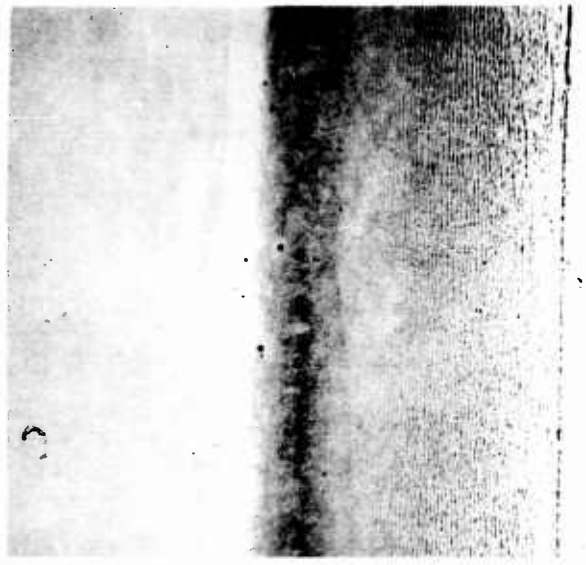

NH_4F, HF ETCH 3514 100 X

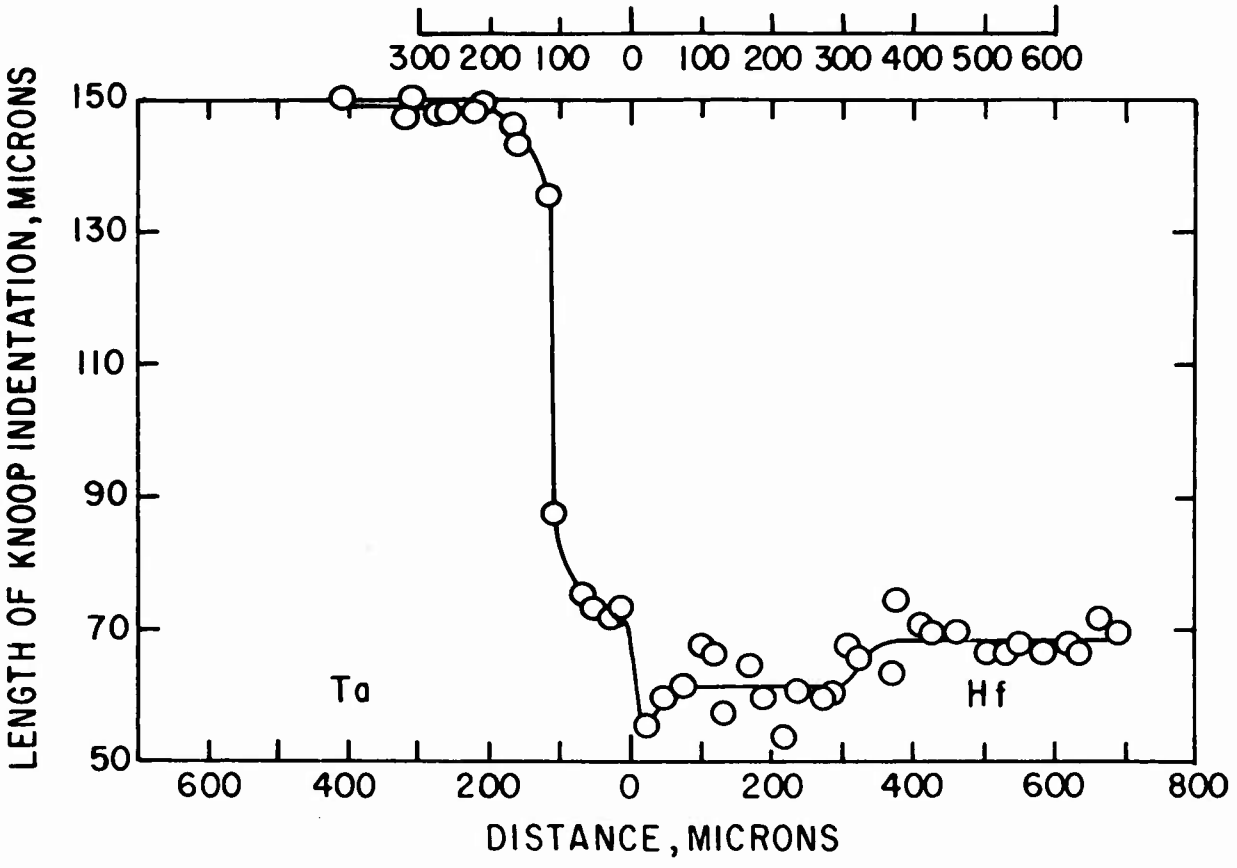

Fig. 26 - Ta - Hf, pressure weld no. 6b, annealed 4 hours at 1700 °C

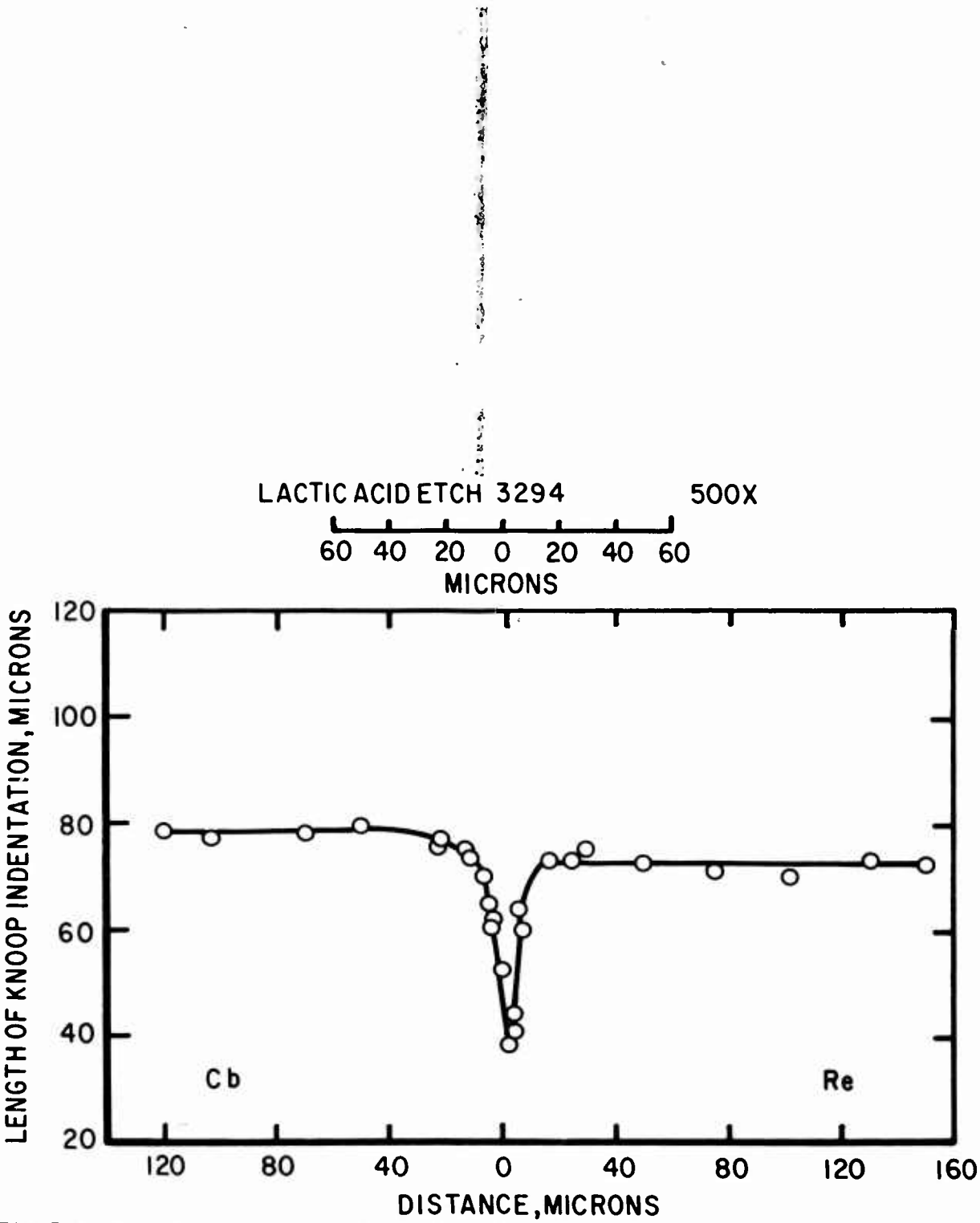

Fig.27-Cb – Re, pressure weld no. 4b – 4; microstructure and microindentation measurements of interdiffusion after annealing 4 hours at 1700° C.

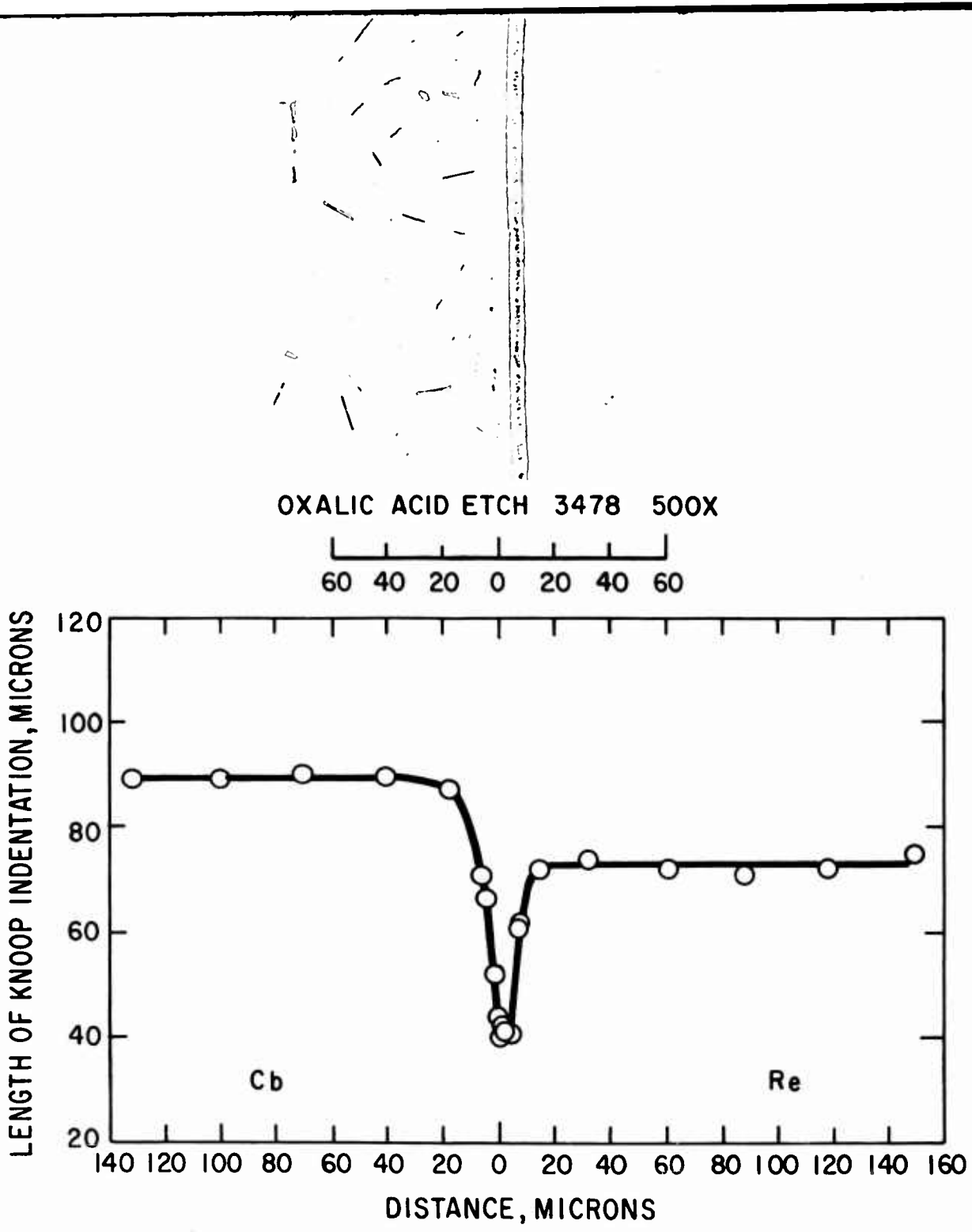

Fig.28- Cb - Re, pressure weld no. 6c, annealed 4 hours at 1700°C

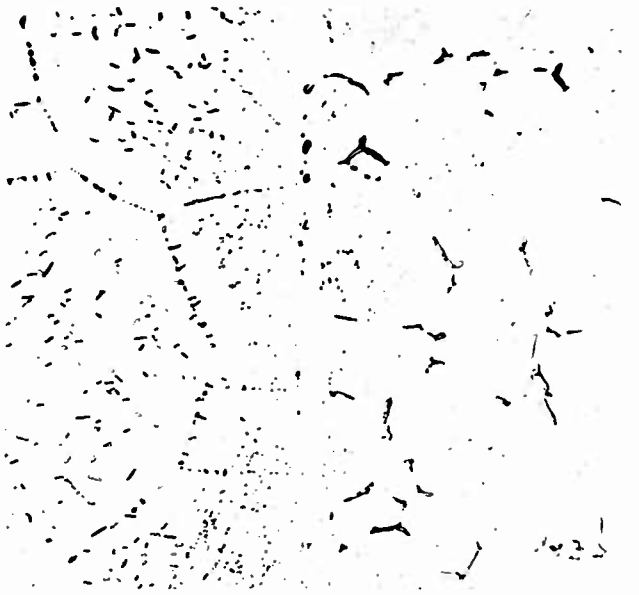

Fig.29-Cb-Ta, pressure weld no. 4b-4; microstructure and microindentation measurements of interdiffusion after annealing 4 hours at 1700°C.

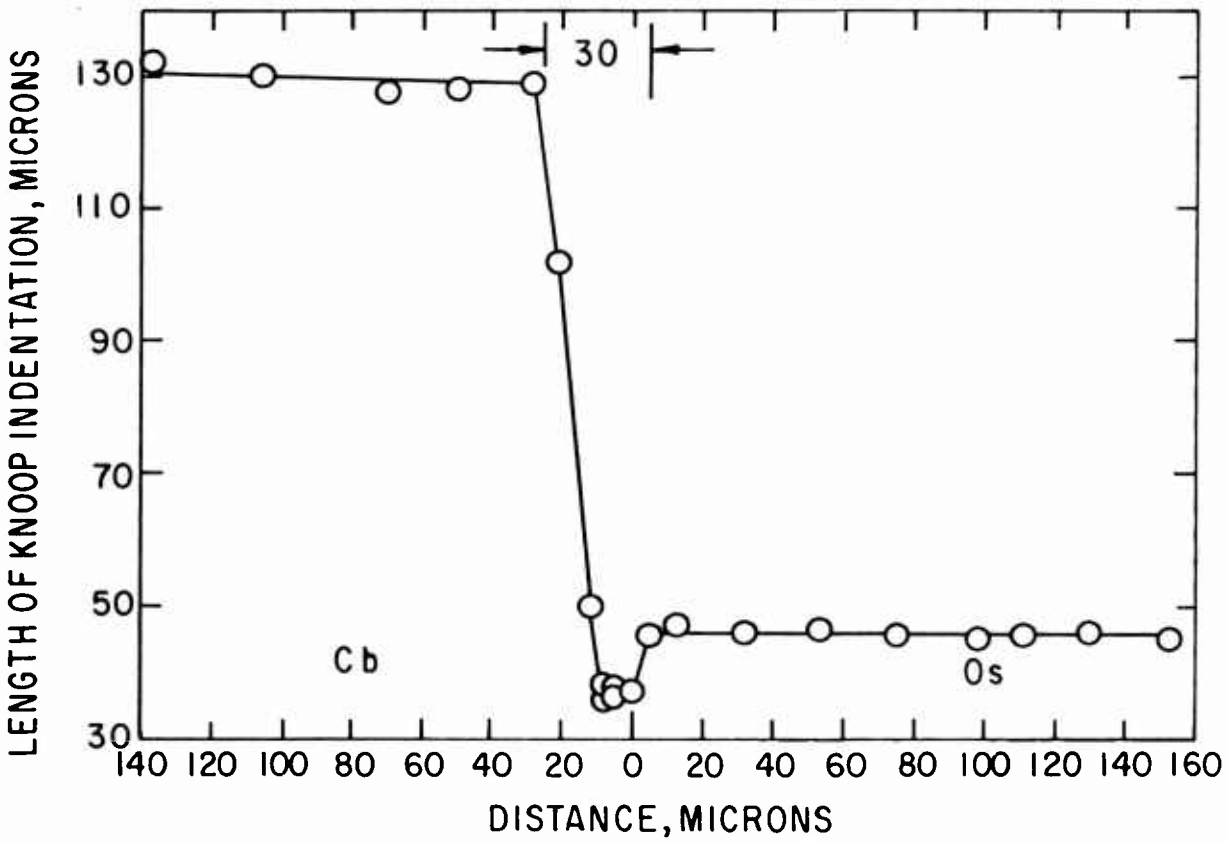

Fig.30-Cb-Os, pressure weld no. 6b, annealed 4 hours at 1700°C

Fig.31-Cb-Ir, pressure weld no. 4b-4; microstructure and microindentation measurements of interdiffusion after annealing 4 hours at 1700°C.

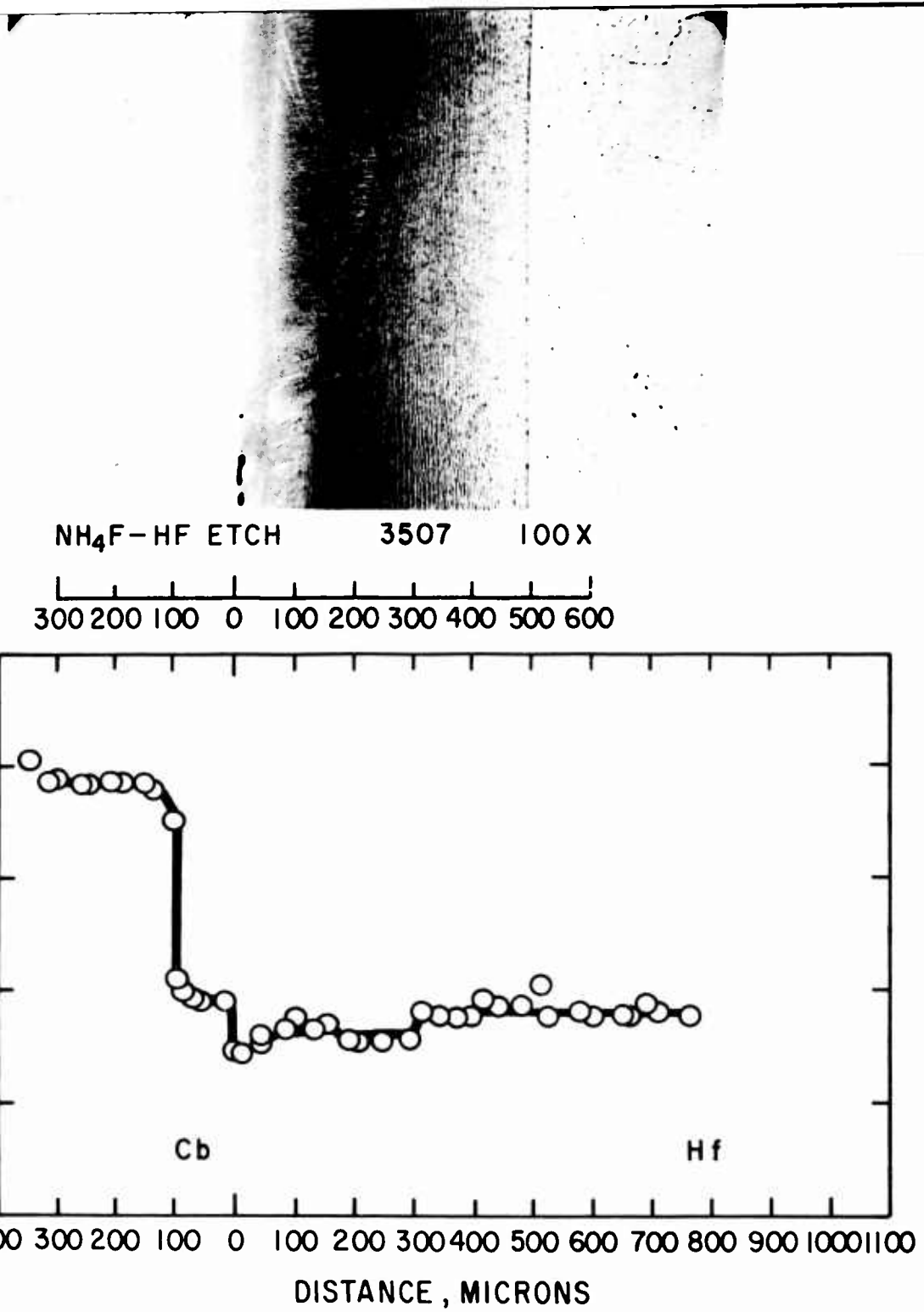

Fig.32- Cb-Hf, pressure weld no.6b, annealed 4 hours at 1700 °C

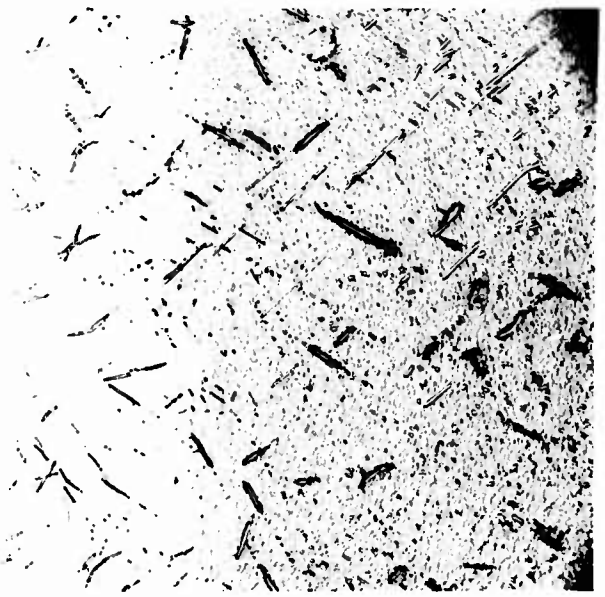

LACTIC ACID ETCH 3590 500X

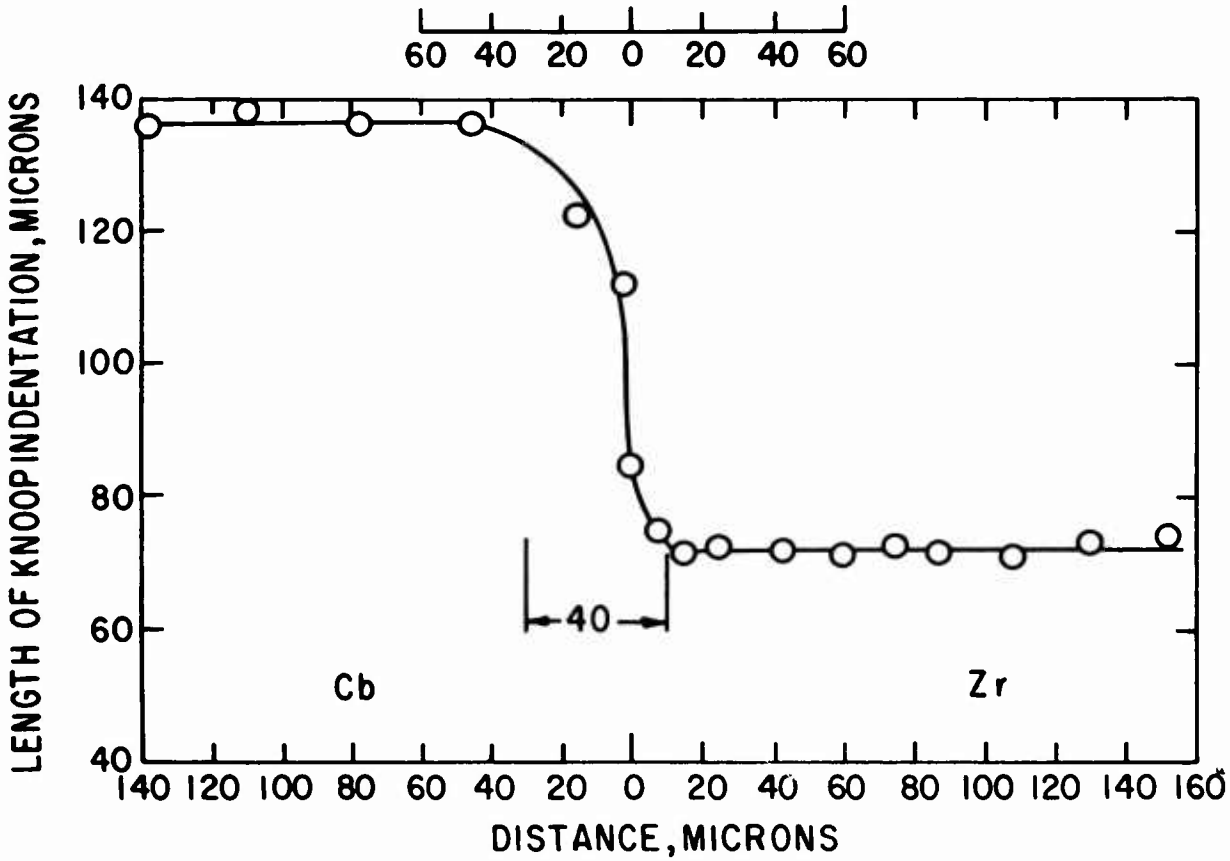

Fig.33- Cb-Zr, pressure weld no.6b, annealed 4 hours at 1700°C

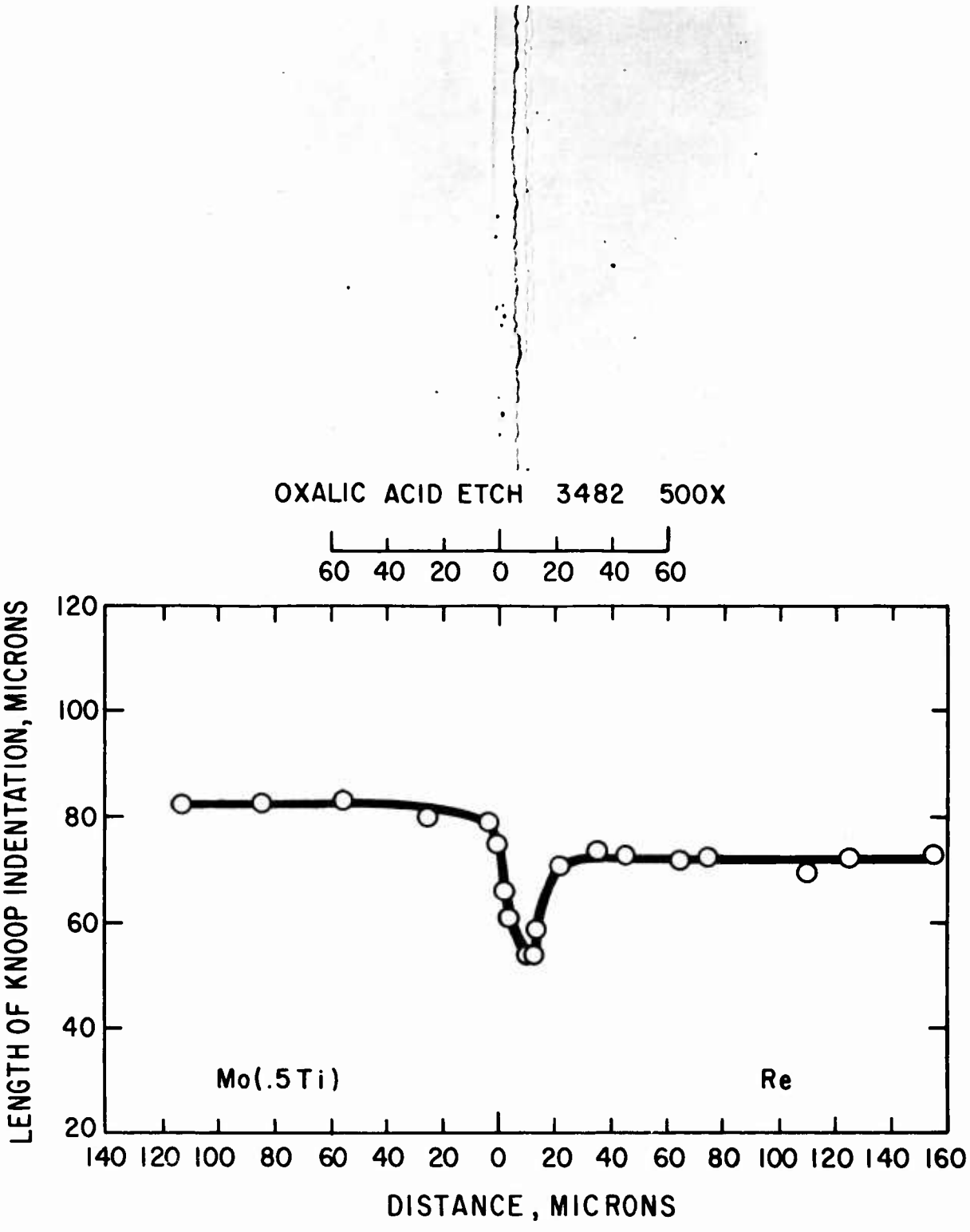

Fig.34- Mo (.5 Ti) – Re, pressure weld no.6c, annealed 4 hours at 1700°C

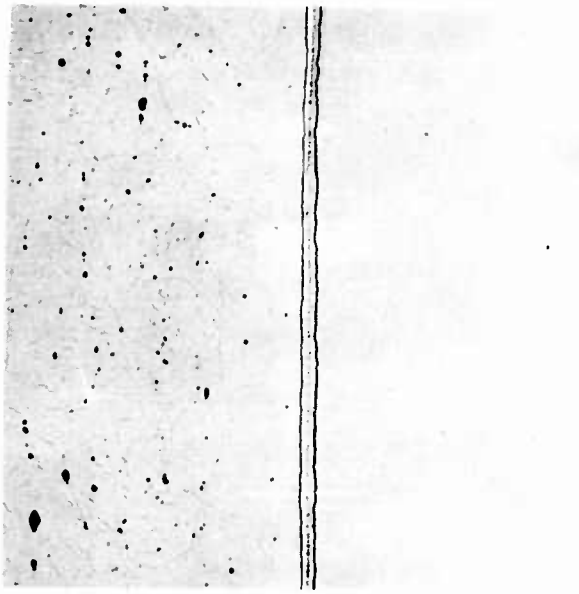

LACTIC ACID ETCH 3480 500X

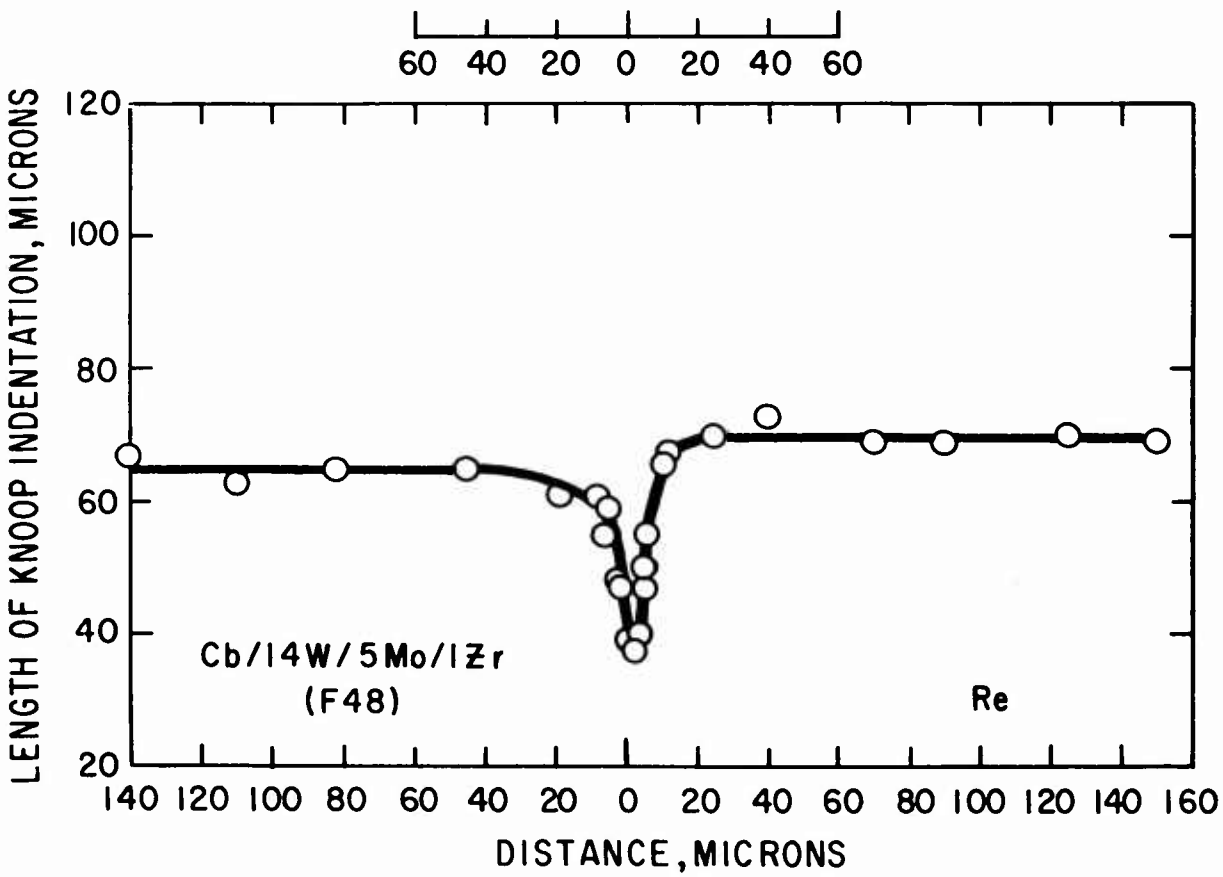

Fig.35- Cb(F48)-Re, pressure weld no.6c, annealed 4 hours at 1700°C

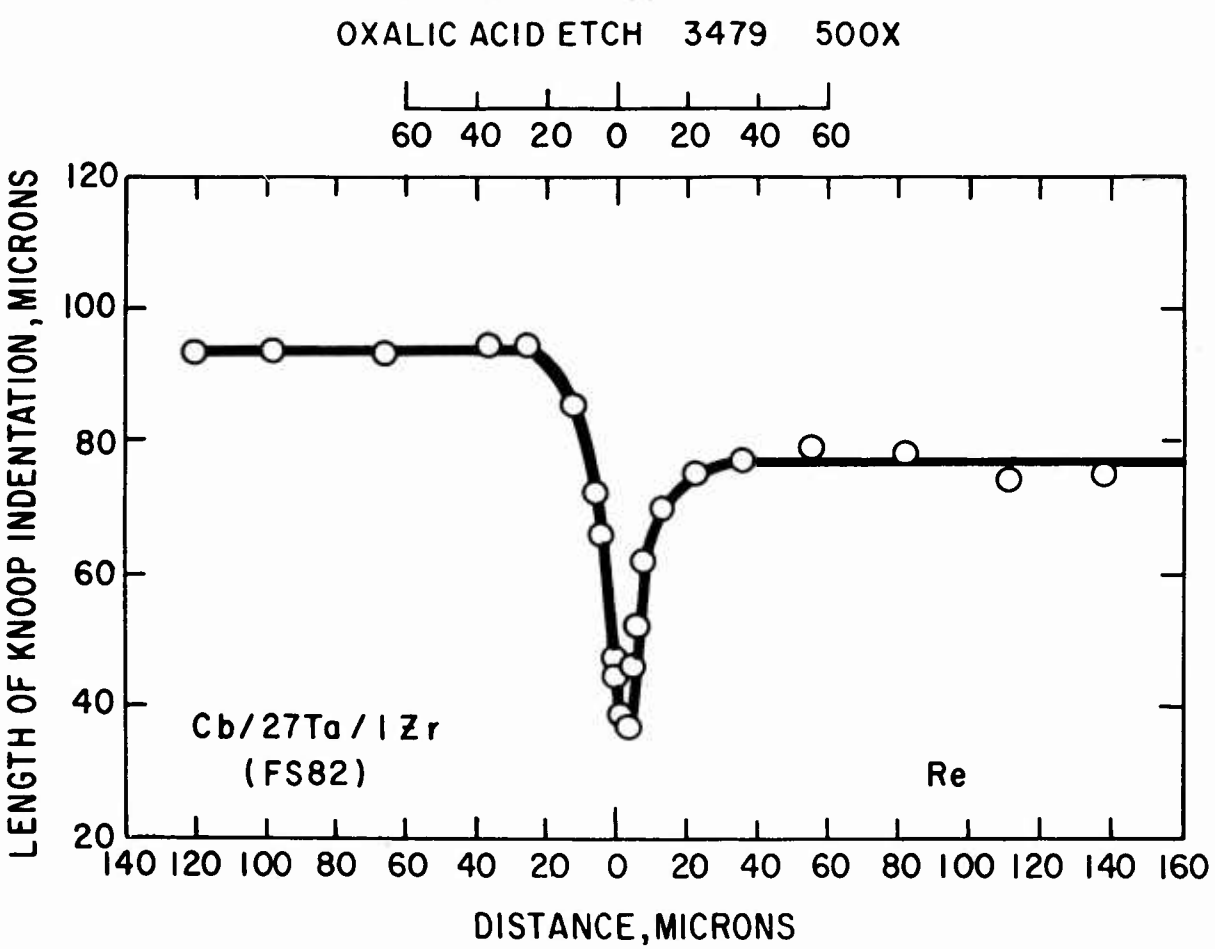

Fig. 36- Cb (FS82)- Re, pressure weld no. 6c, annealed 4 hours at 1700°C

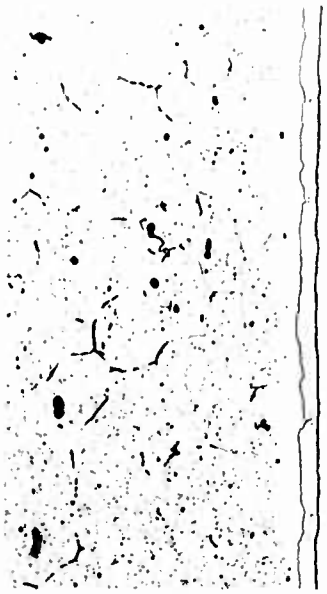

OXALIC ACID ETCH 3481 500X

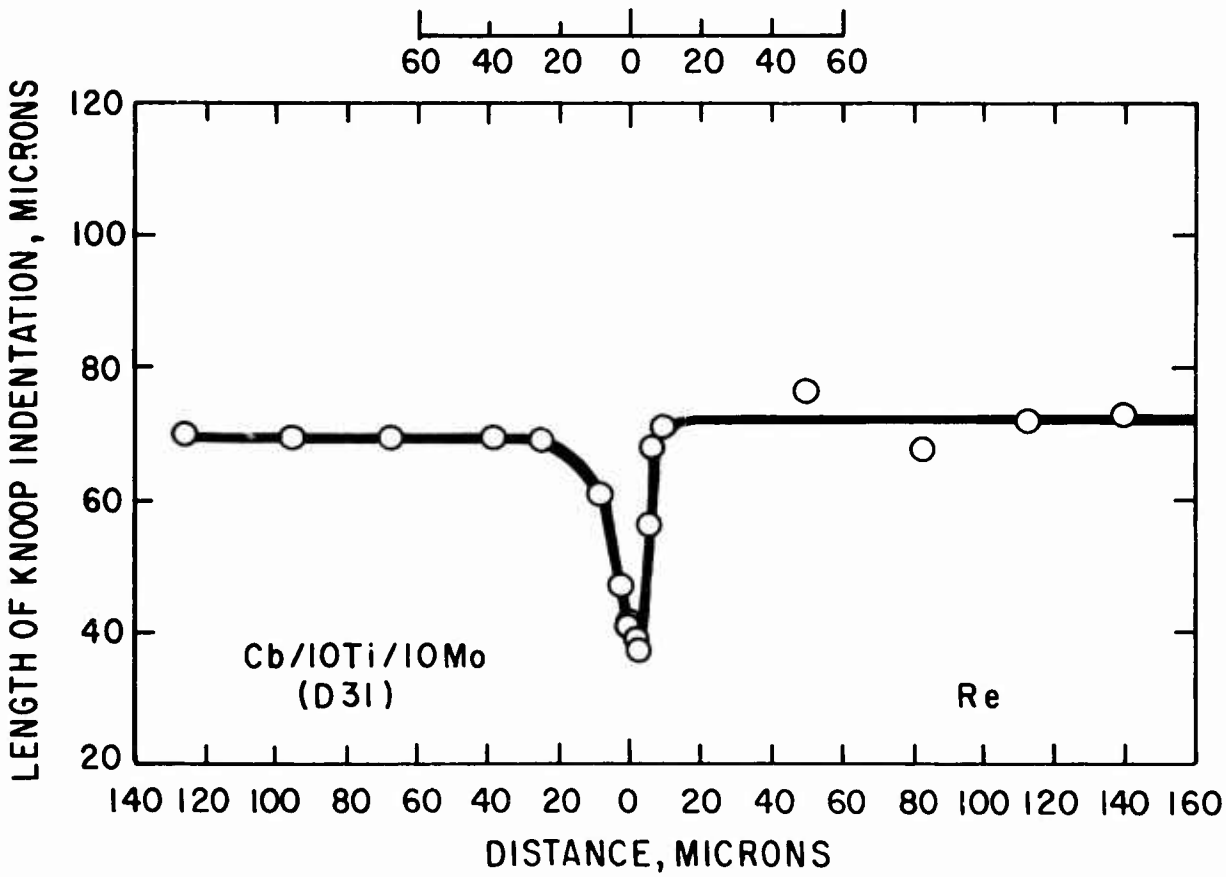

Fig.37- Cb (D31)–Re , pressure weld no.6c, annealed 4 hours at 1700 °C

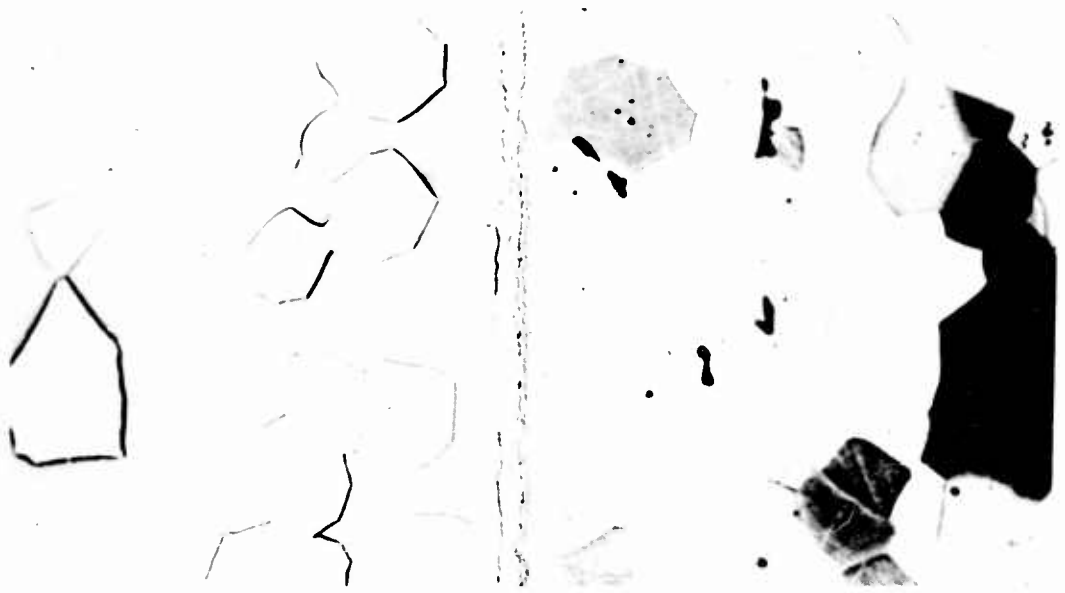

OXALIC ACID ETCH 3899 500 X

POLARIZED LIGHT

60 40 20 0 20 40 60

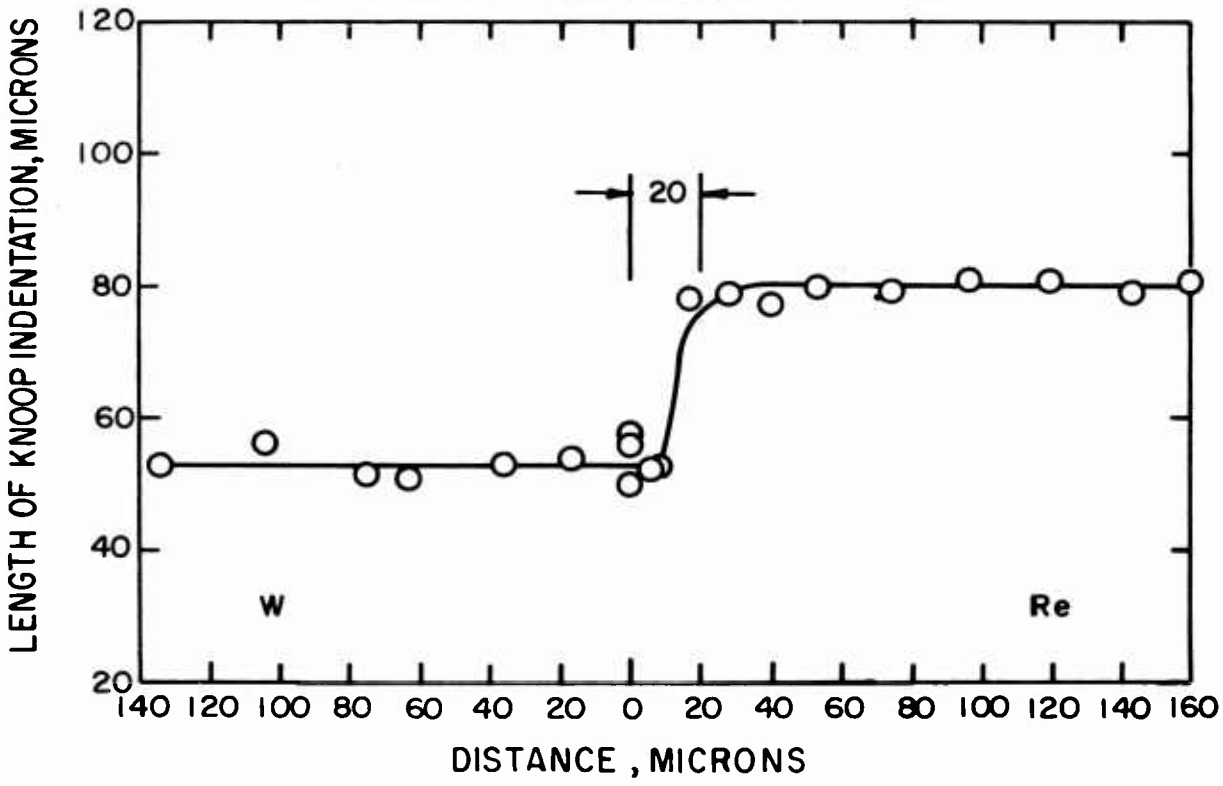

Fig.38-W-Re, pressure weld no. 7a, annealed 3 hours at 1800°C

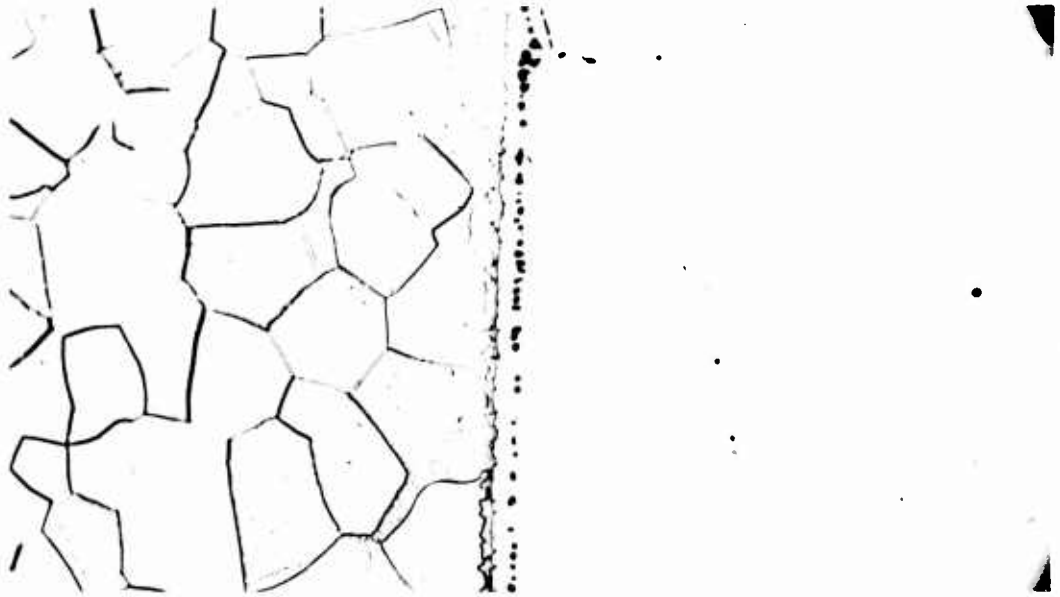

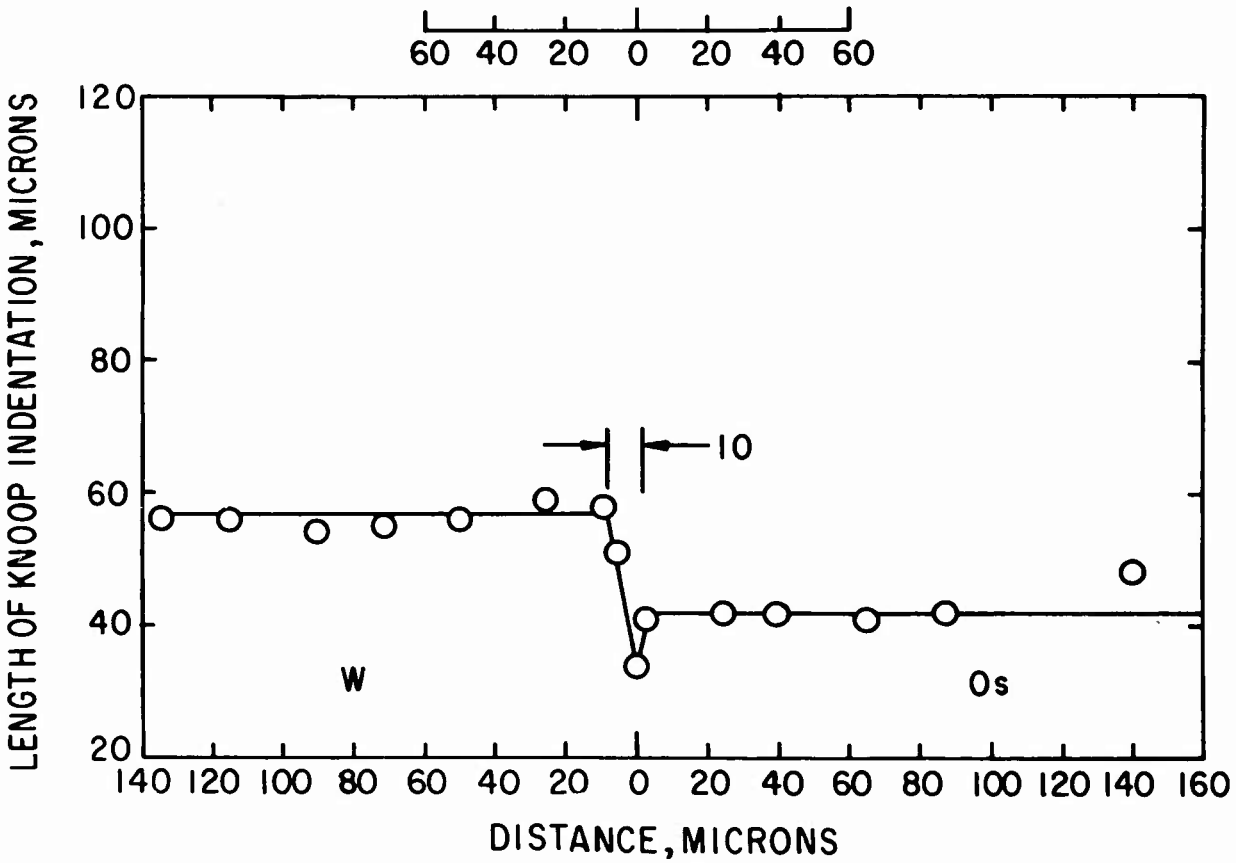

Fig.39- W – Os, pressure weld no. 7 b, annealed 3 hours at 1800°C

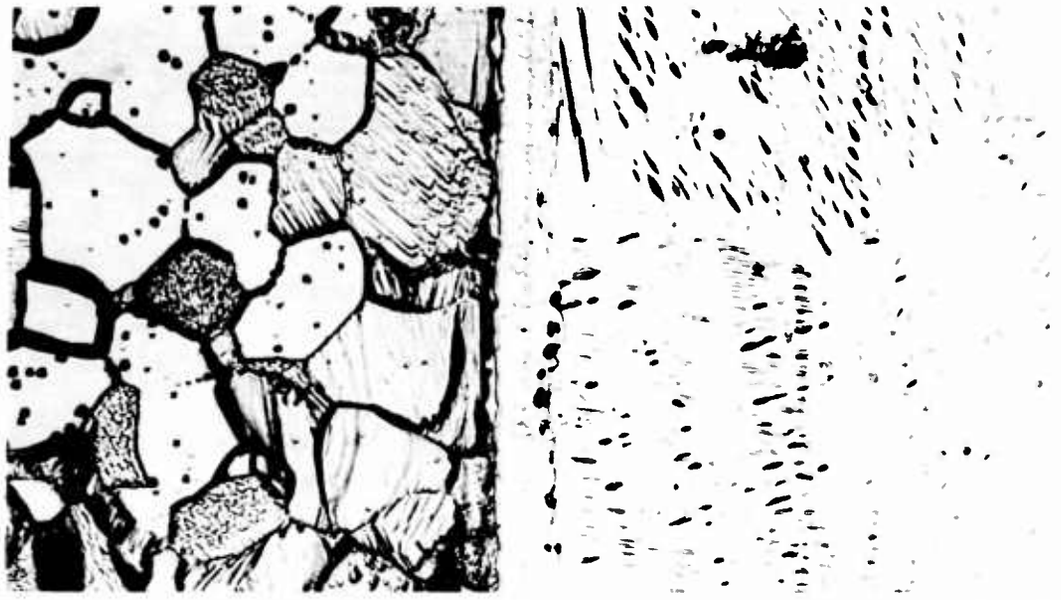

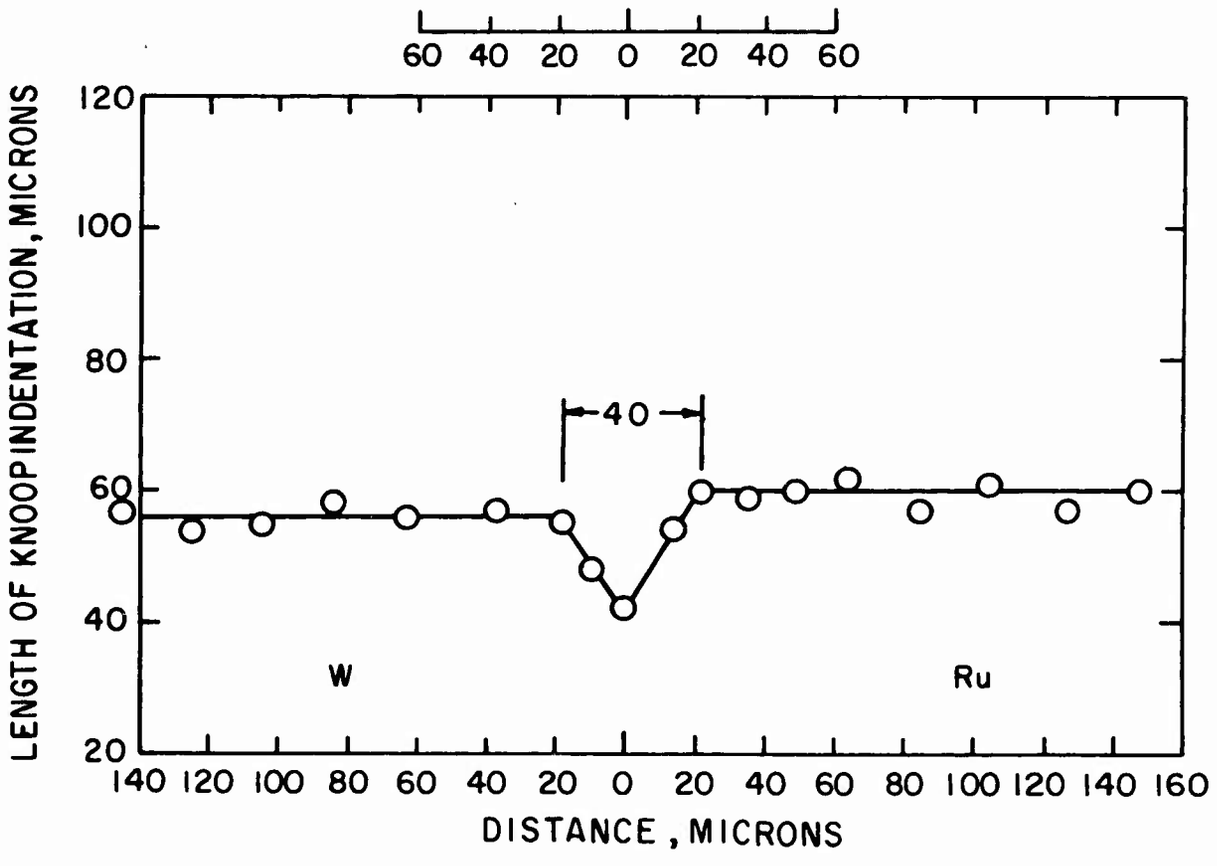

Fig 40- W – Ru, pressure weld no. 7a, annealed 3 hours at 1800°C

KOH, $K_3Fe(CN)_6$ ETCH 3895 500 X

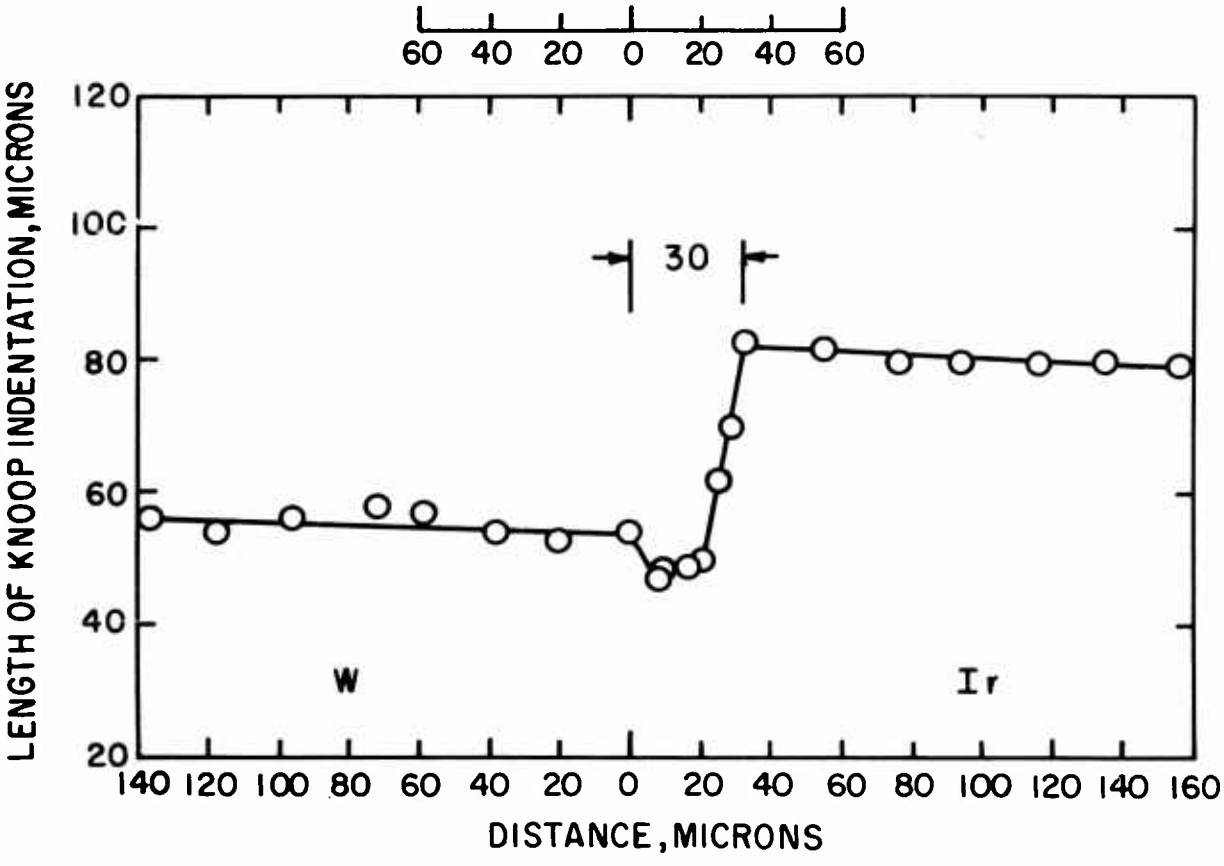

Fig 41- W-Ir, pressure weld no. 7a, annealed 3 hours at 1800°C

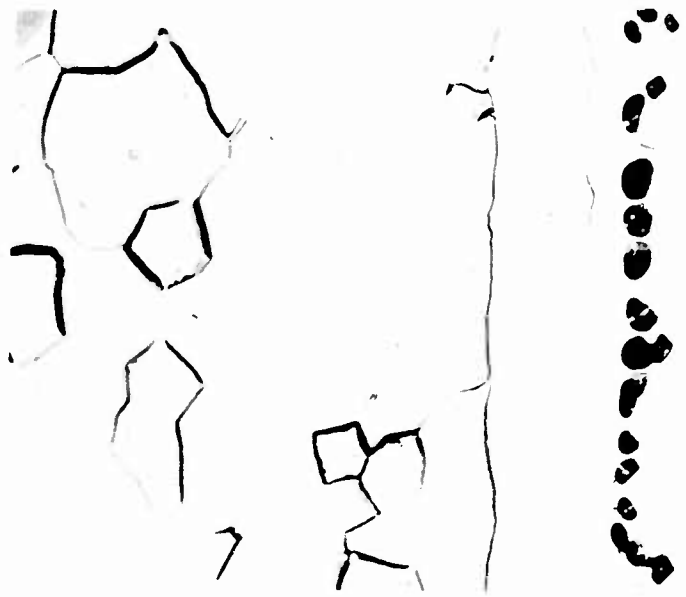

KOH, $K_3Fe(CN)_6$ ETCH 3896 500X

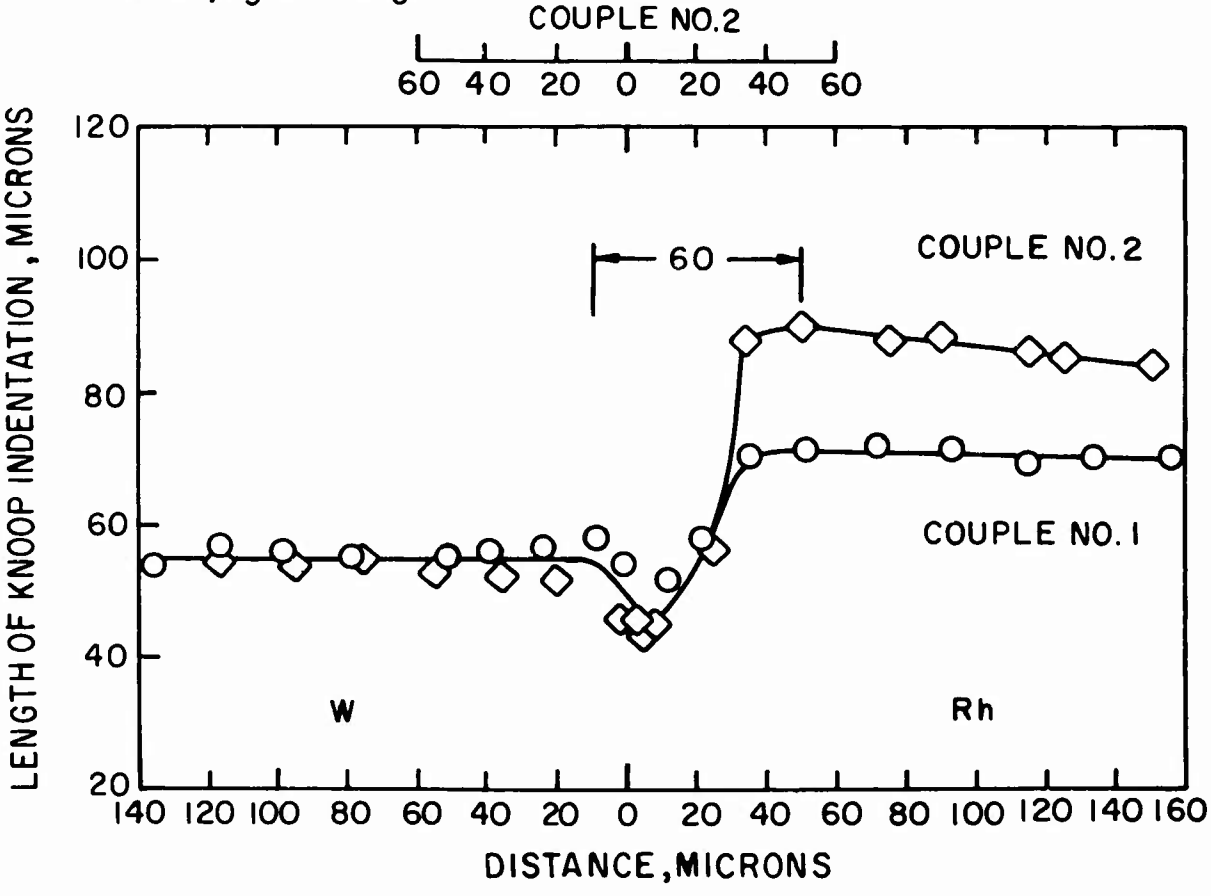

Fig.42- W-Rh, pressure weld no. 7a, annealed 3 hours at 1800 °C

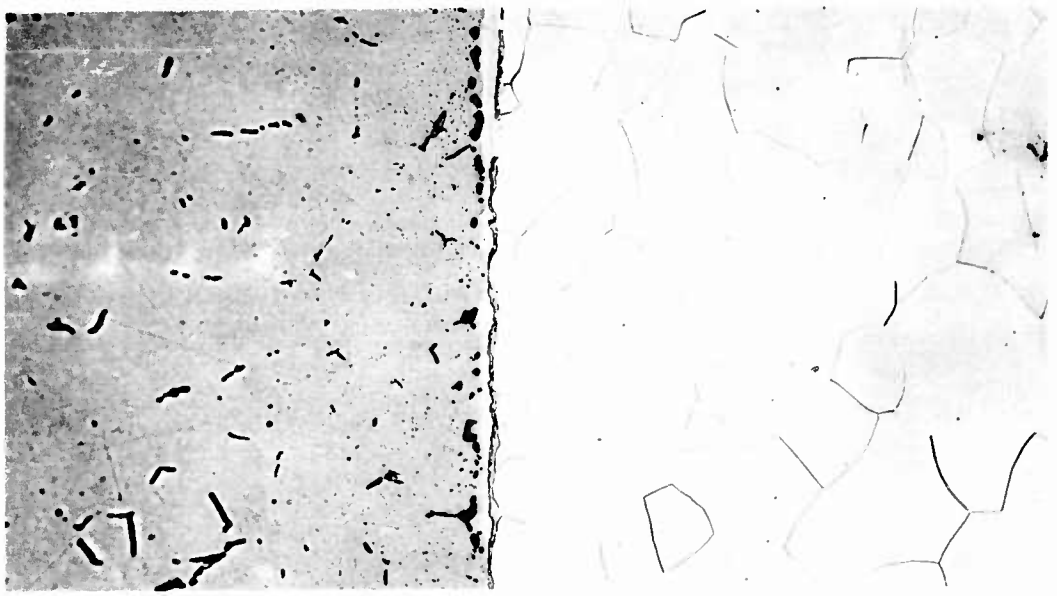

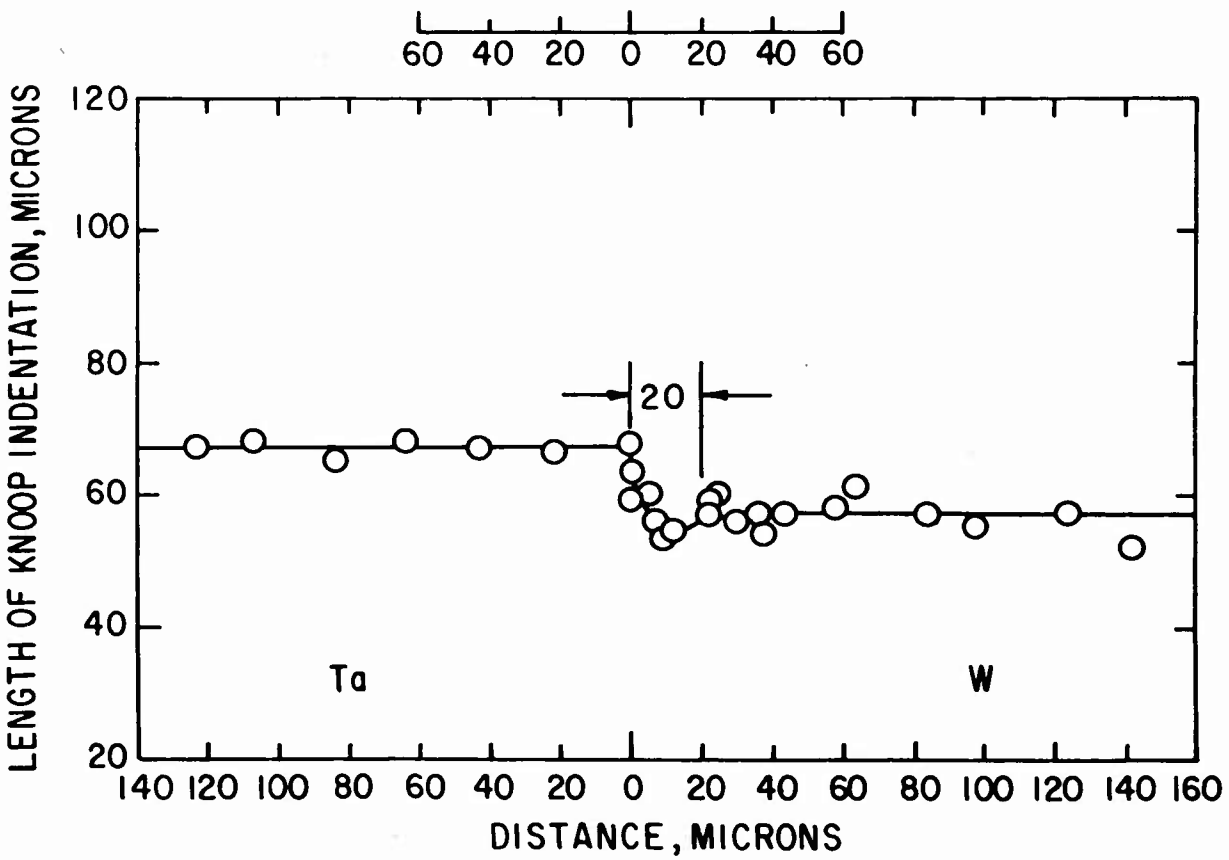

Fig.43- Ta–W, pressure weld no. 7b, annealed 3 hours at 1800°C

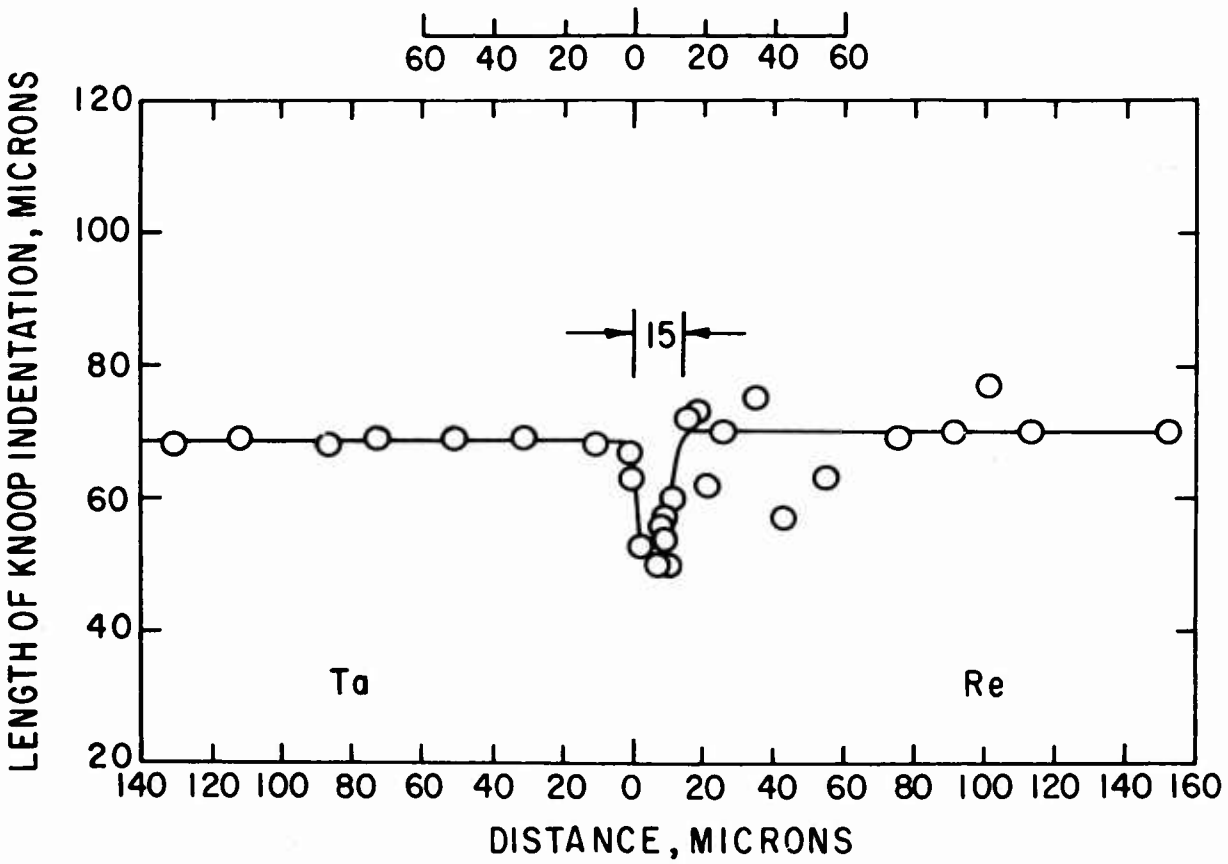

Fig.44-Ta-Re, pressure weld no.7b, annealed 3 hours at 1800°C

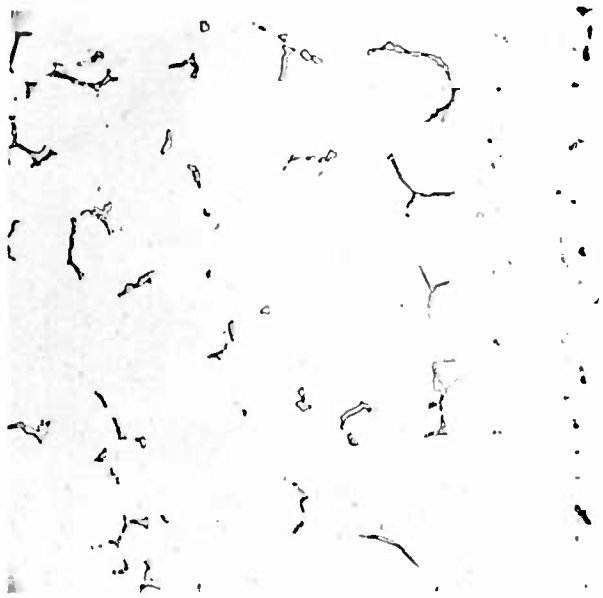

LACTIC ACID ETCH 3659 500X

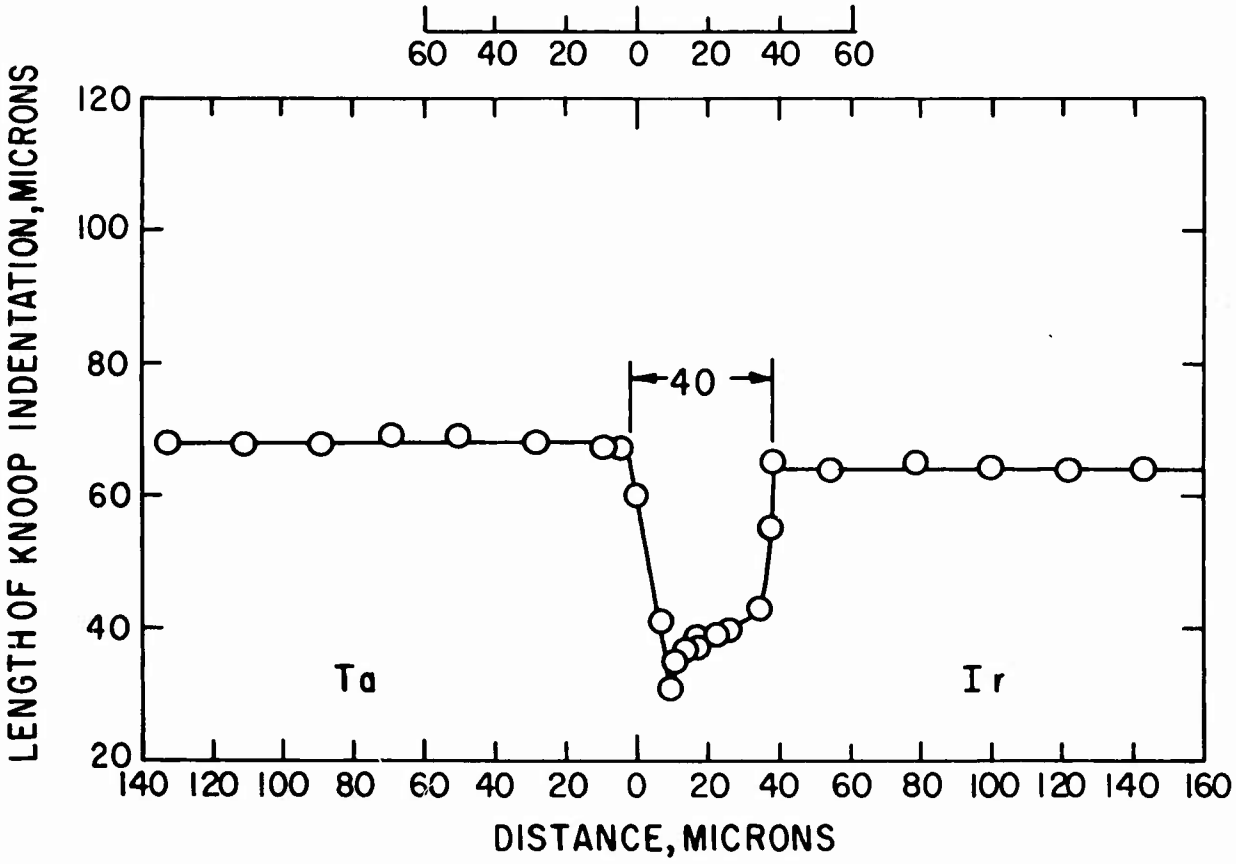

Fig.45- Ta-Ir, pressure weld no. 7b, annealed 3 hours at 1800° C

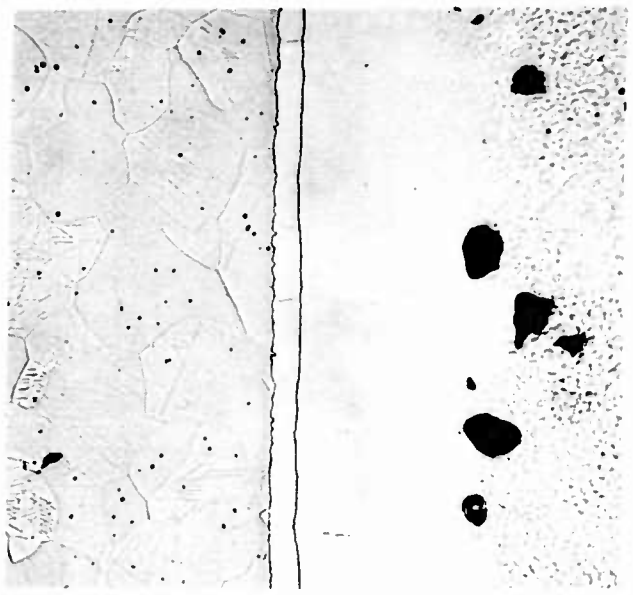

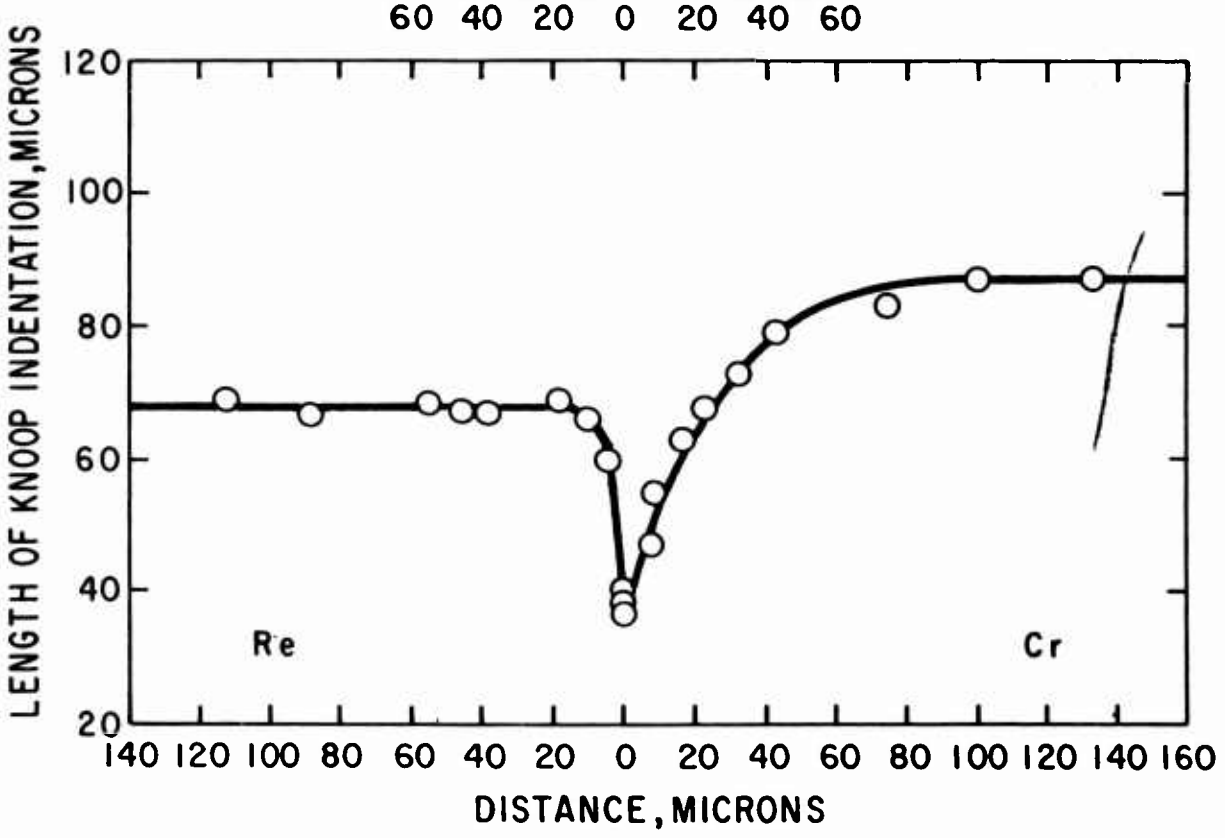

Fig.46- Re-Cr, pressure weld no.5; annealed 1 hour at 1700° C

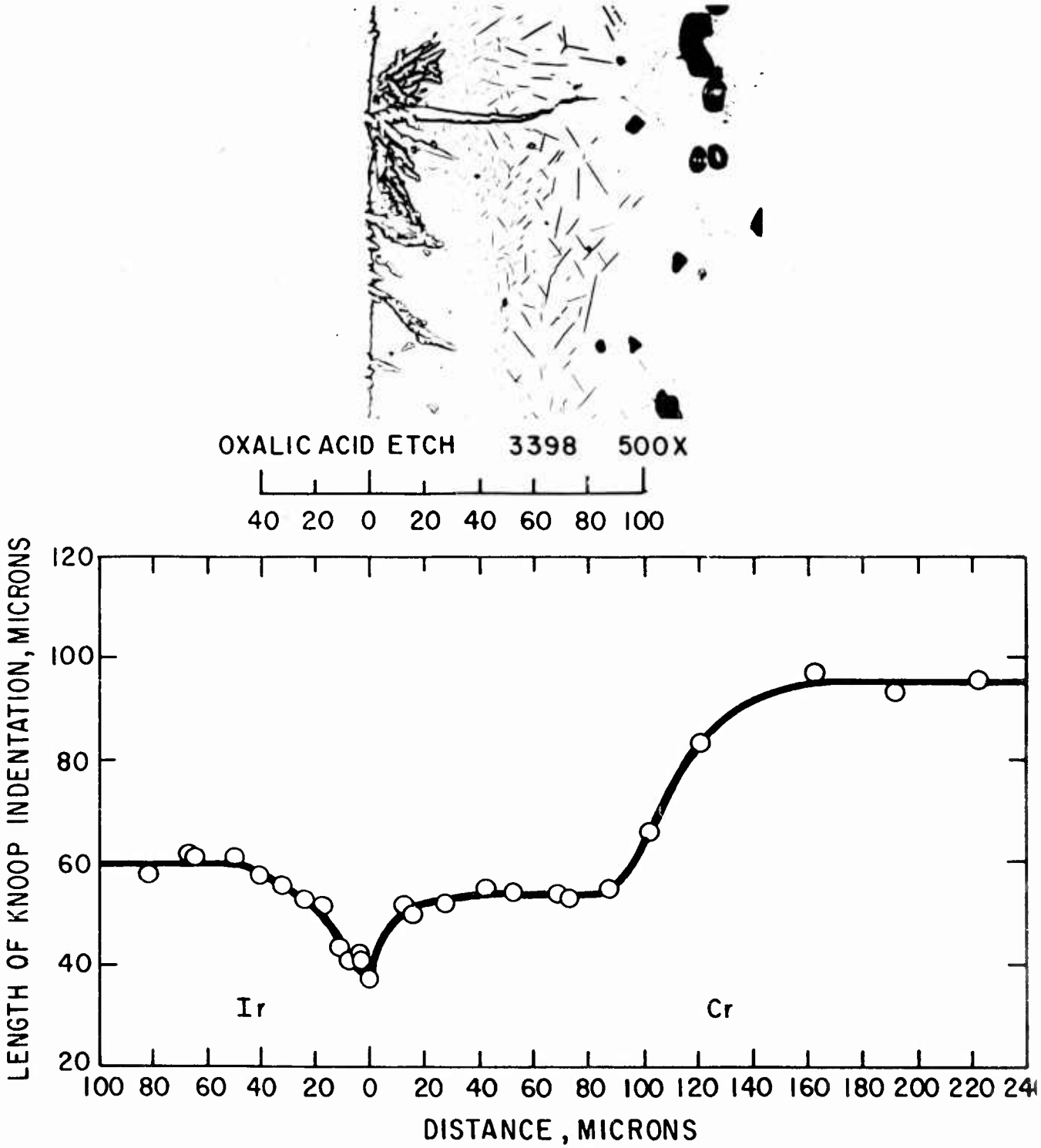

Fig.47- Ir-Cr, pressure weld no.5, annealed 1 hour at 1700 °C

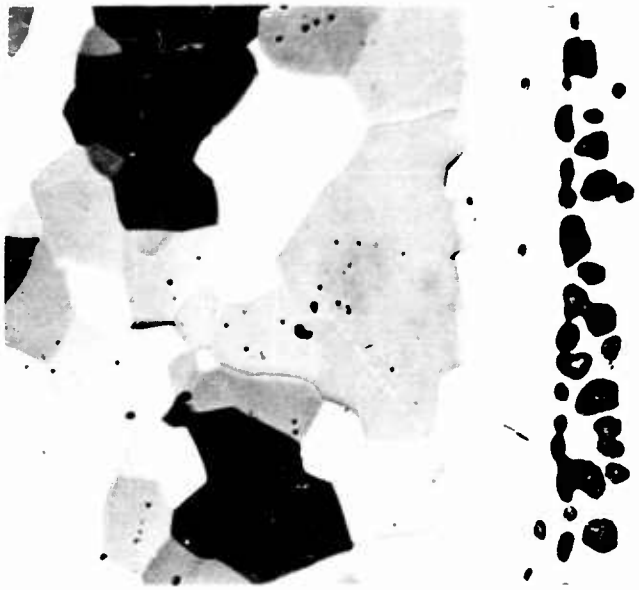

OXALIC ACID ETCH 3898 500X

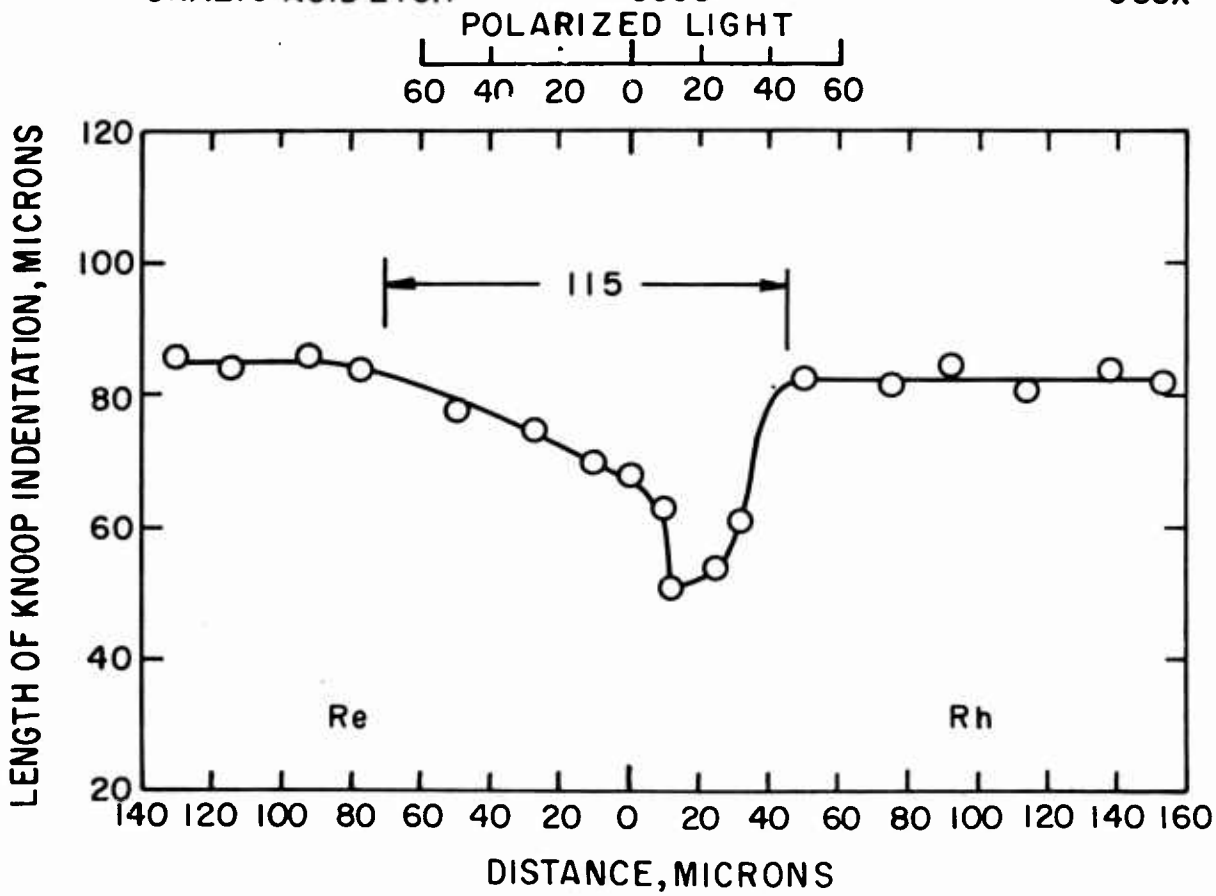

Fig48- Re – Rh, pressure weld no. 7a, annealed 3 hours at 1800 °C

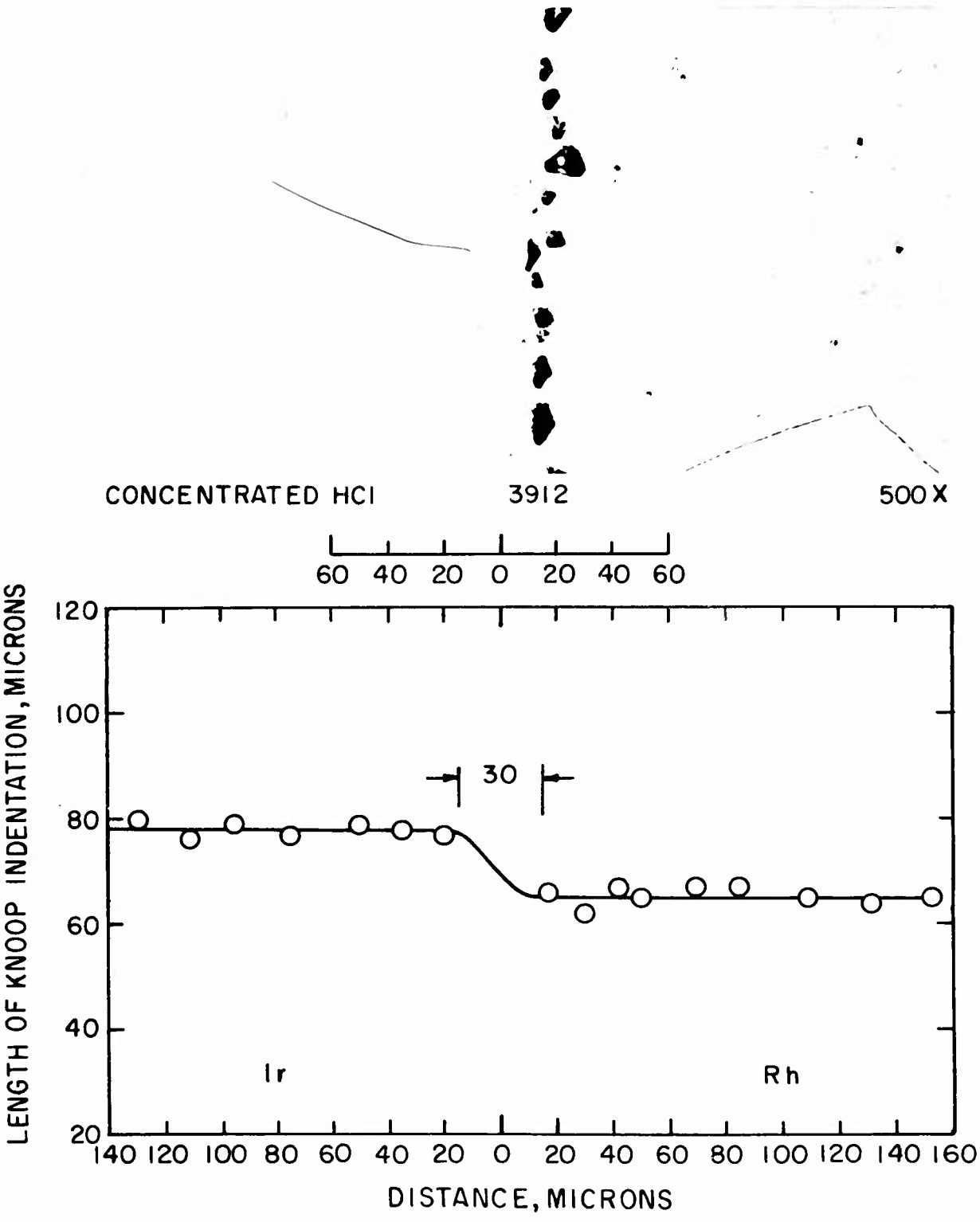

Fig.49- Ir - Rh, pressure weld no. 7a, annealed 3 hours at 1800°C

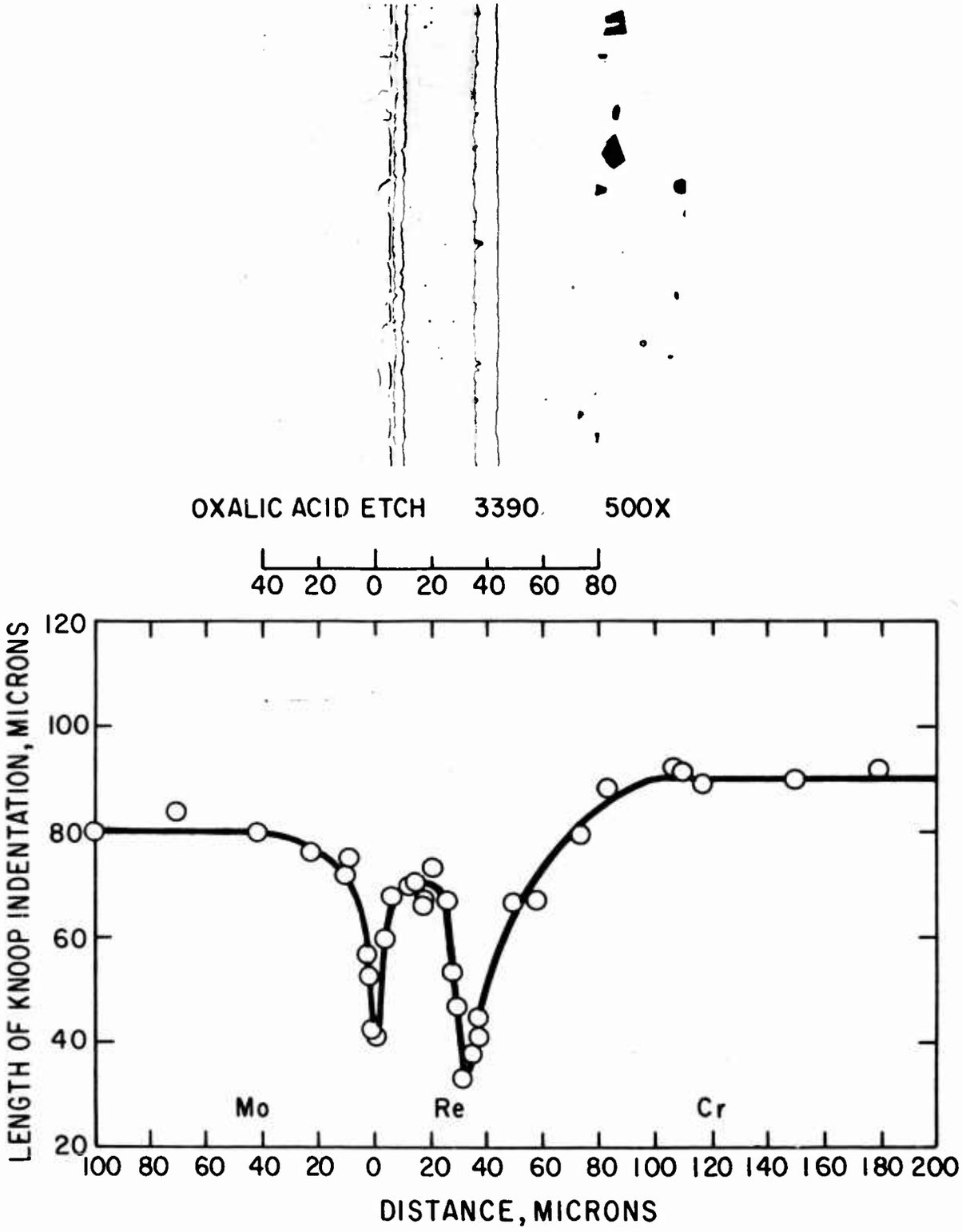

Fig.50- Mo – Re – Cr, pressure weld no.5, annealed 1 hour at 1700 °C

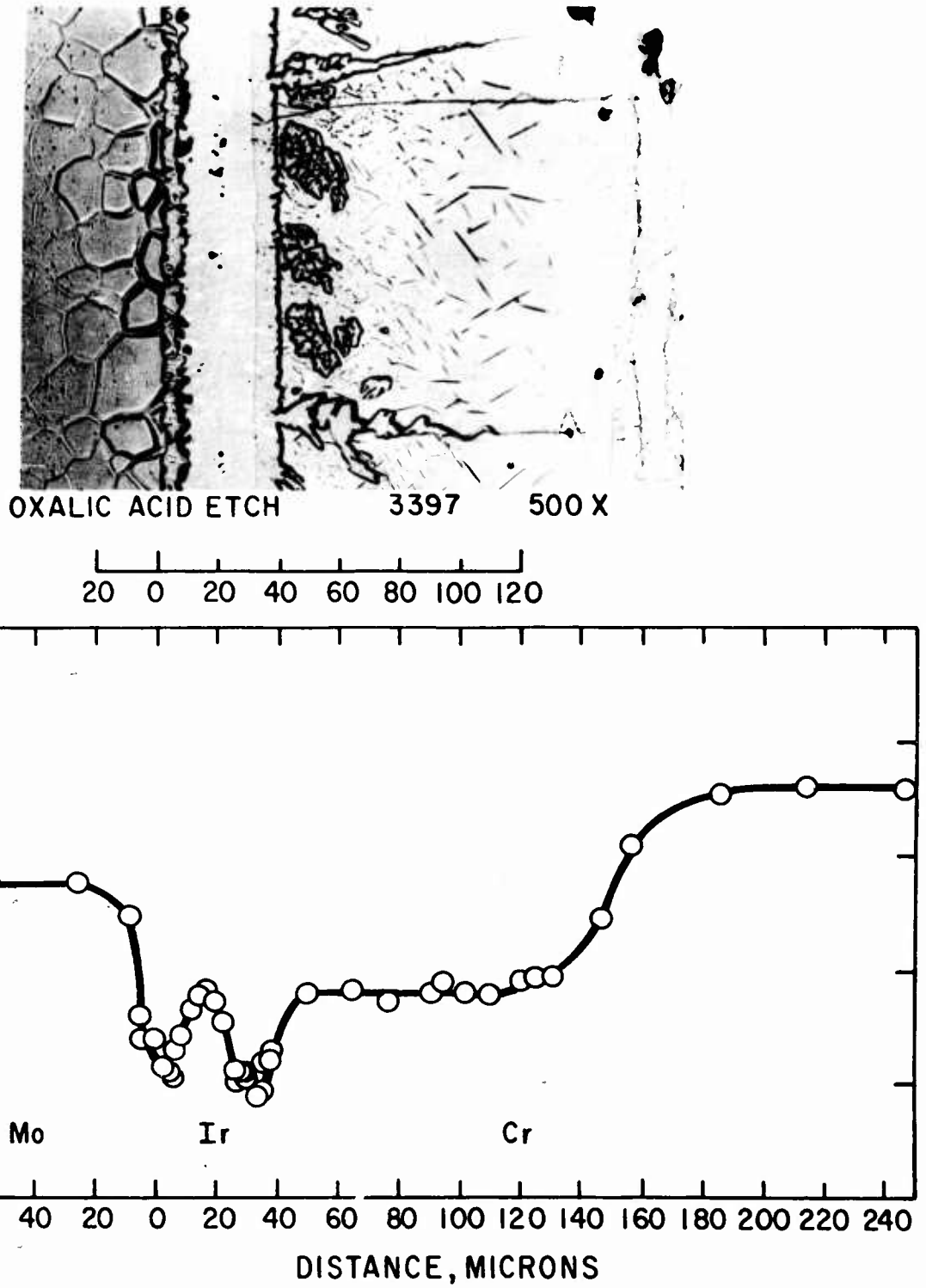

Fig.51- Mo-Ir-Cr, pressure weld no.5, annealed 1 hour at 1700 °C

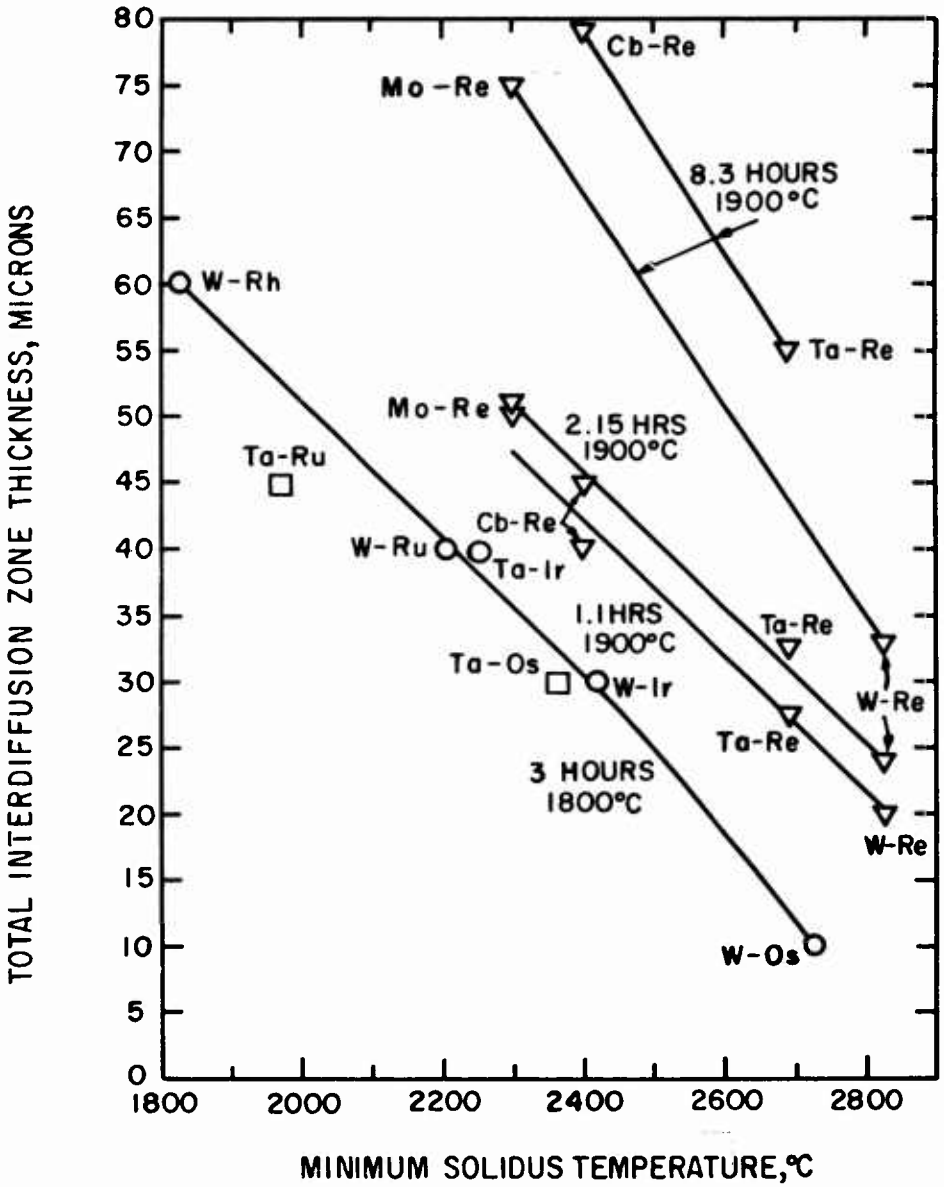

Fig. 52 - Relationship between extent of interdiffusion and the minimum solidus temperature in several base-barrier alloy systems. Diffusion couples were given the indicated annealing treatments.

9.1 Interfacial Hardness and Hardness Increment — The magnitudes of the hardness and the hardness increment at the interface were considered as screening criteria, since hard, and presumably brittle, phases might prohibit good bonding. However, the relation between hardness and brittleness is not definite and it is difficult to set levels above which these hardness parameters can be considered deleterious. As a rough judgment, only the W-Os and Ta-Ir combinations are considered undesirable because of high interfacial hardness.

9.2 Porosity — The porosity evident in many combinations, as indicated in Tables 4 and 5, may also inhibit good bonding. Some combinations with Os and Ru barriers, especially W-Os, also exhibit a pronounced tendency to crack near the interface. Because of such characteristics the W-Os and Ta-Os combinations are considered undesirable.

9.3 Barrier Oxidation Resistance and Barrier-Coating Interdiffusion — Although the barrier is intended to be covered with a protective coating, its oxidation behavior is still important because of possible exposure to the atmosphere through the coating and because of interdiffusion between the barrier and the coating. The only promising barrier metals that exhibit relatively good resistance to oxidation are Rh, Ir, and to a lesser extent, Ru. Barrier-coating interdiffusion was investigated for the cases of Cr and Rh as oxidation-resistant coating components. In general, it may be assumed that barrier-coating interdiffusion should be at a minimum for non-oxidation-resistant barriers. The Mo-Ta, Cb-Ta, and Cb-Mo combinations are not considered desirable because the barrier metal has poor oxidation and interdiffusion characteristics.

After consideration of the factors discussed above, the 20 promising combinations have been reduced to the following 14 optimum ones.

-	Mo-W	Ta-W	Cb-W
W-Re	Mo-Re	Ta-Re	Cb-Re
-	-	-	Cb-Os
W-Ru	-	Ta-Ru	-
W-Ir	-	Ta-Ir	-
-	Mo-V	-	Cb-Zr

B. Interdiffusion Kinetics in Some Optimum Combinations

Microstructures of the interdiffusion zones of W-Re, Mo-Re, Ta-Re and Cb-Re diffusion couples are shown in Figs. 53 to 56, together with graphs showing the variations in microindentation length with distance, normal to the interface. The photomicrographs represent the longest annealing times at 1900°C which were used for each combination, whereas the microindentation data is shown for all annealing times. Two intermediate phases, sigma and chi, are observed in the W-Re and Mo-Re couples, whereas only one, sigma, is formed in the Ta-Re and Cb-Re couples (see Table 7). Solid solution regions are present on either side of the intermediate phase layers. Porosity was found in the diffusion zones of all except the W-Re combination. In the Mo-Re, Ta-Re, and Cb-Re combinations, the predominant diffusion direction is toward the Re,

Table 7

Solid Solubilities and Intermediate Phases at 1900°C in Some Optimum Combinations

Combination	Solubility of Base in Barrier a/o	Solubility of Barrier in Base a/o	Intermediate Phases with Stable Compositional Ranges a/o	Reference
W-Re	11 W	29 Re	chi (23 to 27 W) sigma (35 to 57 W)	(15)
Mo-Re	1 Mo	51 Re	chi (13 to 16 Mo) sigma (18 to 32 Mo)	(5)
Ta-Re	3 Ta	46 Re	chi (21 to 37 Ta)	(3)
Cb-Re	< 2 Cb	41.5 to 43 Re	chi (13 to 37 Cb)	(8, 9, 10)

with the result that the intermediate phase layers are located entirely on the Re side of the original interface. A line of porosity is present on the Mo, Ta, or Cb side of the interface in each case, at approximately the extreme limit of the Mo, Ta, or Cb-rich solid solution. In the W-Re combination, on the other hand, the intermediate phase layer is roughly centered on the original interface, and no porosity is present.

In general, the total extent of interdiffusion as indicated by the thicknesses of the interdiffusion zones (determined from microindentation measurements) seems to be a more significant parameter representing the interdiffusion behavior than the intermediate phase thickness, since the interdiffusion zone is less distorted by unequal diffusion rates. In the presence of such inequality, the intermediate phase layer thickness indicates a lesser extent of interdiffusion than actually occurs.

In Figs. 57 to 59 are plotted values of intermediate phase layer thicknesses and total interdiffusion zones versus annealing time at 1900°C on a log-log scale for each combination. Both parameters follow approximately straight lines in all cases, except for the chi phases in the W-Re and Mo-Re combinations at short annealing times. This behavior indicates that interdiffusion follows a relationship of the form $X^n = kt$, where X is either the interdiffusion zone thickness or intermediate phase width, t is annealing time, and n and k are constants. The values of n and k determined for each combination are listed in Table 8.

The sigma phase layers in both the W-Re and Mo-Re combinations followed approximately the same relationship, whereas growth of the chi phase is somewhat erratic, especially in Mo-Re. In W-Re, chi grows rapidly between the 1.1 and 2.15 hour anneals, remains constant until 8.3 hours, and then grows at a rate governed by the above relationship. In Mo-Re, a similar behavior was observed, except that the width remained approximately constant up to a longer time, 18.1 hours, before growing more rapidly. With respect to the two Mo-Re specimens annealed 41.5 hours, a chi phase layer was found in one specimen but not in the other. It is possible that a relatively slight increase in the rate of movement of the sigma/chi interface with respect to that of the chi/Re interface can reduce the width of the chi phase layer below the detectable limit (about 0.3 to 0.5 micron). Such an occurrence is more likely in the Mo-Re than in the W-Re combination because the diffusion is predominantly from the Mo into the Re whereas diffusion in W-Re is approximately the same in each direction. Thus, all the Mo-Re interfaces would be expected to move in the same direction, into the Re, and more rapid interface movement should occur (for a given layer width) than in the W-Re combination. Under such conditions relatively slight fluctuations in rates of interface movement in Mo-Re could have a substantial effect on the width of the narrower of the phase layers.

Several authors have considered mathematical techniques for treating interdiffusion in the presence of intermediate phases. Castleman[25] has examined analytically certain idealized cases of interdiffusion in three-phase systems. Although many approximations were made, the mathematics is still complicated. A number of investigators have studied the growth of intermediate phase in binary systems, and have also found that it usually follows a parabolic relation of the form $X^n = kt$, where n is between 1 and 4[26,27]. Mathematical treatments of

Table 8

Constants in the Equation, $X^n = kt$, Relating Intermediate Phase and Total Interdiffusion Zone Thicknesses to Diffusion-Annealing Time at 1900°C

Combination	Region	n	k (microns^n/hr)	Ds (cm^2/sec)
W-Re	Total Zone	4.9	2.4×10^6	3.4×10^{-6}
	Total Phase Layer	2.5	0.87×10^2	
	Sigma	3.3	4.4×10^2	
	Chi	1.4	0.004×10^2	
Mo-Re	Total Zone	4.6	6.4×10^7	9.0×10^{-5}
	Total Phase Layer	2.6	2.0×10^2	
	Sigma	3.2	8.5×10^2	
Ta-Re	Total Zone	2.9	1.4×10^4	1.9×10^{-8}
	Total Phase Layer (Chi)	3.4	1.2×10^2	
Cb-Re	Total Zone	2.9	3.7×10^4	5.1×10^{-8}
	Total Phase Layer (Chi)	3.4	2.4×10^2	

phase growth based on volume diffusion are valid only where $n = 2$, as is sometimes the case after long times at high temperatures[27, 28, 29]. The temperature-dependent rate constant, k, is approximately equal to $2D_s$, where D_s can be considered as an approximate over-all interdiffusion coefficient[27]. Values of D_s for each case studied here are also listed in Table 8.

Based on growth kinetics studies and assuming that the concentration-penetration curves were linear, Heumann[29] obtained diffusion coefficients in the beta, gamma, and epsilon phases of the Ag-Zn system by applying the Matano analysis which Jost had shown earlier is valid for such cases. Using a somewhat different analytical approach, Castleman[29] obtained diffusion coefficients and activation energies in the gamma and beta phases of the Al-Ni system from growth kinetics. Castleman[30] applied with a similar approach to diffusion in beta-brass, however, the results did not show good agreement with those obtained from a Matano analysis of the concentration-penetration curve as determined by an electron microbeam probe.

In the interdiffusion studies made here, however, only the interdiffusion zone and intermediate phase layer thicknesses were measured and not the penetration rates of the phase boundaries. Consequently, the over-all "interdiffusion coefficient", D_s, in the equation $X^n = 2D_s t$, is probably the significant parameter describing the interdiffusion behavior. In all cases studied here, n is between 1.44 and 4.87, indicating that volume diffusion is not the predominant process occurring, since for pure volume diffusion, n is theoretically equal to 2[27].

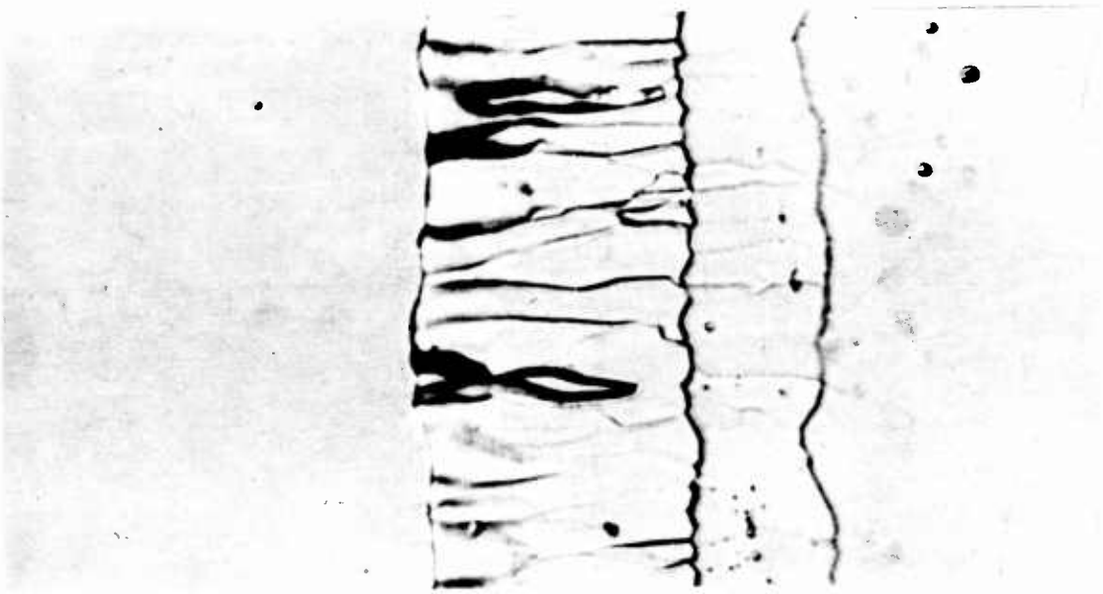

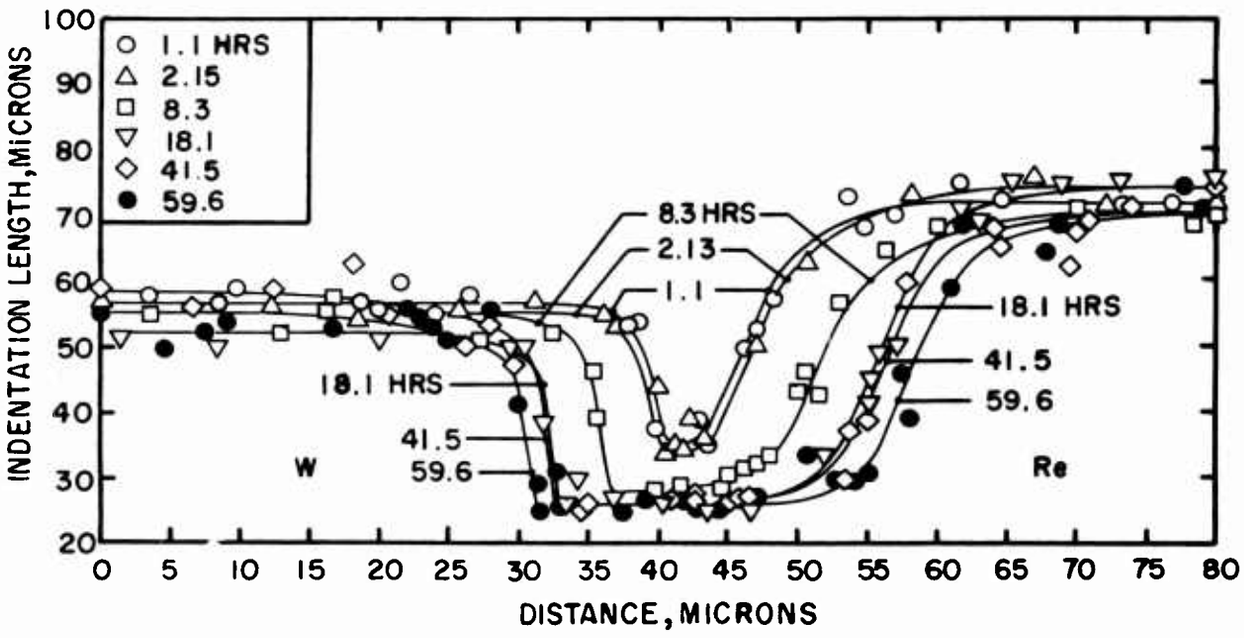

Fig.53 - Variation of knoop indentation length with distance, normal to the interface, in tungsten-rhenium diffusion couples after annealing at 1900°C

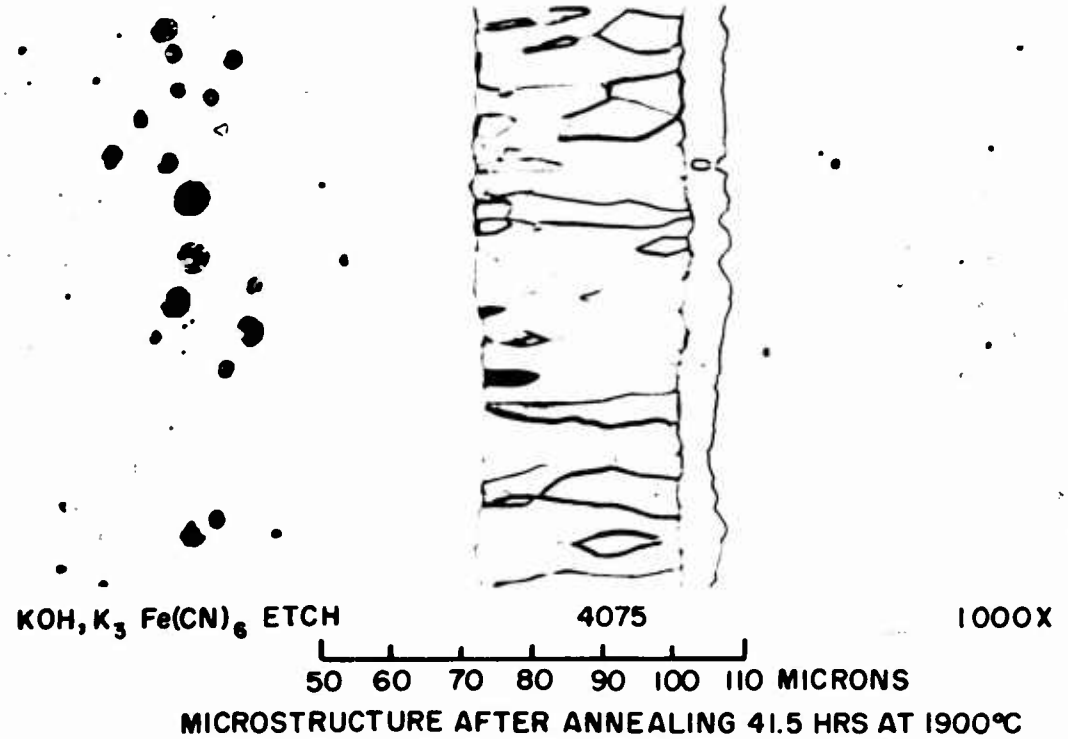

Fig.54 - Variation of knoop indentation length with distance, normal to the interface, in molybdenum-rhenium diffusion couples after annealing at 1900°C

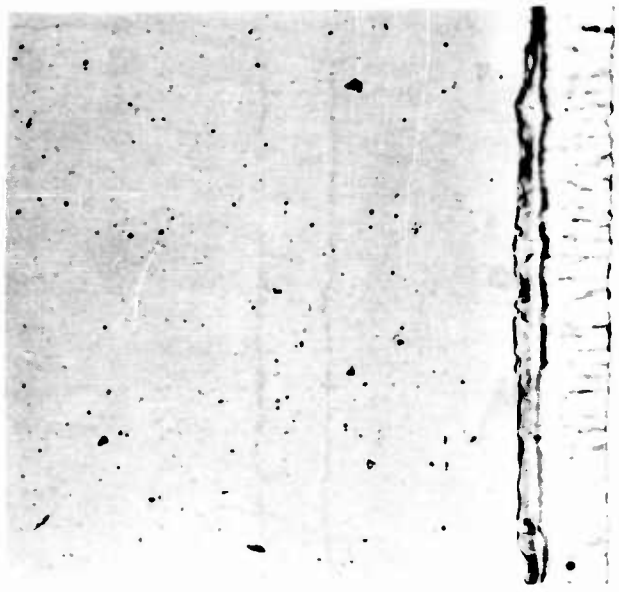

LACTIC ACID ETCH 4078 1000X

50 60 70 80 90 100 110 MICRONS

MICROSTRUCTURE AFTER ANNEALING 8.3 HRS AT 1900°C

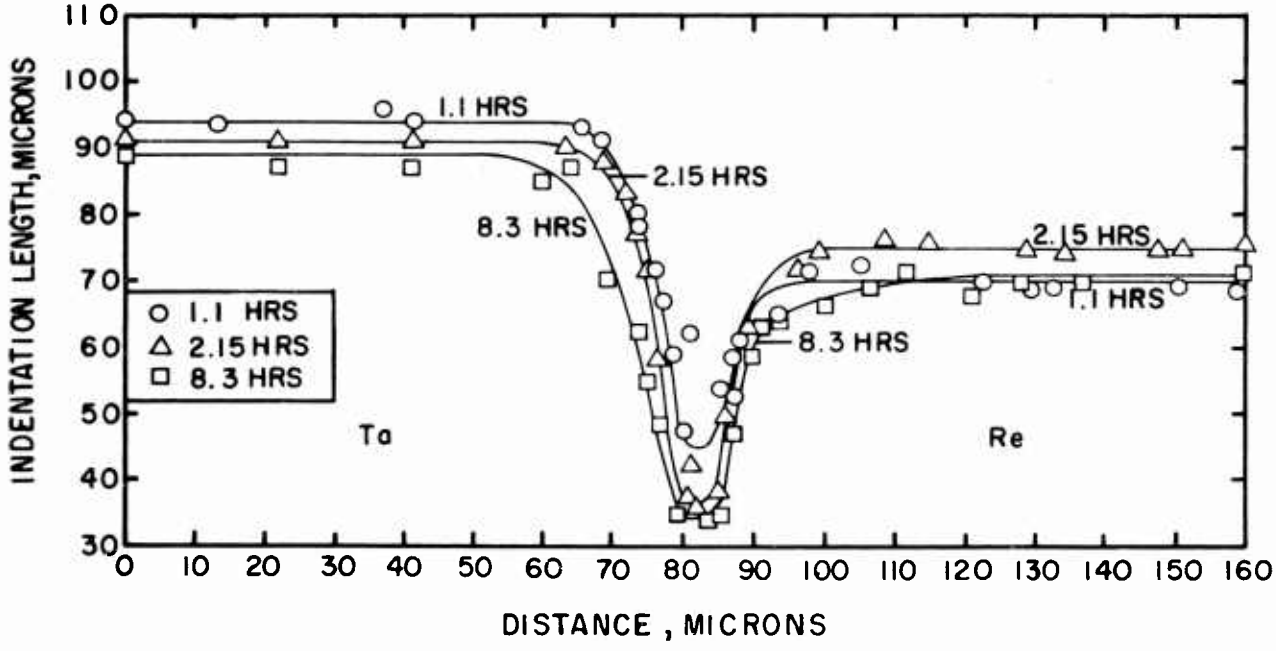

Fig.55 - Variation of knoop indentation length with distance, normal to the interface, in tantalum-rhenium diffusion couples after annealing at 1900°C

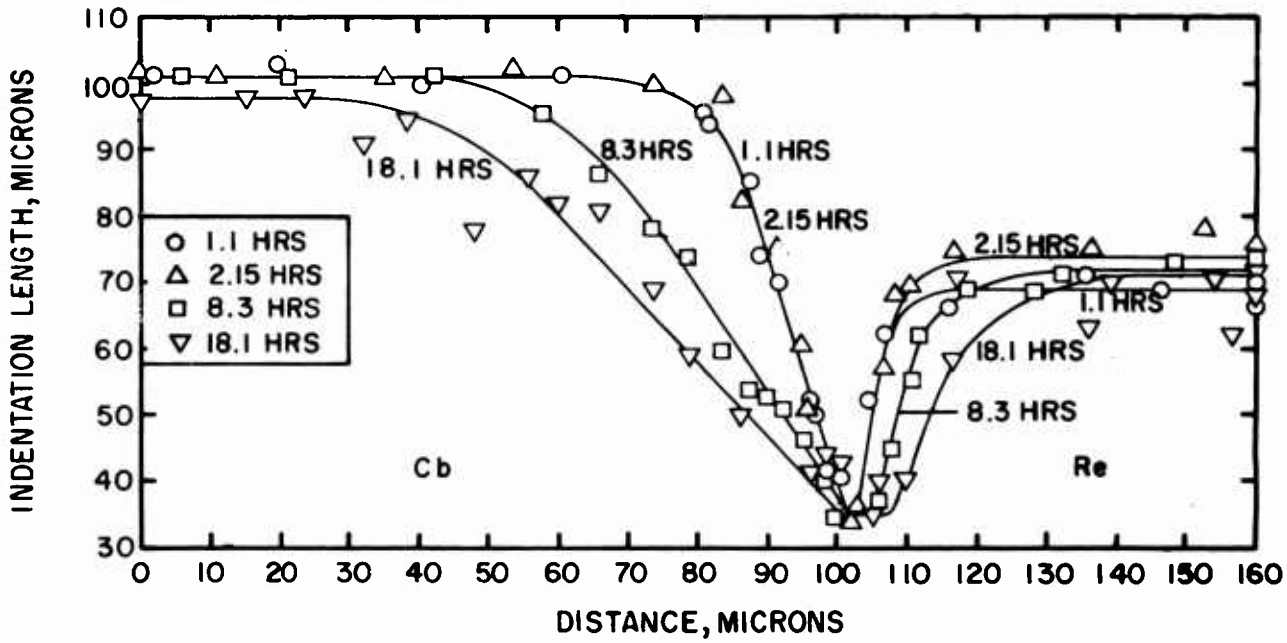

Fig.56 – Variation of knoop indentation length with distance, normal to the interface, in columbium-rhenium diffusion couples after annealing at 1900°C

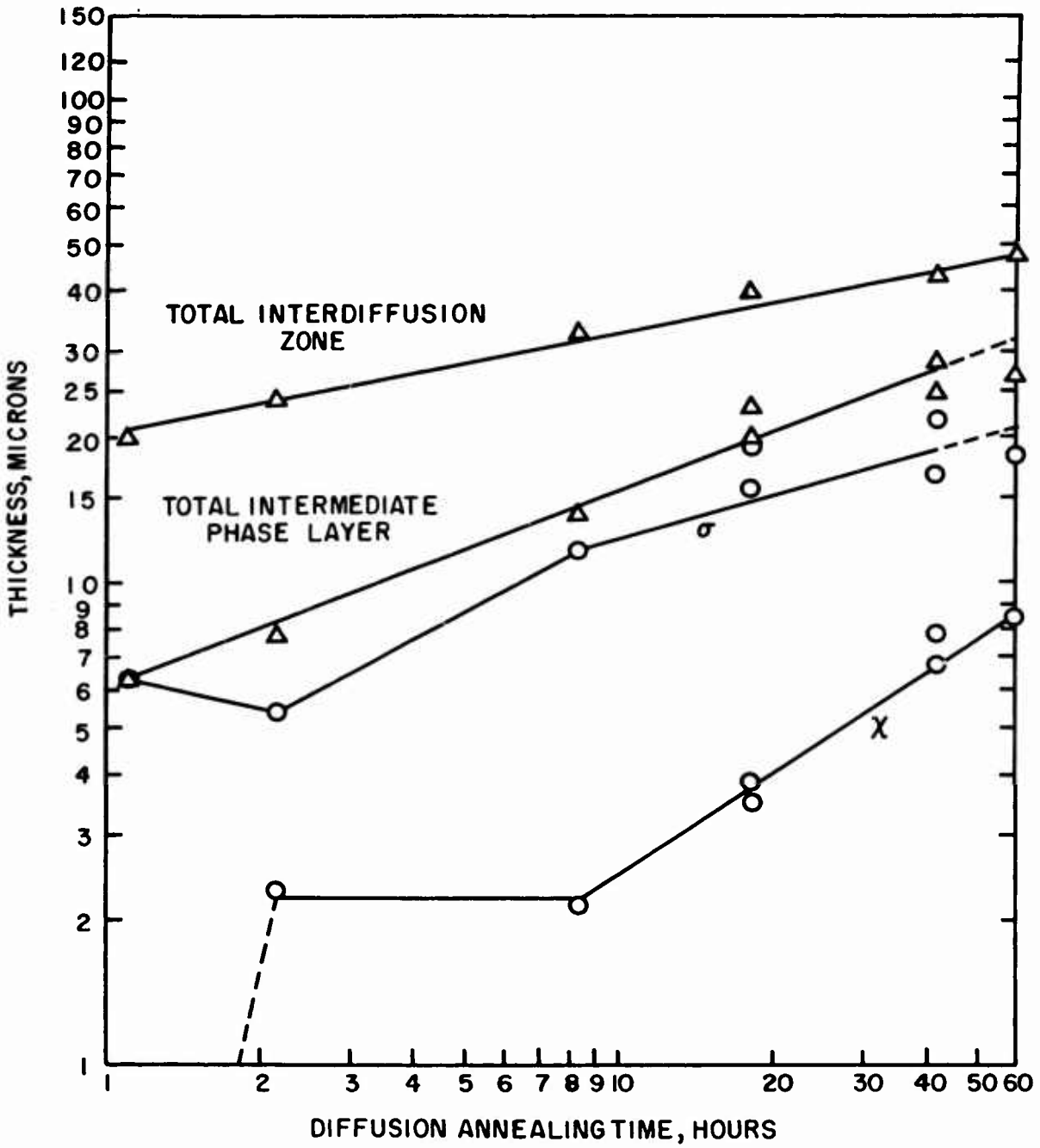

Fig.57–Growth of interdiffusion zone and intermediate phases in tungsten-rhenium diffusion couples annealed at 1900°C

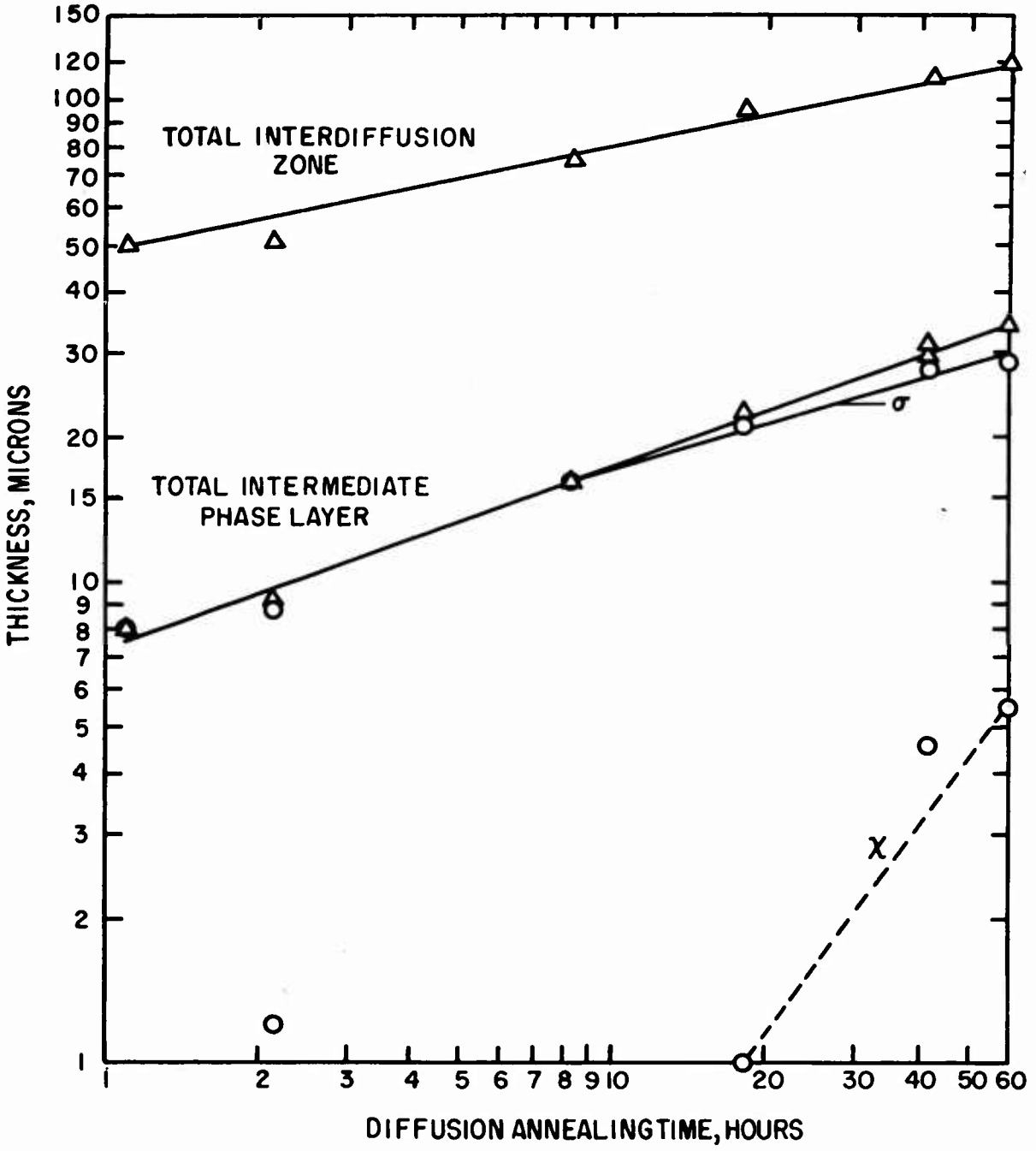

Fig.58 - Growth of interdiffusion zone and intermediate phases in molybdenum-rhenium diffusion couples annealed at 1900°C

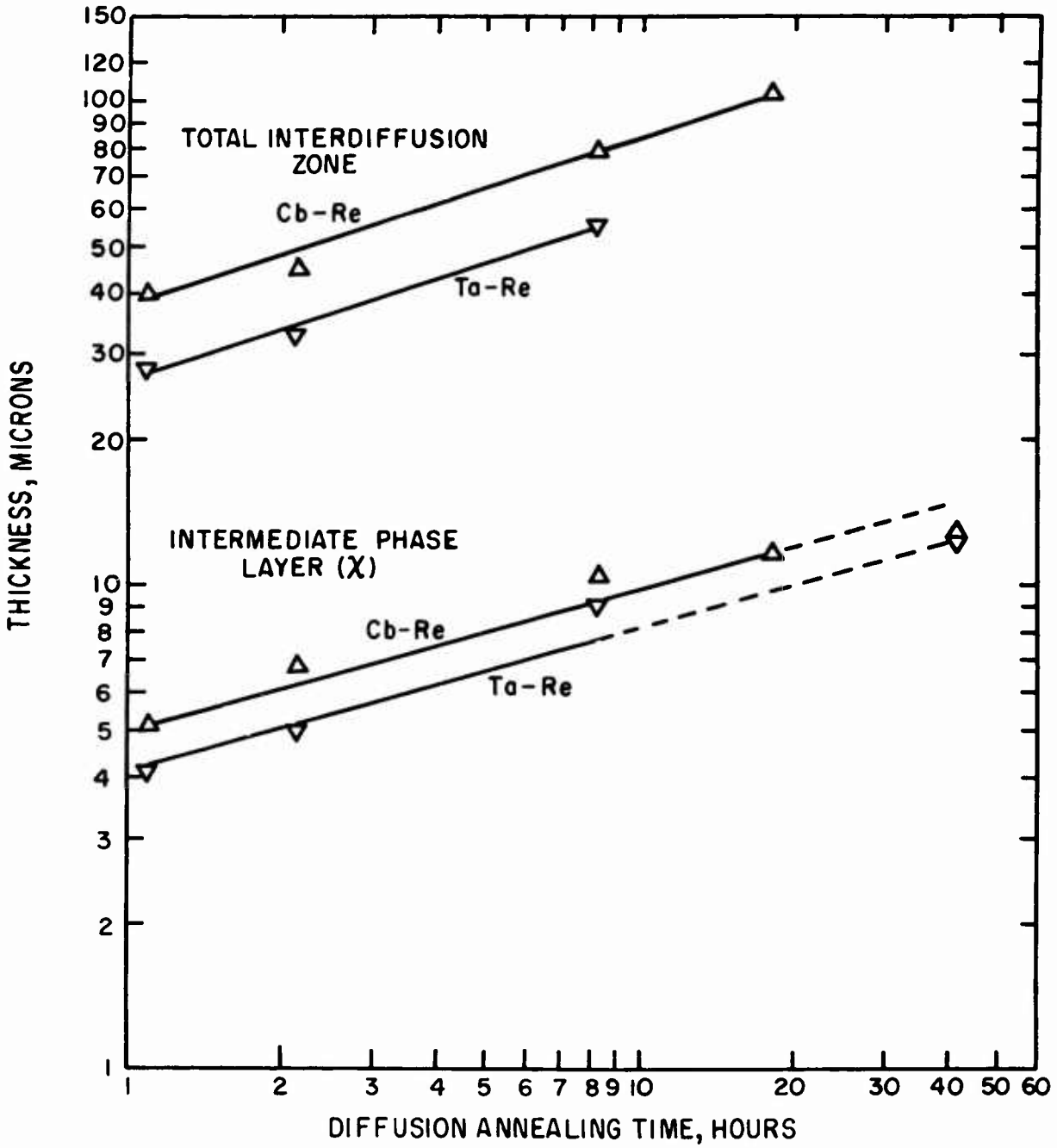

Fig.59- Growth of interdiffusion zone and intermediate phases in tantalum-rhenium and columbium-rhenium diffusion couples annealed at 1900°C

IV. SUMMARY OF RESULTS

A. Thirty-three base-barrier combinations were evaluated for relative extents of interdiffusion by metallographic examination and microhardness tests on diffusion couples prepared by pressure-welding and annealing at 1700°C.

B. Wide variations in the total interdiffusion zone thicknesses from over 600 microns in the Mo-Hf, Ta-Hf, and Cb-Hf combinations to 30 microns in the Ta-Os combination, were found to occur after diffusion-annealing for four hours.

C. A rough correlation of the extent of interdiffusion with the minimum base-barrier alloy solidus temperature was found. Combinations with solidus temperatures over 2100°C exhibit only limited interdiffusion, whereas up to 2100°C wide variations occur.

D. Using criteria of 30 microns maximum interdiffusion after a one-hour anneal and 60 microns after a four-hour anneal at 1700°C, 20 promising combinations were selected for further study.

E. Alloying of Mo and Cb base metals was found to produce no observable effect on base-barrier interdiffusion with Re as the barrier metal.

F. Interdiffusion studies on the three-layer combinations Mo-Re-Cr and Mo-Ir-Cr, where Cr simulated a typical oxidation-resistant coating metal, indicate that the use of a Re barrier can reduce interdiffusion by amounts up to 45% as compared to the Mo-Cr combination alone.

G. In further evaluation experiments on eight promising W and Ta-base combinations after diffusion-annealing for three hours at 1800°C, the extents of interdiffusion found in combinations of W base metal with Pt-group barrier metals such as Rh, Ir, Ru, and Os were found to decrease with increasing alloy solidus temperature. Insufficient data were obtained to ascertain whether a similar relationship exists for Ta base metal. However, similar relationships were found for the W-Re, Mo-Re, Ta-Re, and Cb-Re combinations after annealing at 1900°C.

H. The results of the base-barrier interdiffusion studies were supplemented by consideration of such factors as alloy melting point, interfacial hardnesses, porosity formation, tendency toward interfacial cracking, barrier-coating metal (Cr and Rh) interdiffusion, and barrier metal properties. The following 14 combinations were chosen as optimum:

-	Mo-W	Ta-W	Cb-W
W-Re	Mo-Re	Ta-Re	Cb-Re
-	-	-	Cb-Os
W-Ru	-	Ta-Ru	-
W-Ir	-	Ta-Ir	-
-	Mo-V	-	Cb-Zr

I. Quantitative interdiffusion studies on optimum combinations involving W, Mo, Ta, and Cb base metals with Re barrier metal at a diffusion-annealing temperature of 1900°C have shown that the thickness (X) of the total interdiffusion zone and of the intermediate phase layers increase with time (t) in accordance with $X^n = kt$, with n varying between 1.4 and 4.9.

J. These values of n indicate that processes other than pure volume diffusion, for which n is theoretically equal to 2, are occurring.

K. Values of an over-all interdiffusion coefficient, D_s, calculated from the growth kinetics of the interdiffusion zones at 1900°C, were 3.4×10^{-6} cm^2/sec for the W-Re combination, 9.0×10^{-5} for Mo-Re, 1.9×10^{-8} for Ta-Re, and 5.1×10^{-8} for Cb-Re. No published values were available for comparison.

References

(1) E. M. Passmore, J. E. Boyd, L. P. Neal, C. A. Andersson, B. S. Lement; Investigation of Diffusion Barriers for Refractory Metals, WADD TR 60-343 (August 1960).

(2) W. Rostoker, A Study of Ternary Phase Diagrams of Tungsten and Tantalum, WADC TR 59-492 (March 1960).

(3) A. R. Kaufmann, et. al., Refractory Metal Constitution Diagrams, WADD TR 60-343 (June 1960).

(4) W. Rostoker, op. cit.

(5) Ibid.

(6) S. A. Komjathy, et. al., Phase Relationships in Selected Binary and Ternary Vanadium-Base Alloys Systems, WADC TR 59-483 January 1960.

(7) J. J. English, Binary and Ternary Phase Diagrams of Columbium, Molybdenum, Tantalum and Tungsten, DMIC Report 152 (April 1961).

(8) P. Levesque, et. al., Trans. ASM, 53, (1961) 215-226.

(9) B. C. Geissen, et. al., Trans. AIME, 221, (1961) 1009-1013.

(10) A. G. Knapton, J. Less-Common Metals, 2, (1961) 113-124.

(11) M. Hansen, Constitution of Binary Alloys, McGraw-Hill Book Co., New York, (1958).

(12) G. L. Miller, Tantalum and Niobium, Buttersworth Scientific Publications, London (1959).

(13) M. Hansen, op. cit.

(14) G. L. Miller, op. cit.

(15) J. M. Dickinson and L. S. Richardson, Trans. ASM, 51, (1959) 758-771.

(16) A. R. Kaufmann, et. al., op. cit.

(17) E. J. Rapperport, Refractory Metal Phase Diagrams, Quarterly Progress Report, NMI-9235, (June 30, 1961).

References (cont.)

(18) E. Anderson and W. Hume-Rothery, J. Less-Common Metals, 2, (1960) 443-450.

(19) E. Anderson and W. Hume-Rothery, J. Less-Common Metals, 2, (1960) 19-28.

(20) C. S. Hartley, et. al., Phase Relationships in Tantalum-Rich Tantalum-Ruthenium Alloys at 1500°C, WADD TN 60-288, (March 1961).

(21) J. A. Misencik, The Chromium-Columbium Binary System, WAL TR 805.5/1 (March 1960).

(22) J. D. Baird, J. Nucl. Energy, Part A: Reactor Science, 11, (1960), 81-88.

(23) R. S. Barnes and D. J. Mazey, Acta Met., 6, (1958), 1-7.

(24) R. I. Jaffee, A Brief Review of the Refractory Metals, DMIC Memorandum 40 (1959).

(25) L. S. Castleman, "An Analytical Approach to the Diffusion Bonding Problem", Nuc. Sci. and Eng., 4 (1958) 209.

(26) L. S. Castleman and L. L. Seigle, "Layer Growth During Interdiffusion in the Aluminum-Nickel Alloy System", Trans AIME, 212, (1958), 589.

(27) J. D. Baird, op. cit.

(28) L. S. Castleman, H. A. Froot, and L. L. Seigle, "Fundamentals of Diffusional Bonding - VI", SEP-258 (July 26, 1961).

(29) L. S. Castleman and L. L. Seigle, op. cit.

(30) L. S. Castleman, H. A. Froot and L. L. Seigle, op. cit.

Aeronautical Systems Division, Dir/Materials & Processes, Metals & Ceramics Lab, Wright-Patterson AFB, Ohio.
Rpt Nr ASD-TDR-62-432, INVESTIGATION OF DIFFUSION BARRIERS FOR REFRACTORY METALS. Final report, July 1962, 95 p., incl. illus., tables & 30 refs.

Unclassified Report

Thirty-three base barrier combinations involving the four refractory metals W, Mo, Ta, and Cb and 12 potential barrier metals having melting points over 1700°C were evaluated for relative interdiffusion behavior at 1700°C and 1800°C. The relative extent of interdiffusion decreases with increasing base-barrier solidus temperature, although wide variations occur for melting points up to

(over)

2100°C. Interdiffusion in the Mo-Cr combination was found to be substantially reduced by the presence of a Re barrier.

Re, Ru, and Ir barriers appear optimum for W base metal; W, Re, Ru, and Ir appear optimum for Ta; and W, Re, Os, and Zr appear optimum for Cb.

The thickness (X) of the total interdiffusion zone as well as of the intermediate phase layers in the W-Re, Mo-Re, Ta-Re, and Cb-Re combinations was found to increase with time (t) in accordance with the relationship $X^n = kt$, with values of n in the range 1.4 to 4.9.

1. Barrier Coatings
2. Interdiffusion
3. Refractory Metals

I. AFSC Project 7312 Task 731201
II. Contract AF 33(616)-6354
III. ManLabs, Inc., Cambridge, Mass.
IV. E. M. Passmore, J. E. Boyd, B. S. Lement
V. Aval fr OTS
VI. In ASTIA collection

Aeronautical Systems Division, Dir/Materials & Processes, Metals & Ceramics Lab, Wright-Patterson AFB, Ohio.
Rpt Nr ASD-TDR-62-432, INVESTIGATION OF DIFFUSION BARRIERS FOR REFRACTORY METALS. Final report, July 1962, 95 p., incl. illus., tables & 30 refs.

Unclassified Report

Thirty-three base barrier combinations involving the four refractory metals W, Mo, Ta, and Cb and 12 potential barrier metals having melting points over 1700°C were evaluated for relative interdiffusion behavior at 1700°C and 1800°C. The relative extent of interdiffusion decreases with increasing base-barrier solidus temperature, although wide variations occur for melting points up to

(over)

2100°C. Interdiffusion in the Mo-Cr combination was found to be substantially reduced by the presence of a Re barrier.

Re, Ru, and Ir barriers appear optimum for W base metal; W, Re, Ru, and Ir appear optimum for Ta; and W, Re, Os, and Zr appear optimum for Cb.

The thickness (X) of the total interdiffusion zone as well as of the intermediate phase layers in the W-Re, Mo-Re, Ta-Re, and Cb-Re combinations was found to increase with time (t) in accordance with the relationship $X^n = kt$, with values of n in the range 1.4 to 4.9.

1. Barrier Coatings
2. Interdiffusion
3. Refractory Metals

I. AFSC Project 7312 Task 731201
II. Contract AF 33(616)-6354
III. ManLabs, Inc., Cambridge, Mass.
IV. E. M. Passmore, J. E. Boyd, B. S. Lement
V. Aval fr OTS
VI. In ASTIA collection

Aeronautical Systems Division, Dir/Materials & Processes, Metals & Ceramics Lab, Wright-Patterson AFB, Ohio.
Rpt Nr ASD-TDR-62-432, INVESTIGATION OF DIFFUSION BARRIERS FOR REFRACTORY METALS. Final report, July 1962, 95 p., incl. illus., tables & 30 refs.

Unclassified Report

Thirty-three base barrier combinations involving the four refractory metals W, Mo, Ta, and Cb and 12 potential barrier metals having melting points over 1700°C were evaluated for relative interdiffusion behavior at 1700°C and 1800°C. The relative extent of interdiffusion decreases with increasing base-barrier solidus temperature, although wide variations occur for melting points up to

(over)

1. Barrier Coatings
2. Interdiffusion
3. Refractory Metals

I. AFSC Project 7312 Task 731201
II. Contract AF 33(616)-6354
III. ManLabs, Inc., Cambridge, Mass.
IV. E. M. Passmore, J. E. Boyd, B. S. Lement
V. Aval fr OTS
VI. In ASTIA collection

Aeronautical Systems Division, Dir/Materials & Processes, Metals & Ceramics Lab, Wright-Patterson AFB, Ohio.
Rpt Nr ASD-TDR-62-432, INVESTIGATION OF DIFFUSION BARRIERS FOR REFRACTORY METALS. Final report, July 1962, 95 p., incl. illus., tables & 30 refs.

Unclassified Report

Thirty-three base barrier combinations involving the four refractory metals W, Mo, Ta, and Cb and 12 potential barrier metals having melting points over 1700°C were evaluated for relative interdiffusion behavior at 1700°C and 1800°C. The relative extent of interdiffusion decreases with increasing base-barrier solidus temperature, although wide variations occur for melting points up to

(over)

1. Barrier Coatings
2. Interdiffusion
3. Refractory Metals

I. AFSC Project 7312 Task 731201
II. Contract AF 33(616)-6354
III. ManLabs, Inc., Cambridge, Mass.
IV. E. M. Passmore, J. E. Boyd, B. S. Lement
V. Aval fr OTS
VI. In ASTIA collection

2100°C. Interdiffusion in the Mo-Cr combination was found to be substantially reduced by the presence of a Re barrier.

Re, Ru, and Ir barriers appear optimum for W base metal; W, Re, Ru, and Ir appear optimum for Ta; and W, Re, Os, and Zr appear optimum for Cb.

The thickness (X) of the total interdiffusion zone as well as of the intermediate phase layers in the W-Re, Mo-Re, Ta-Re, and Cb-Re combinations was found to increase with time (t) in accordance with the relationship $X^n = kt$, with values of n in the range 1.4 to 4.9.

2100°C. Interdiffusion in the Mo-Cr combination was found to be substantially reduced by the presence of a Re barrier.

Re, Ru, and Ir barriers appear optimum for W base metal; W, Re, Ru, and Ir appear optimum for Ta; and W, Re, Os, and Zr appear optimum for Cb.

The thickness (X) of the total interdiffusion zone as well as of the intermediate phase layers in the W-Re, Mo-Re, Ta-Re, and Cb-Re combinations was found to increase with time (t) in accordance with the relationship $X^n = kt$, with values of n in the range 1.4 to 4.9.